



Università degli Studi di Cagliari

**DOTTORATO IN SCIENZE E TECNOLOGIE FARMACEUTICHE**  
**Ciclo XXVIII**

**DESIGN AND SYNTHESIS OF NEW POTENTIAL ANTICANCER AGENTS AND HIGH-  
SELECTIVE A2B ANTAGONISTS**

**CHIM08**

Presentata da:

Antonella Arridu

Coordinatore Dottorato e Tutor:

Prof. Elias Maccioni

Esame finale anno accademico 2014-2015



## ABSTRACT

The synthesis of antitumor agents covers a large part of current medicinal chemistry efforts. This thesis mainly focuses on the synthesis of different scaffolds as new potential anticancer agents.

Two different approaches were applied: a hybrid concept and a rational based drug design. In the first case, the hybrid concept is useful since it allows combining multiple active scaffolds in a unique molecule. As a consequence, several targets could be hit simultaneously, making this solution particularly attractive for multi-factorial diseases like cancer. Within this category, several isatin-thiazolinone-pyrazoline hybrids were synthesized. Some of them were submitted to biological assays, demonstrating good activity toward different solid tumour cell-lines. In the second class of compounds, the synthetic efforts were combined to computational tools in order to achieve detailed information about the structure-activity relationships. Following this approach, psoralen derivatives, thought as DNA G-quadruplex stabilizers, were synthesized. For these compounds no biological assays were performed so far.

Finally, the last part of the thesis has been dedicated to the synthesis of 1-alkyl-8-(piperazine-1-sulphonyl)phenyl xanthines as high-selective  $A_{2B}$  antagonists. Even though the leading role of adenosine and their receptors in cancer pathogenesis were extensively documented, the high therapeutic potential of these compounds requires a wider analysis of their pharmacological properties. Also in this case, several compounds were synthesized. Some of them were tested in a radioligand binding assay to evaluate the affinity and selectivity toward  $A_{2B}R$  subtype, further confirming the high potential of these compounds as  $A_{2B}$  antagonists.

## CONTENTS

THESIS OVERVIEW .....	1
REFERENCES.....	3
SECTION I.....	5
ANTITUMOR AGENTS.....	5
STATE OF THE ART OF CANCER TREATMENT AND MENAGEMENT.....	5
REFERENCES.....	12
1    SYNTHESIS OF SUBSTITUTED ISATIN, THIAZOLIDINONE AND ARYL-PYRAZOLINE BASED HYBRIDS AS ANTICANCER AGENTS.....	14
1.1    INTRODUCTION.....	14
1.2    COMBINATION OF ISATIN-THIAZOLIDINONE-PYRAZOLINE MOIETIES .....	16
1.2.1    Background.....	16
1.2.2    Synthetic pathway.....	20
1.2.3    A promising pharmacophore hybrid approach.....	25
1.3    CONCLUSIONS.....	29
1.4    EXPERIMENTAL SECTION .....	29
1.4.1    Materials and methods.....	29
1.4.2    Chemistry and structural characterization.....	30
1.4.3    Biological assays.....	46
1.4    REFERENCES.....	48
2    DESIGN AND SYNTHESIS OF PSORALEN DERIVATIVES AS DNA G-QUADRUPLEX STABILISERS.....	50
2.1    INTRODUCTION.....	50
2.2    G-QUADRUPLEX: STRUCTURE AND CONFORMATIONS.....	50
2.3    DNA G-QUADRUPLEX: GENOMIC LOCALIZATION AND BIOLOGICAL ROLE	53
2.3.1    DNA G-quadruplex in telomeric ends.....	54
2.3.2    DNA G-quadruplex in oncogene promoter regions.....	54
2.4    SMALL MOLECULES TARGETING G-QUADRUPLEX DNA .....	55
2.5    RATIONAL DESIGN OF PSORALEN DERIVATIVES.....	57
2.5.1    Computational study.....	57
2.5.2    Synthetic strategy.....	62

2.6	EXPERIMENTAL SECTION .....	67
2.6.1	Experimental section. Materials and methods.....	67
2.6.2	Experimental section. Chemistry and structural characterization .....	68
2.7	CONCLUSIONS.....	72
2.8	REFERENCES .....	73
SECTION II.....		78
A2B ANTAGONISTS.....		78
ADENOSINE RECEPTORS: STRUCTURE, DISTRIBUTION AND BIOLOGICAL FUNCTIONS.....		78
REFERENCES.....		84
3	SYNTHESIS AND BIOLOGICAL EVALUATION OF 1-PROPYL-8-(PIPERAZINE-1- SOLPHONYL)PHENYL XANTHINES AS SELECTIVE ANTAGONISTS OF ADENOSINE A <sub>2B</sub> RECEPTORS.....	88
3.1	INTRODUCTION TO A <sub>2B</sub> RECEPTOR .....	88
3.1.1	A2B receptor. Structure and therapeutic potential .....	88
3.1.2	A2B receptor. Agonists and antagonists.....	91
3.2	SYNTHESIS OF 1,8-SUBSTITUED XANYHINES AS SELECTIVE ANTAGONISTS OF A2BAR.....	94
3.2.1	Synthesis of 1,8-substituted xanthines as selective antagonists ofA2BAR. Structural features and synthetic pathway .....	94
3.3	CONCLUSIONS.....	102
3.4	EXPERIMENTAL SECTION .....	103
3.4.1	Materials and methods.....	103
3.4.2	Chemistry and structural characterization .....	103
3.5	REFERENCES.....	112

## THESIS OVERVIEW

*The discovery and exploitation of new drug targets are the main focus for both academic research and pharmaceutical industry. Drug target identification and validation has radically changed and evolved over the last decades, translating the serendipitous drug discovery into a rational and reliable process. In this respect, pharmaceutical chemistry is among the most rapidly advancing fields, with constant improvements in methods and techniques. The present state of the art in medicinal chemistry has been reached, in part, with a rational combination of innovative knowledges derived from different areas of life and chemistry sciences.<sup>1,2</sup>*

*In particular, the advent of computational chemistry and molecular biology is having a deep impact on drug discovery. Recombinant proteins and monoclonal antibodies, generated using molecular biology knowledges and tools, have greatly enriched the therapeutic armamentarium. Moreover, the combination of genome science with the computational power of bioinformatics, are facilitating the dissection of the genetic basis of multifactorial diseases and the identification of the most suitable druggable sites for future medicines.<sup>2-4</sup>*

*At the same time, synthetic chemistry is becoming progressively structure based, using physical organic, crystallographic techniques and computational chemistry.*

*Therefore, the drug discovery process includes an elaborated experimentation set that requires a multidisciplinary intervention and aims to identify the molecular driver of a specific disease, to deep the knowledge of its physio-pathological pathways, and to demonstrate that the pharmacological modulation of this target leads to a real clinical benefit in the considered pathologic state.<sup>5</sup>*

*The majority of targets currently selected for drug discovery are proteins (receptors and enzymes)<sup>6</sup> while the most common indications are antihypertensive,<sup>7, 8</sup> antineoplastic<sup>9,10</sup> and anti-inflammatory activities.<sup>10,11</sup>*

*This work is mainly focused on the synthesis of different classes of compounds expected to exhibit antitumor activity. To simplify the discussion, the thesis has been divided in two sections.*

*The first section is in turn subdivided in two chapters and concerns the synthesis of different compounds endowed with antitumor activity. More in detail, the first chapter describes the synthesis of hybrid molecules, whose molecular skeleton was built by a combination of small units, for which anticancer activity has been proven. These combinations provide hybrid entities, also defined chimeric structures, ideally equipped with a dual mechanism of action.<sup>12</sup> Since the hybrids retain the pharmacophoric features of each element it is possible to observe synergistic effects on the targeted bio-molecules. As illustrated in the chapter, the hybrid approach offers a potential tool to overcome the most common problems related to conventional cancer therapy. Therefore, using as*

starting point the encouraging data reported in the literature for isatin-thiazolinone- and pyrazoline based hybrids,<sup>13</sup> several compounds were synthesized and some of them were submitted to biological assays. The tested compounds show a good activity toward different solid tumors. Even though the mechanism of action of synthesized compounds has not been established yet, the obtained data validate the hybrid pharmacophore approach as a useful means to amplify the activity of individual building blocks.

The second chapter illustrates the rational design and the subsequent synthesis of psoralene derivatives thought as DNA G-quadruplex stabilizers. G-quadruplexes are four-stranded DNA and RNA structures found in specific and crucial portion of nucleic acids, such as telomeric ends, promoter region of several oncogenes such as MYC, KIT and KRAS. In addition, RNA G-quadruplexes has been found in 5'-untranslated region (UTR) of the small GTPase NRAS.<sup>14</sup> Considering the role played by these elements in cancer development is clear that the selective recognition and stabilization of quadruplexes instead of duplex DNA could provide a powerful and selective anticancer strategy.<sup>15, 16</sup>

The second section is focused on the synthesis of 1-alkyl-8-(piperazine-1-sulphonyl)phenyl xanthines as selective antagonists of adenosine A<sub>2B</sub> receptors. Because of their low affinity, the adenosine is produced locally at high concentrations to interact with A<sub>2B</sub> receptors. Often this process is associated with ischemic events, during which the activation of these receptors promotes angiogenesis to compensate for the lack of oxygen. It is well established that solid tumors are hypoxic tissues and that their development and metastatic spread are strictly dependent on angiogenesis processes.<sup>17</sup> Even if the antagonists of A<sub>2B</sub> receptors exert antitumor activity, the high therapeutic potential of these pharmacological agents in numerous pathological states such as asthma, diabetes, diabetic retinopathy, and inflammatory pain,<sup>18, 19</sup> requires a broader and more general discussion on the pharmacology, distribution and structural features of synthesized antagonists. In fact, considering the ubiquitous distribution of adenosine receptors and, consequently the large variety of biological effects related to their activation, high selectivity is mandatory to prevent the side effect related to the generalized functional antagonism of all adenosine receptor subtypes.<sup>20</sup>

## REFERENCES

1. Erhardt, P. W. Medicinal Chemistry in the New Millennium: A Glance into the Future. In *Drug Discovery and Development*; John Wiley & Sons, Inc.: 2006, pp 17-102.
2. Manning, A. M. Target Identification and Validation. In *Drug Discovery*; John Wiley & Sons, Inc.: 2013, pp 43-65.
3. Ortega, S. S.; Cara, L. C.; Salvador, M. K., In silico pharmacology for a multidisciplinary drug discovery process. *Drug Metabol. Drug Interact.* **2012**, 27, 199-207.
4. Jacoby, E.; Schuffenhauer, A.; Azzaoui, K.; Popov, M.; Dressler, S.; Glick, M.; Jenkins, J.; Davies, J.; Roggo, S. Small molecules for chemogenomics-based drug discovery. 2006; Imperial College Press: 2006; pp 1-38.
5. Hughes, J. P.; Rees, S.; Kalindjian, S. B.; Philpott, K. L., Principles of early drug discovery. *Br. J. Pharmacol.* **2011**, 162, 1239-1249.
6. Imming, P.; Sinning, C.; Meyer, A., Drugs, their targets and the nature and number of drug targets. *Nat. Rev. Drug Discov.* **2006**, 5, 821-834.
7. Inoue, R.; Mori, Y., New target molecules in the drug control of blood pressure and circulation. *Curr. Drug Targets: Cardiovasc. & Haematol. Disord.* **2003**, 3, 59-72.
8. Carpino, P. A.; Flynn, D., Review of companies and drug classes in the 2007-2011 antihypertensive patent literature. *Pharm. Pat. Anal.* **2012**, 1, 45-64.
9. Chandra, A.; Soni, R. K.; Sharma, U.; Jain, S. K.; Yadav, P., A review updated on chemotherapeutics. *J. Drug Delivery Ther.* **2013**, 3, 192-197.
10. Lu, D.-Y.; Lu, T.-R.; Wu, H.-Y., Combination chemical agents with biological means in cancer therapy. *Res. Rev. BioSci.* **2013**, 7, 153-155.
11. Koc, E.; Kucukguzel, S. G., Medicinal chemistry and anti-inflammatory activity of nitric oxide-releasing NSAID drugs. *Mini-Rev. Med. Chem.* **2009**, 9, 611-619.
12. Meunier, B., Hybrid molecules with a dual mode of action: dream or reality? *Acc. Chem. Res.* **2008**, 41, 69-77.
13. Havrylyuk, D.; Zimenkovsky, B.; Vasylenko, O.; Gzella, A.; Lesyk, R., Synthesis of new 4-thiazolidinone-, pyrazoline-, and isatin-based conjugates with promising antitumor activity. *J. Med. Chem.* **2012**, 55, 8630-41.



14. Balasubramanian, S.; Hurley, L. H.; Neidle, S., Targeting G-quadruplexes in gene promoters: a novel anticancer strategy? *Nat. Rev. Drug Discov.* **2011**, *10*, 261-275.
15. Ou, T. M.; Lu, Y. J.; Tan, J. H.; Huang, Z. S.; Wong, K. Y.; Gu, L. Q., G-quadruplexes: targets in anticancer drug design. *ChemMedChem* **2008**, *3*, 690-713.
16. Brazda, V.; Haronikova, L.; Liao, J. C.; Fojta, M., DNA and RNA quadruplex-binding proteins. *Int. J. Mol. Sci.* **2014**, *15*, 17493-517.
17. Morello, S.; Miele, L., Targeting the adenosine A2b receptor in the tumor microenvironment overcomes local immunosuppression by myeloid-derived suppressor cells. *Oncoimmunology* **2014**, *3*, e27989.
18. Zablocki, J.; Elzein, E.; Kalla, R., A2B adenosine receptor antagonists and their potential indications. *Expert Opin. Ther. Pat.* **2006**, *16*, 1347-1357.
19. Ortore, G.; Martinelli, A., A2B receptor ligands: past, present and future trends. *Curr. Top. Med. Chem.* **2010**, *10*, 923-40.
20. Baraldi, P. G.; Tabrizi, M. A.; Fruttarolo, F.; Romagnoli, R.; Preti, D., Recent improvements in the development of A(2B) adenosine receptor agonists. *Purinergic Signalling* **2008**, *4*, 287-303.

## SECTION I ANTITUMOR AGENTS

### STATE OF THE ART OF CANCER TREATMENT AND MANAGEMENT

Cancer represents a collection of different genetic diseases associable each other by specific and redundant hallmarks. Cancer pathogenesis is a progressive, multistep and mutagenic process during which the cells acquire some typical properties including unlimited proliferation potential, self-sufficiency in growth signals, resistance to anti-proliferative and apoptotic signals, angiogenesis promotion and capability to escape immune system detection and to metastasize distal organs *Errore. L'origine riferimento non è stata trovata.*. The acquisition of this phenotypic set of features is supported by surrounding stromal cells, so that tumor microenvironment support can be included in the list of cancer hallmarks.<sup>1</sup>

Many of these phenotypic traits are brought by genetic alterations that involve the gain of function of key oncogenes as a result of mutation, amplification and over-expression events, generally associated with a simultaneous loss of functions of tumor-suppressor genes due to mutation, deletion end/or epigenetic silencing.<sup>1,2</sup>

This genetic instability allows the reactivation or modification of existing molecular programs normally used during the development or maintenance of tissue homeostasis. Therefore, tumorigenesis evolves through random mutations and epigenetic changes that alter these pathways, followed by a clonal selection of cells that can survive and proliferate under conditions that would normally be deleterious.<sup>2</sup>

The complexity of alterations in cancer presents an enormous challenge in anticancer therapeutic discovery and development. Although tumorigenesis derives from well-established phenomena, cancer is a set of different syndromes showing tissue and organ specificity, which contributes to further complicate the scenario related to a multifactorial disease with a series of implications in the anti-neoplastic agents development, cancer treatment and management.

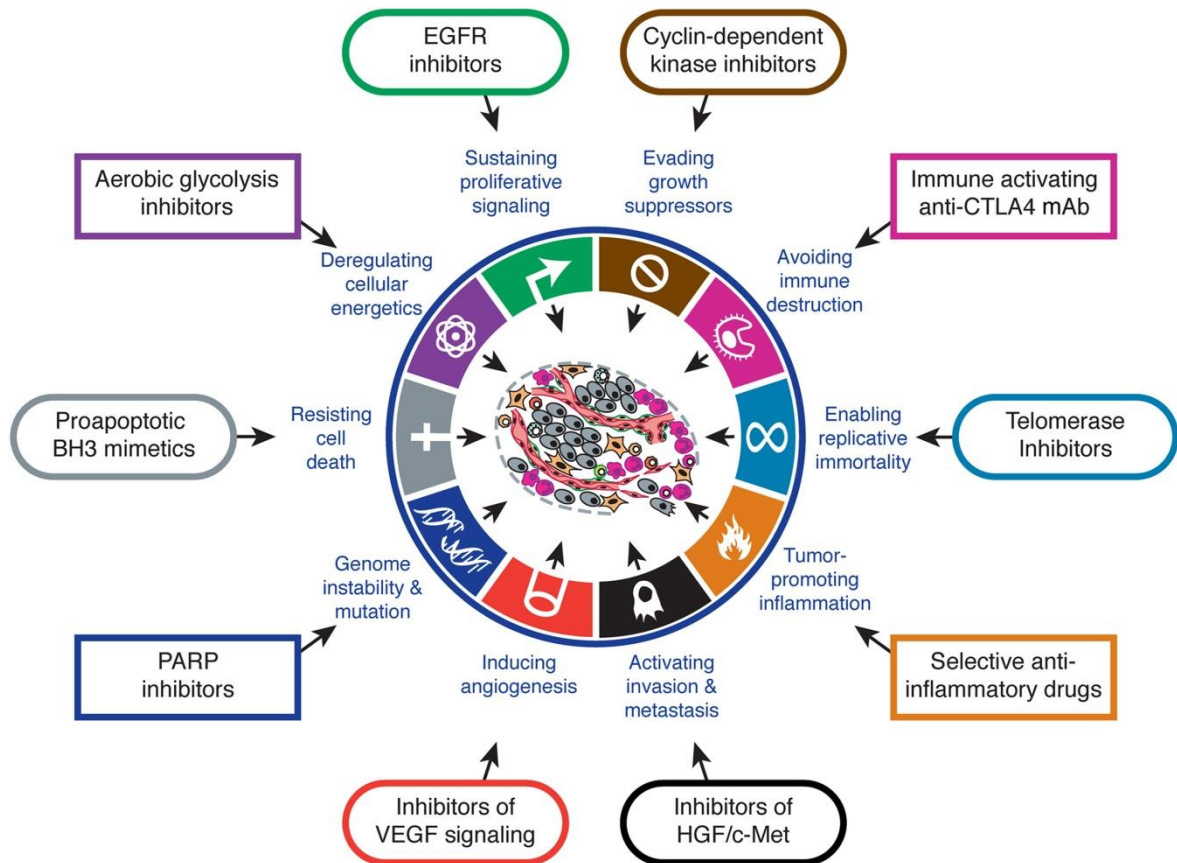


**Figure 1.** Therapeutic Targeting of the Hallmarks of Cancer.<sup>1</sup>

Conventional anticancer discovery has been focused for a long time on cytotoxic or cytostatic agents able to exert their activity on tumor cell lines and tumor regression in murine models (Table 1, Figure 2). These agents were discovered mainly by serendipity or inhibiting metabolic pathways critical for cell division.<sup>3</sup>

**Table 1.** Examples of antineoplastic drugs.

<b>Alkylating agents</b>	<b>Antimetabolites</b>	<b>Topoisomerase inhibitors</b>	<b>Miscellaneous</b>
busulfan	cytarabine	dactinomycin	arsenic trioxide
carmustine	clofarabine	daunomycin	asparaginase
cyclophosphamide	fludarabine	doxorubicin	bleomycin
dacarbazine	gemcitabine	etoposide	dexamethasone
ifosfamide	mercaptopurine	idarubicin	hydroxyurea
lomustine	methotrexate	irinotecan	mitotane
mechlorethamine	nelarabine	mitoxantrone	
melphalan	thioguanine	teniposide	
procarbazine	Tubulin binders	topotecan	
temozolomide	docetaxel	<b>Hormonal drugs</b>	
thiotepa	paclitaxel	Prednisone	
Cisplatin	vinblastine	fosfestrol	
Carboplatin	vincristine	tamoxifen	
Oxaliplatin	vinorelbine	letrozole	

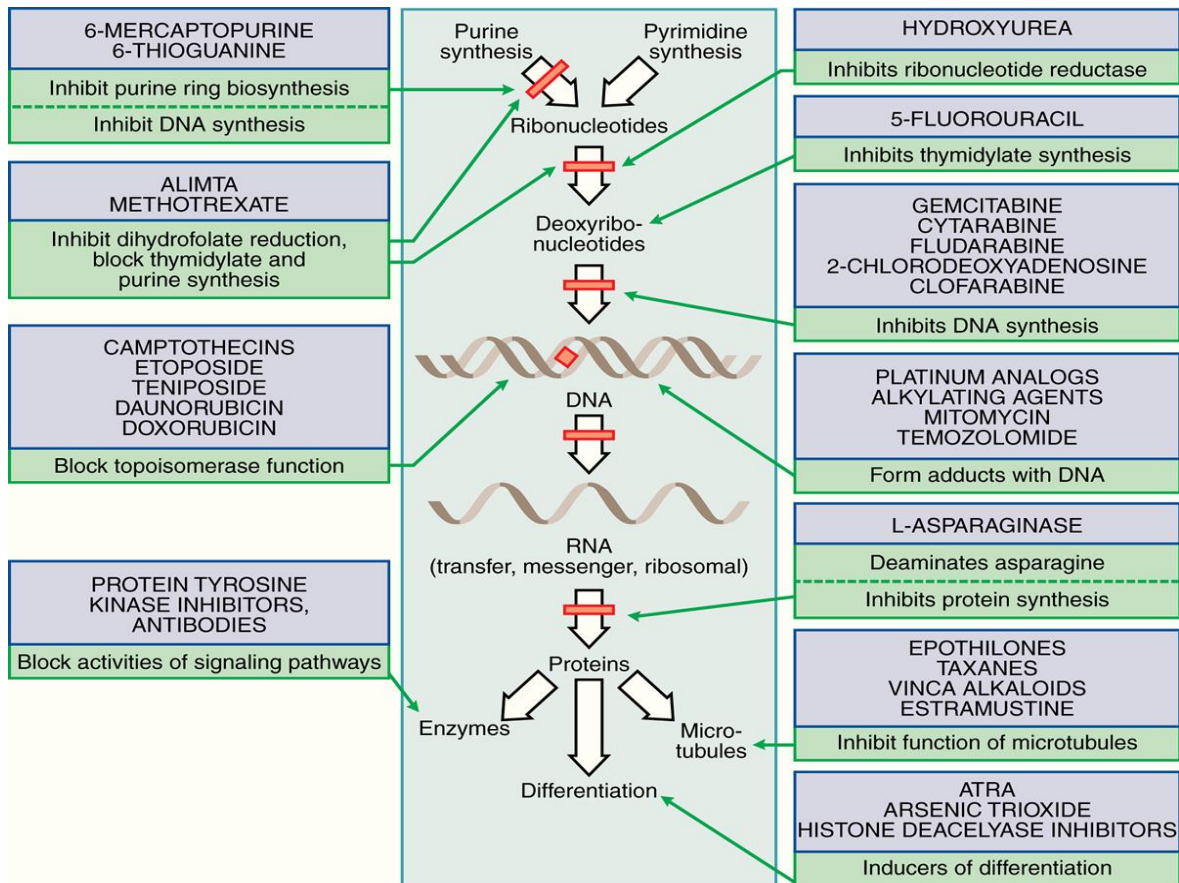


**Figure 2.** Chemotherapy: mechanisms of action of anticancer drugs.

Even if these strategies provided numerous anticancer agents used in oncology so far, their low therapeutic index and the development of molecular biology technologies, associated with a deeper and deeper understanding of etiopathology of cancer at a molecular level, oriented the anticancer research toward a target-based approach.<sup>4</sup> The paradigm of this new concept of anticancer drug discovery is the rational design of molecules created to interact or modify a specific molecular target, expressed on the tumor cells or on their microenvironment, playing a key role in tumor growth, survival and progression. Several target-based compounds have emerged over the last years and some of them have been approved for the clinical use. Examples of target-based compounds are Imatinib mesylate (Tyrosine Protein Kinase Inhibitor), Gefitinib (Epidermal growth factor (EGF) receptor inhibitor), Bortezomib (Proteasome Inhibitor), Trastuzumab (an monoclonal antibody that binds human epidermal growth factor receptor 2 (HER2)).<sup>4, 5</sup>

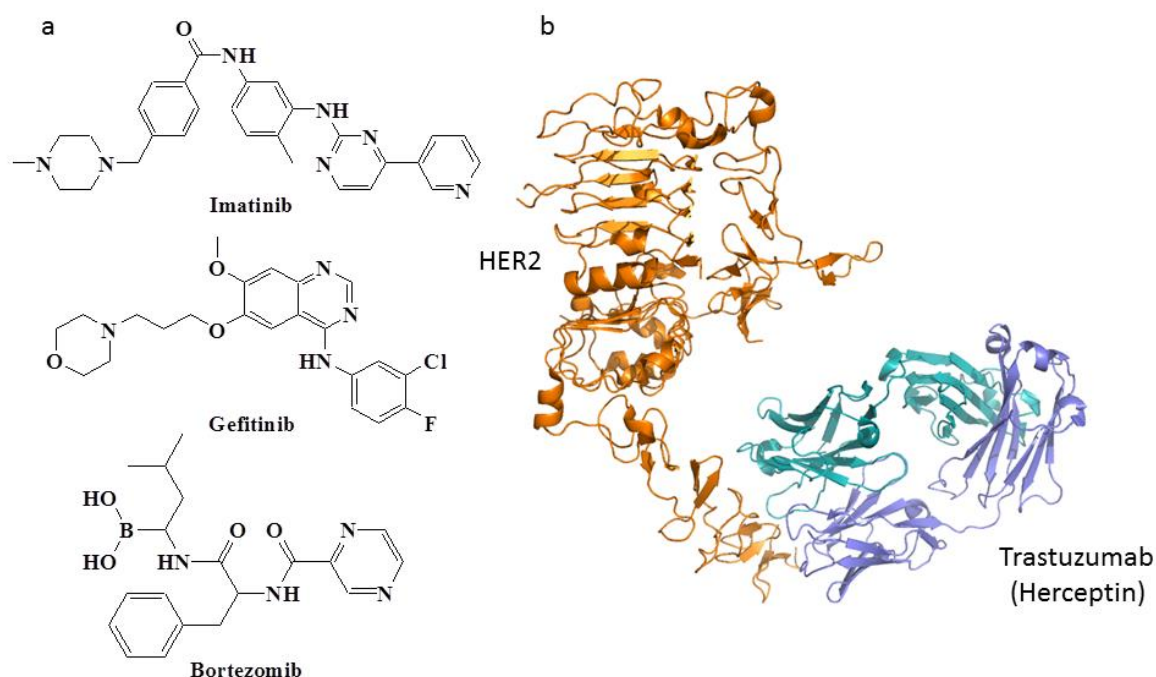


**Figure 3.** Target based compounds: a) small molecules; b) Trastuzumab (trade name Herceptin), a monoclonal antibody that interferes with the HER2 receptor extracellular region.<sup>6</sup>

New anticancer agents are categorized in different classes based upon their origin, chemistry, bioactivity profile, and mechanism of action.

Targeted therapies comprise monoclonal antibodies and small molecules inhibitors, routinely used in the therapy for several common malignancies, including breast, colorectal, lung and pancreatic cancers as well as lymphoma, leukemia, and multiple myeloma.<sup>5, 7-10</sup> Targeted therapies are, in most of cases, better tolerated than conventional chemotherapy. However, also these new generation drugs cause severe toxic effects, such as hypertension, cardiac dysfunctions, thrombosis, acneiform rash and proteinuria. In addition, some small molecules inhibitors are metabolized by P450 enzymes thus, multiple drug-drug interactions are possible.<sup>11, 12</sup>

The clinical use of these compounds is usually proposed in combination with the conventional therapy based on cytotoxic and hormonal agents.

The high number of antitumor drugs currently available enables thousands of possible combinations. Drugs used in combination possess, ideally, a set of *a priori* defined characteristics, such as different mechanisms of action, different spectrum of cell kill, different toxicity profile, and different profiles of resistance. Synergistic or additive cell kill effects, without increasing of toxicity, is a frequent goal of drug combination. Generally, combinations of drugs showing additive therapeutic effects are given at full doses to increase the percent of cell kill, reduce the number of chemotherapy cycles, avoid the onset of drug resistance, and improve clinical outcome and patient survival possibilities.<sup>13-15</sup> Classical cytotoxic drugs are commonly dosed in short-duration high-

dose cycles rather than a continuous low-dose administration. The short-duration high-dose administration is related with both short-term side effects, which disappear at the end of therapy, and long-term side effects.

Severe short-term side effects related to classical cytotoxic therapy have a deep impact on the design of drug combinations on the bases of their toxicity profiles. As abovementioned, these agents are dosed to the highest tolerated level to achieve the maximum therapeutic effect. Thus, toxic effects are often caused by an extension and exacerbation of therapeutic effects even on non-cancerous cells, reflecting the mechanism of action based on the killing of rapidly-growing normal cells (hair follicle, gastrointestinal surface epithelia, and stem cells).

The late-onset of side effects can be associated with any kind of cancer treatment and, generally, shows organ specificity on the basis of cancer therapy. For example, chemotherapy to the chest can cause heart or lung problems, including congestive heart failure (CHF), coronary artery disease, arrhythmia and difficult breathing. The use of Doxorubicin, Trastuzumab, Daunorubicin, Epirubicin and Cyclophosphamide has been associated with higher probabilities to induce heart diseases in cancer survivors.<sup>11, 13</sup> Recently, the introduction of novel target-based anticancer agents has allowed changes in the regimens to include continuous low-dosages administration of targeted drugs. This approach has proven to be successful in the antiangiogenic-based treatment and has been named low-dose metronomic (LDM) chemotherapy.<sup>4</sup>

In addition to cytotoxic and molecularly targeted anticancer agents, drugs acting through several indirect mechanisms are used in cancer management. All these agents are aimed at improving the quality of life of cancer patients, increase the compliance, and reduce the hospitalization due to side effects. These include chemo-protective agents, multidrug resistance reversing agents, analgesic, anti-emetics, and bone marrow growth factors.<sup>16, 17</sup> Many of these agents are available through a wide variety of drug delivery options including immediate and sustained release formulation, transdermal products and depot formulation.<sup>18</sup>

Despite continuing advances in the treatment of neoplastic diseases and the advent of new molecular target therapy that changed the prognosis for different malignancies, the standard cytotoxic therapy continues to be the first choice in the treatment of many cancer types.

In addition to prolong survival in patients with certain cancers, targeted therapies provide treatment options for some patients who may not otherwise be candidates for anticancer therapy. For instance, non-small cell lung cancer and non-Hodgkin's lymphoma primarily affect elderly patients, many of whom have medical comorbidities that limit the use of standard chemotherapy. Targeted therapies are often less toxic and better tolerated than the traditional ones, offering these patients additional treatment opportunities.<sup>13</sup>

Although the targeted therapy is conceived as a rational approach able to compensate for the lack of selectivity of the traditional chemotherapy, it presents a series of limitations. Firstly, the onset of drug resistance, inherently related to the high genetic variability of tumors is not a solved problem.

In addition, the target specificity does not eliminate the short and long term side effects. Therefore, exploiting and rationalizing all the information coming from the related disciplines, the goal of medicinal chemistry is to design and synthesize new drugs which, either as single entities or in combination, can improve selectivity, reduce toxicity, prevent the onset of drug resistance and promote the patient adherence to the treatment regimens, by developing oral or easily administrating formulations.



## REFERENCES

1. Hanahan, D.; Weinberg, R. A., Hallmarks of cancer: the next generation. *Cell* **2011**, 144, 646-74.
2. Luo, J.; Solimini, N. L.; Elledge, S. J., Principles of cancer therapy: oncogene and non-oncogene addiction. *Cell* **2009**, 136, 823-37.
3. Cancer Chemotherapy In *Basic & Clinical Pharmacology*, B. G. Katzung, S. B. M., A. J. Trevor, Ed.
4. Narang, A. S.; Desai, D. S. Anticancer drug development unique aspects of pharmaceutical development. 2009; Springer: 2009; pp 49-92.
5. Ambhaikar, N. B. Cancer Drugs. In *Drug Discovery*; John Wiley & Sons, Inc.: 2013, pp 287-336.
6. Cho, H.-S.; Mason, K.; Ramyar, K. X.; Stanley, A. M.; Gabelli, S. B.; Denney, D. W.; Leahy, D. J., Structure of the extracellular region of HER2 alone and in complex with the Herceptin Fab. *Nature* **2003**, 421, 756-760.
7. Larsen, J. E.; Cascone, T.; Gerber, D. E.; Heymach, J. V.; Minna, J. D., Targeted Therapies for Lung Cancer: Clinical Experience and Novel Agents. *Cancer J.* **2011**, 17, 512-527.
8. Downing, J. R., Targeted therapy in leukemia. *Mod. Pathol.* **2008**, 21 Suppl 2, S2-7.
9. El Zouhairi, M.; Charabaty, A.; Pishvaian, M. J., Molecularly Targeted Therapy for Metastatic Colon Cancer: Proven Treatments and Promising New Agents. *Gastrointestinal Cancer Research : GCR* **2011**, 4, 15-21.
10. Johnston, P. B.; Yuan, R.; Cavalli, F.; Witzig, T. E., Targeted therapy in lymphoma. *J. Hematol. Oncol.* **2010**, 3, 1-10.
11. Cross, S. S., The molecular pathology of new anti-cancer agents. *Current Diagnostic Pathology* **2005**, 11, 329-339.
12. Chen, E. X.; Siu, L. L., Development of molecular targeted anticancer agents: successes, failures and future directions. *Curr. Pharm. Des.* **2005**, 11, 265-72.
13. Gerber, D. E., Targeted therapies: a new generation of cancer treatments. *Am. Fam. Physician* **2008**, 77, 311-9.

14. Conlin, A. K.; Seidman, A. D., Beyond cytotoxic chemotherapy for the first-line treatment of HER2-negative, hormone-insensitive metastatic breast cancer: current status and future opportunities. *Clin. Breast Cancer* **2008**, *8*, 215-23.
15. Retter, A. S.; Figg, W. D.; Dahut, W. L., The combination of antiangiogenic and cytotoxic agents in the treatment of prostate cancer. *Clin Prostate Cancer* **2003**, *2*, 153-9.
16. Morjani, H.; Madoulet, C., Immunosuppressors as multidrug resistance reversal agents. *Methods Mol. Biol.* **2010**, *596*, 433-46.
17. Rayburn, E. R.; Ezell, S. J.; Zhang, R., Anti-Inflammatory Agents for Cancer Therapy. *Molecular and cellular pharmacology* **2009**, *1*, 29-43.
18. Skaer, T. L., Transdermal opioids for cancer pain. *Health Qual. Life Outcomes* **2006**, *4*, 24-24.

# 1 SYNTHESIS OF SUBSTITUTED ISATIN, THIAZOLIDINONE AND ARYL-PYRAZOLINE BASED HYBRIDS AS ANTICANCER AGENTS

## 1.1 INTRODUCTION

Over the years, the design of chemotherapeutics has become increasingly sophisticated. Despite this, to date there is not cancer treatment that is totally effective against disseminated cancer.<sup>1</sup> Genomic complexity and genetic heterogeneity are the main responsible for the limited and transient response of the majority of solid tumors to selective one-target therapy. This heterogeneity and, in particular, the possibility of having genetically distinct cell subpopulations, results both in the impossibility to adopt mono-drug regimens and in a dynamic and unpredictable response to the conventional pharmacological treatment *Errore. L'origine riferimento non è stata trovata.*<sup>2</sup> This feature has been recognized as a key factor in the drug resistance phenomena, even though the latter is due to a combination of genetic differences and alteration of cancer cells, and host factors.<sup>3</sup>

Currently, the most widespread strategy used by clinicians for the treatment of metastatic or irresponsive patients is based on the combination therapies. Often, these antineoplastic combinations are administrated following specific co-therapy protocols taking into account the activity and toxicity spectra, in order to amplify the therapeutic benefits and to minimize the overlapping of side effects at their optimal doses, and considering the known resistance mechanism of each component. In several cases, the individual components of combination are co-formulated as a single dosage form, making simpler the therapeutic regimens.<sup>3,4</sup> In both instances, these associations aim to obtain a multi-target action and, consequently, prevent the onset of drug resistance and delay the occurrence of relapse, showing more effectiveness over the long term. In the complex scenario of multi-factorial diseases, the combination of theoretical and empirical observations tends to emphasize the importance of multi-targeted therapies in the symptom management and disease remission, leading the search toward the concept "one molecule - multiple targets".<sup>1,3,4</sup>

The modulation of different targets simultaneously can be achieved either by cocktail drugs or by single chemical entities, containing two or more fragments, that could interact with different molecular targets of a multi-factorial disease. Obviously, these approaches are not mutually exclusive and, current data support the idea of a possible combination of multi-target agents with conventional chemotherapeutics. These combinations offer the possibility to achieve the block of different pathways in a vertical (different steps of a single pathway) or in horizontal (more than one pathway) mode.<sup>1,2</sup>

In this respect, the design of molecular hybrids, able to interact with different molecular targets, could have a series of considerable advantages, including the

possibility to improve the patient compliance, call off the probability of drug-drug interactions, overcome the serious side effects generally related to the combined therapy and facilitate clinical trial design. In addition, the use of these hybrids allows to solve the issues commonly related to the co-formulation, including chemical and physical incompatibilities that affect the pharmacokinetic of each drug, or technical problems, inherent to the production process itself.<sup>5</sup>

Therefore, molecular hybridization can be defined as a strategy of rational drug design based on the combination of two bioactive pharmacophoric units in a single molecule. Thus, through the suitable fusion of these sub-structures, it is possible to obtain a new highly active architecture that maintains or improves the activity and characteristics of the parent molecules.<sup>1</sup>

Hybrid drugs can be designed using “*post hoc*” or “*ad hoc*” approaches. In the “*post hoc*” method the hybrids are derived from well-known drugs, while in the “*ad hoc*” method conjugates are derived by leads affected by *in vivo* instability or by missing drug-like properties. In general, hybrid approaches could be exploited in the early phase of drug development to obtain the lead optimization, both in pharmacodynamics and pharmacokinetic profiles.<sup>3</sup> There are several options to combine the units constituting a molecular hybrid. More in detail, multi-target action can be achieved by linking two units by cleavable or non-cleavable spacers or by overlapping structural motifs derived from different drugs.<sup>3,6</sup> Until now, several examples of molecular hybrids have been reported for the cancer treatment.<sup>7-13</sup>

## 1.2 COMBINATION OF ISATIN-THIAZOLIDINONE-PYRAZOLINE MOIETIES

### 1.2.1 Background

As above mentioned, molecular hybridization techniques have been largely used to discover new promising scaffolds with a significant anticancer profile and several examples have been reported for microtubule inhibition. In this specific case, some well-known microtubule inhibitors such as taxol, vinca alkaloids, combretasatin and colchicine have been included in hybrid molecules, obtaining compounds that exhibit inhibitor activity at nanomolar level.<sup>1</sup>

Most in general, several heteroaryl based hybrids have been exploited as antitumor agents and, among these, isatin based hybrids have been the object of intense research due to the isatin moiety favorable features. In particular, the isatin is a privileged scaffold because it not only offers wide possibilities for chemical modifications but also exhibits a broad spectrum of biological properties. Among these properties, cytotoxic and antineoplastic activities have been related to its inhibition capability of several enzymes, such as tyrosine kinase, serine/threonine kinases (e.g. cyclin-dependent kinases, CDKs) and carbonic anhydrase isozymes.<sup>14, 15</sup> Therefore, the chemical plasticity and the ability of isatin to inhibit different enzymes make it one of the most exploited fragment to obtain new active multifunctional hybrids. For these reasons, several isatin based hybrids have been synthesized. The hybrids, belonging to this class, most frequently reported in the literature include conjugates of isatin with uracil, triazole, benzothiazole, pyrazolines, calchones and thiazolidinone moieties.<sup>1, 16-18</sup>

Based on the interesting data reported in literature<sup>18</sup> and on the activity displayed by single fragments, in this work the attention has been focused on isatin-thiazolinone-pyrazoline conjugates. In this structure the thiazolinone portion acts as essential linker between the pyrazoline and isatin moieties. Even if, from a formal point of view, the thiazolinone is a molecular bridge between the isatin and pyrazoline units, each element of the hybrid contributes to the anti-tumor activity. In fact, similarly to indolinone, pyrazolines and thiazolinones and their correlated heterocycles exhibit a variety of pharmacological activities, including antifungal, antidepressant, anti-epileptic, anti-inflammatory, antibacterial and antitumor activities.<sup>19</sup> In particular, with respect to these molecules, the anti-proliferative effect has been related to their ability to interfere with several molecular targets. Regarding the pyrazolines, the antitumor behavior has been related to the inhibition of cyclin-dependent kinase, heat shock proteins, vascular endothelium growth factor (VEGF), and P-glycoprotein,<sup>18</sup> while in the case of the thiazolinone, the activity has been associated with their affinity for the tumor necrosis factor (TNF), antiapoptotic complex Bcl-XL-BH3, JNK-stimulating phosphatase-1 (JNK-1) and non-membrane protein tyrosine phosphatase (SHP-2).<sup>18,20</sup> Thus, in principle, the association of the three nuclei provides to the molecule a potential, in terms of activity,

substantially higher than those associated to each single element or to the possible combinations of two of them.<sup>18</sup> Several data are reported in the literature about the SARs of these conjugates that contribute to validate the hybrid approach as a potential tool to obtain multifunctional compounds. More in detail, these data highlight that the antitumor activity is strictly dependent on the presence of the three heterocycles on the hybrid. It is important to point out that the distribution of the three moieties on the hybrid is not random and the role of the thiazolinone as a spacer is required to optimize the antitumor activity. The absence of this linker in the pyrazoline-indolinone hybrids leads to a decreased activity. Furthermore, it is possible to modulate the activity of these molecules on the base of the aryl substituents in position 3 and 5 of pyrazoline and the substituent in position 5 of indolinone. Finally, the best activity is generally related to compounds with unsubstituted nitrogen on the isatin portion.<sup>18</sup>

According to these assumptions, and using as starting point the most active compound reported in literature (Figure 1.1),<sup>18</sup> a high number of structural analogues of this reference compound have been synthesized.

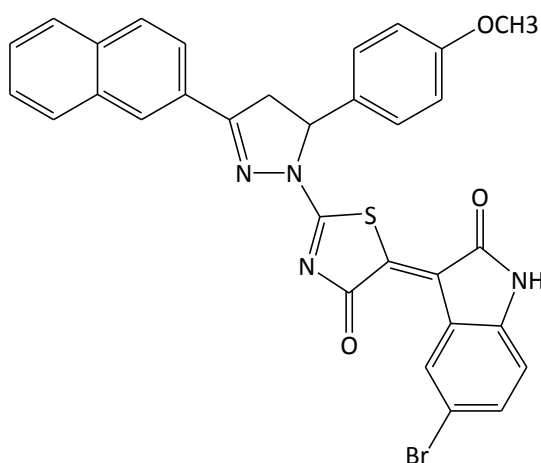


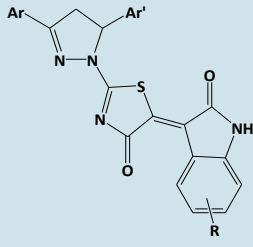
**Figure 1.1.** Most active compounds of previous reported series.<sup>18</sup>

More in detail, this work aims at assessing the contribution to the hybrid activity of different substituents, on the basis of their electronic and steric properties, on the isatin and pyrazoline moieties. To accomplish this goal and simplify the dissertation, these compounds have been grouped into five series (Table 1.1). In each series the molecular skeleton of the hybrid is basically unchanged. Therefore, all the structural modifications have been carried out to obtain:

1. Within each series, the variation of position and type of substituent in the indolinone moiety; these substitution patterns are recursively adopted in each one of the five series;
2. Among different series, the variation of the aryl substituent in position 3 or 5 of the pyrazoline.

In addition, in each series the indolinone moiety has been substituted with a 2-methoxy naphthyl group. The aim of this isosteric substitution was to extensively investigate the impact of the substituted indolinones on the activity. Therefore, the gradual change in the series-specific molecular portions will allow investigating how the steric and electronic features of the substituent affect the interaction between these compounds and their biological targets.

**Table 1.1.** Reference compound **EMAC4000** and new series of analogues compounds synthesized **EMAC4001-4075**.

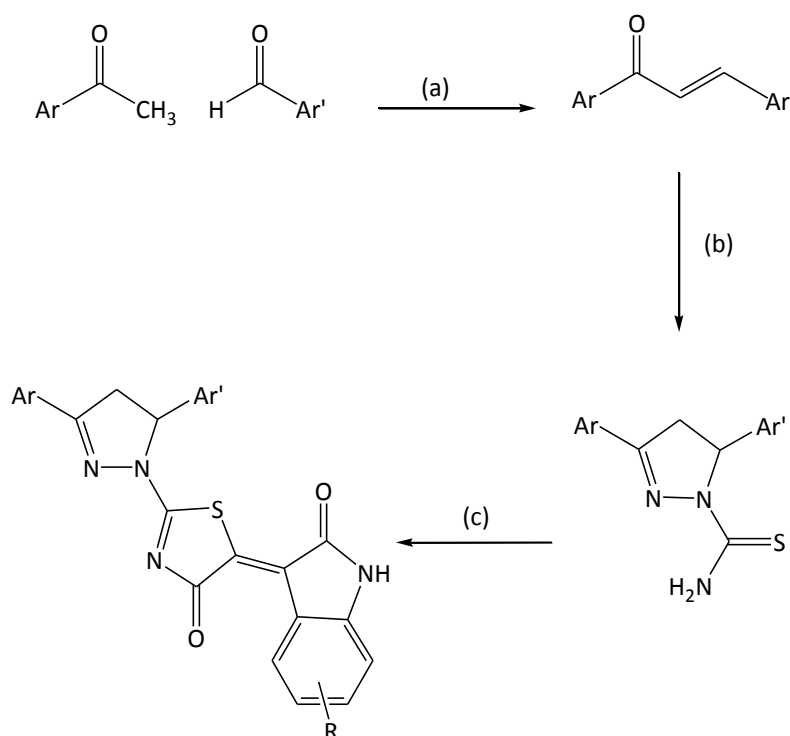
Compound	Series				
	<b>Series 1</b> (EMAC 4000-4009)	<b>Series 2</b> (EMAC 4011-4020)	<b>Series 3</b> (EMAC 4022-4031)	<b>Series 4</b> (EMAC 4033-4042)	<b>Series 5</b> (EMAC 4066-4075)
<b>Isatin group (R)</b>	<b>Ar</b> Naphtalen-2-yl  <b>Ar'</b> 4-methoxy-phenyl	<b>Ar</b> Thiophen-2-yl  <b>Ar'</b> 4-methoxy-phenyl	<b>Ar</b> Naphtalen-2-yl  <b>Ar'</b> 4-fluoro-phenyl	<b>Ar</b> 4-Acetyl biphenyl <b>Ar'</b> 4-methoxy-phenyl	<b>Ar</b> Naphtalen-2-yl  <b>Ar'</b> 4-chloro-phenyl
<b>7-bromo</b>	EMAC 4000	EMAC 4011	EMAC 4022	EMAC 4033	EMAC 4066
<b>5-chloro</b>	EMAC 4001	EMAC 4012	EMAC 4023	EMAC 4034	EMAC 4067
<b>4,7-dichloro</b>	---	---	EMAC 4024	---	---
<b>5,7-dimethyl</b>	EMAC 4003	EMAC 4014	EMAC 4025	---	EMAC 4069
<b>5-fluoro</b>	---	EMAC 4015	EMAC 4026	EMAC 4037	EMAC 4070
<b>7-fluoro</b>	EMAC 4005	EMAC 4016	EMAC 4027	EMAC 4038	EMAC 4071
<b>5-iodio</b>	EMAC 4006	EMAC 4017	---	EMAC 4039	EMAC 4072
<b>5-methoxy</b>	EMAC 4007	EMAC 4018	EMAC 4029	EMAC 4040	EMAC 4073
<b>5-methyl</b>	EMAC 4008	EMAC 4019	EMAC 4030	EMAC 4041	EMAC 4074
<b>5-trifluoromethyl</b>	EMAC 4009	EMAC 4020	EMAC 4031	EMAC 4042	EMAC 4075



### 1.2.2 Synthetic pathway

The synthesis of isatin-thiazolinone-pyrazoline derivatives followed the general method outlined in the **Errore. L'origine riferimento non è stata trovata.** The final compounds have been synthesized via one-pot methodology reacting the 3,5-diaryl-1-thiocarbamoyl-2-pyrazolines with ethyl bromoacetate and the appropriate isatin in the presence of anhydrous sodium acetate, refluxing in glacial acetic acid.<sup>18</sup> More in detail, the synthetic route includes:

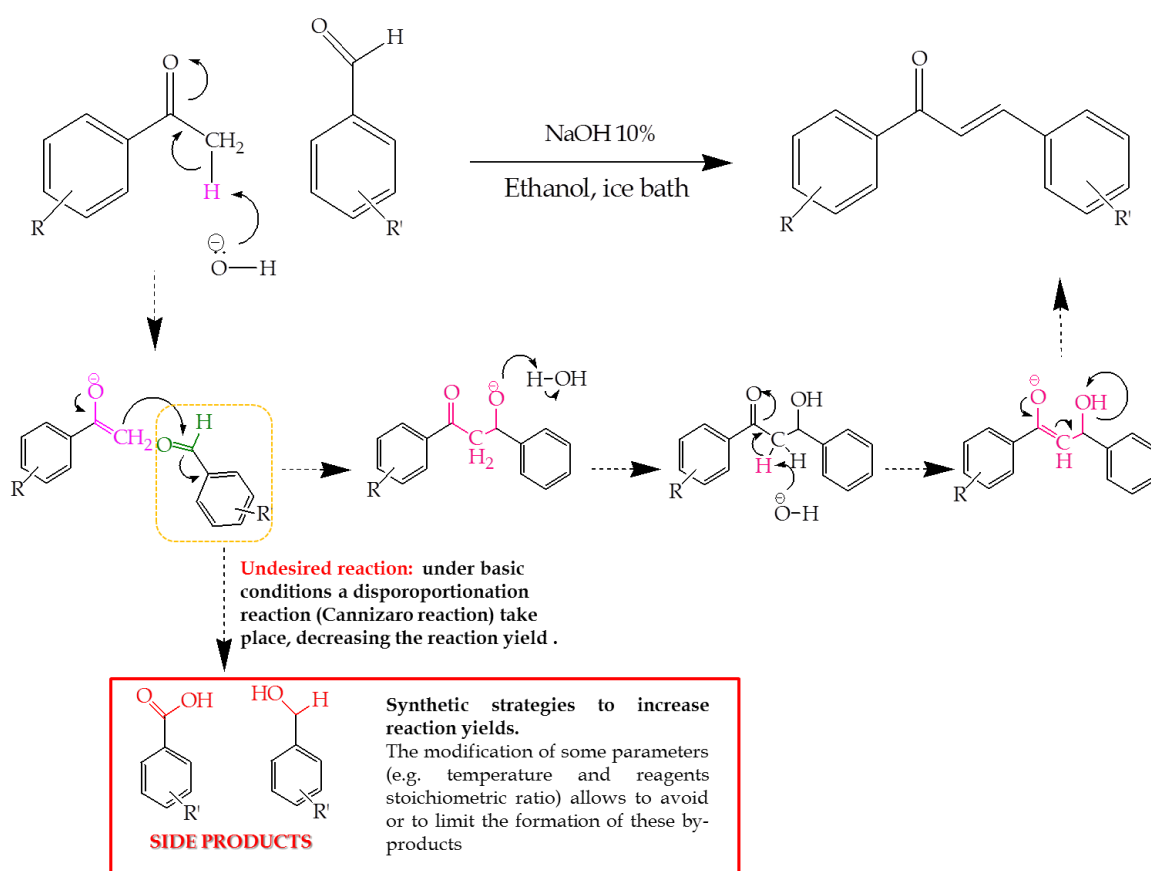
1. The synthesis of 3,5-disubstituted-thiocarbamoyl-2-pyrazolines;
2. The cyclization of 1,3-thiazol-4(5*H*)-one and the subsequent reaction of this neo-formed nucleus with a substituted isatin to obtain the final compounds.



**Scheme 1.1.** Synthetic procedure. Reagents and conditions: (a) NaOH 10%, EtOH, ice bath; (b) KOH 5%, thiosemicarbazide, reflux; ethyl bromo acetate, anhydrous sodium acetate, appropriate isatine, glacial acetic acid, reflux.<sup>18</sup>

The synthesis of 3,5-substituted-1-carbamoyl-2-pyrazolines has been in turn obtained performing two reactions (Scheme 1.1, a and b), including the synthesis of the 1,3-diaryl-2-propen-1-one, followed by the pyrazoline ring closure. The diaryl-2-propenones (chalcones) were synthesized via Claisen-Schmidt condensation, reacting substituted benzaldehydes with aryl methyl ketones in the presence of a strong base (sodium hydroxide 10%) as a catalyst. Usually, this reaction is carried out at room temperature, using equimolar amounts of reagents and an alkali aqueous solution with a

concentration ranging between 10 to 60%. Notably, under these conditions the non-enolizable aldehydes undergo to a disproportionation reaction, known as Cannizaro reaction, forming the correspondent carboxylic acid and alcohol, that strongly affects the reaction yield (Scheme 1.2). To avoid the formation of these by-products, the reaction has been performed keeping the temperature at 0°C and adding the aldehyde dropwise to a basic solution containing the ketone. Furthermore, the use of a slight excess of aldehyde allows to replace this reagent if it is implicate in the Cannizaro reaction. In this way a stable calchone has been obtained, which is reacted in the next step with thiosemicarbazide and potassium hydroxide 5% alcoholic solution, obtaining the expected pyrazoline.<sup>21</sup>



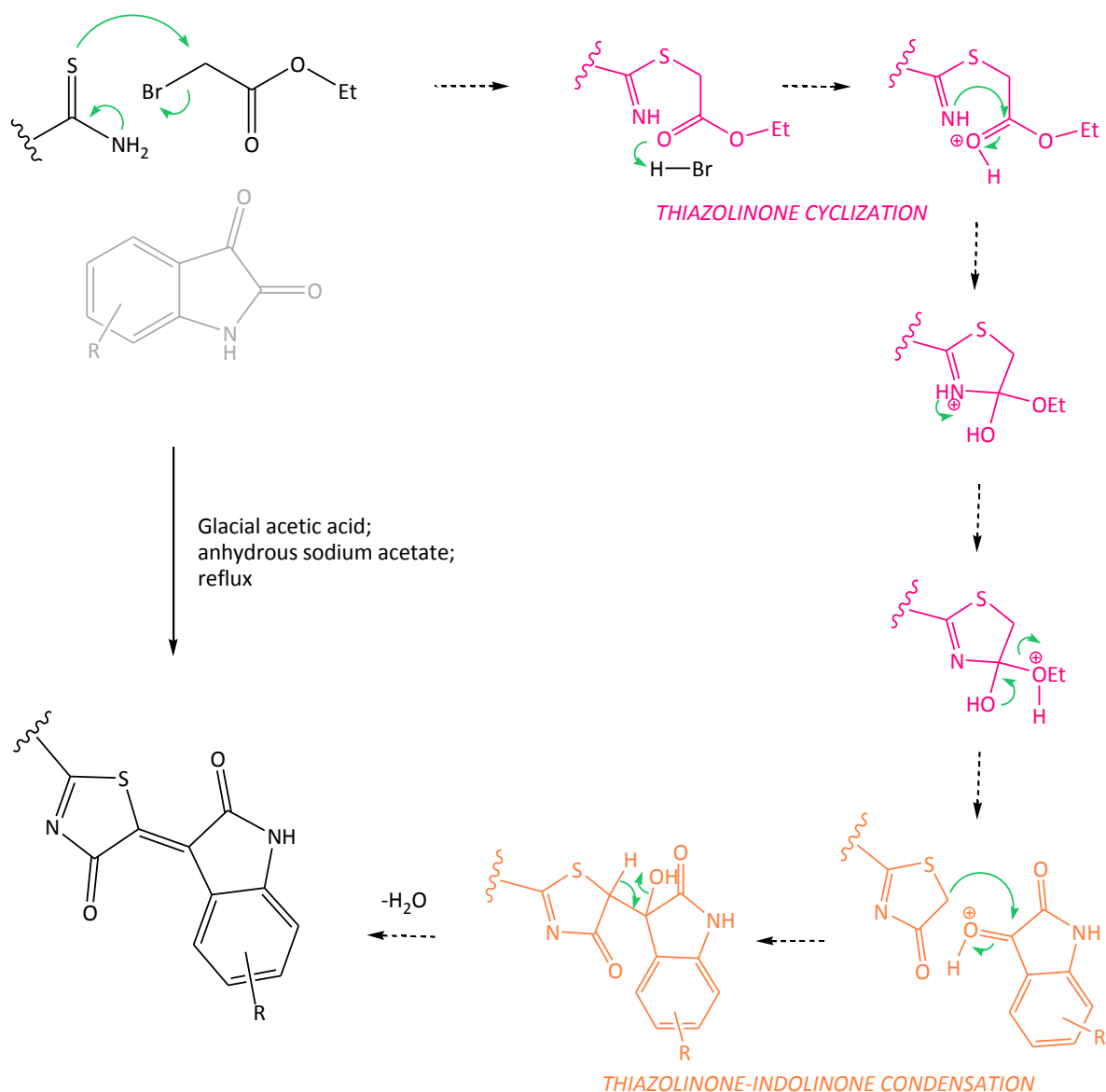
**Scheme 1.2.** Detailed mechanism of Claisen-Schmidt condensation to obtain 1,3-diaryl-2-propen-1-one.

The last step is a three-component (1-thiocarbamoyl-pyrazoline; ethyl bromo acetate, and isatin) one-pot reaction which provides the final compounds, combining two reactions in a unique step. It is worth noting that using this procedure is possible to achieve the formation of the final hybrids without the need of isolating the pyrazoline-thiazolinone intermediate for the condensation with the indolinone (Scheme 1.1, c). A more detailed description of this reaction mechanism is depicted in Scheme 1.3.

More in detail, the cyclization of the thiazolinone, based on Hantzsch's thiazole synthesis, involves the thiocarbamoyl group in position 1 of the pyrazoline and the ethyl bromoacetate. Differently from the synthetic procedure reported in the literature,<sup>18</sup> in which the cyclization is conducted using the chloro acetic acid, this reaction has been performed by using the ethyl bromoacetate. This change in the method can be justified as follows:

1. Esters are more reactive than the corresponding acids in the nucleophilic substitution reactions;
2. The use of an acid results in the formation of water, which interferes with the second part of the reaction.

In fact, the condensation reaction between the methylene at C-5 of the thiazolinone and the carbonyl group in position 3 of the indolinone involves a dehydration reaction. The presence of water in the reaction medium, originating from the previous cyclization, likely shifts the equilibrium to the left leading, presumably, to a reduction of yields. For the majority of the synthesized compounds, it has been observed that the use of the ester with respect to the acid, leads to higher yields. Under these operating conditions (pH weakly acid), the thiazolinone methylene in C-5 is able to react with the carbonyl at the C-3 of the indolinone, leading to the formation of the final product. The pH system is crucial for the success of the reaction and is kept around 5 by the acetic acid/sodium acetate buffer. In fact, this must be sufficiently acid to allow the protonation of the carbonyl oxygen, but not too acid in order to ensure the deprotonation of the thiazolinone methylene that leads to the formation of the nucleophilic centre in this position.



**Scheme 1.3.** Mechanism of the optimized one-pot reaction which provides the final compounds.

Notably, since the reaction of pyrazoline formation is not enantioselective, both enantiomers have been obtained. Therefore, each final compound exists as a couple of enantiomers.

The structure of each compound has been elucidated by <sup>1</sup>HNMR spectroscopy.

The 1,3-diaryl-2-propenones were detected by the typical olefinic proton signals, which appear as two doublets at  $\delta$  7.84-7.70 ppm with a coupling constant  $J$  equal to 15 Hz, typical of *E* isomers.

The 3,5-diaryl carbothioamide pyrazolines were detected by -CH<sub>2</sub> and -CH protons of the ring and, when detectable, by the -NH<sub>2</sub> signal of thiocarbamoyl group that appears as a broad singlet at  $\delta$  7.2-7.1 ppm. In fact, the group -CH<sub>2</sub>CH is part of a AMX system that gives raises to a characteristic set of three doublets of doublets. The AMX system is depicted in the Figure 1.2, where an enlargement of the NMR spectrum shows the

coupling effect on the pyrazoline system. The  $-CH_2$  resonates as a pair of doublets of doublets at  $\delta$  3.14-3.44 ppm ( $H_A$ ), 3.98-4.04 ppm ( $H_M$ ). The  $-CH$  proton appears as a doublet of doublets at  $\delta$  5.64-6.10 ( $H_X$ ) ppm due to vicinal coupling with two magnetically non-equivalent protons of the methylene group at position 4 of the pyrazoline ring ( $J_{AM}$  18.00 Hz,  $J_{AX}$  4 Hz,  $J_{MX}$  11 Hz).

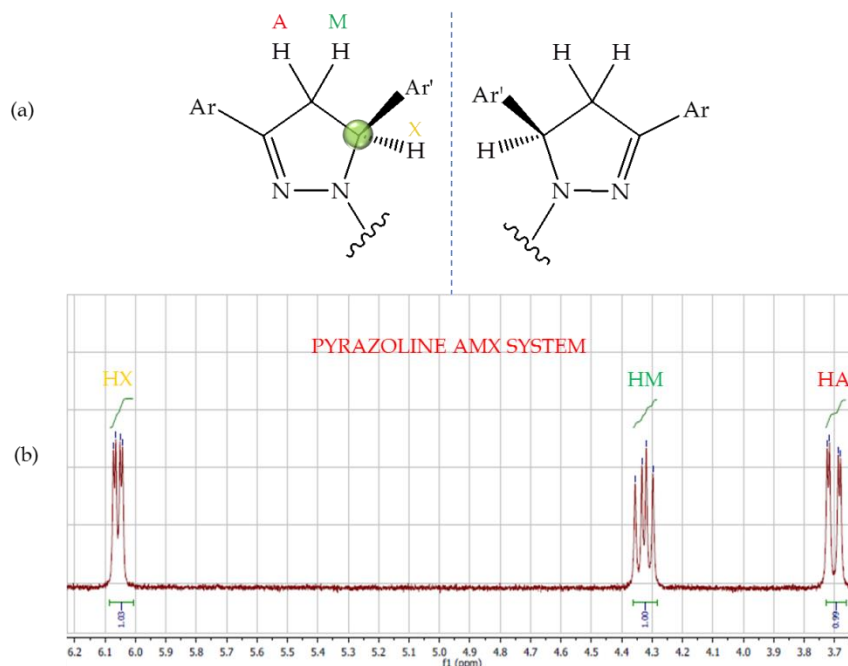


**Figure 1.2.** Coupling effect on the pyrazoline system.

The NMR spectra of final compound show the signals attributable to the protons of the indolinone residue. In each spectrum it is possible to observe a sharp singlet at  $\delta$ ~11 ppm related to the  $-NH$  group in the isatin moiety. Some spectra show two signals for the  $-NH$  group related to a prototropic equilibrium between the enolic and lactamic forms: the first one is detected at 11.92 ppm –e.g. for the compound EMAC 4072- and can be related to the enolic tautomer, while the second isomer is detected at ~11.29 ppm.

All the other aromatic and aliphatic protons, when present, were observed at expected regions.

Due to their poor solubility in the commonly used solvent, the purification process of the final compound is not easily attainable by re-crystallization or chromatographic column. Therefore, when possible the crude reaction products was washed with refluxing ethanol or methanol.

### 1.2.3 A promising pharmacophore hybrid approach

Compounds (Series 1, **EMAC4000-4009**) were submitted to NCI for the preliminary evaluation of their biological activity. Among these, only **EMAC4001** and **EMAC4007** have been selected and tested at both single and five concentration levels. Figure 1.3 shows the structures of both selected and reference compounds. Each compound of this series has the same scaffold of the reference compound. The new compounds only differ for the nature of the substituent in the isatin moiety. In particular, while the reference compound presents a bromine in the position C-5 of the indolinone portion,<sup>18</sup> **EMAC4001** and **EMAC4007** have a chlorine and a methoxy group, respectively. In this way it is possible to assess directly the effect of the isatin substitution pattern.

The biological assays have been performed using a panel of approximately 60 cancer cell lines. This panel includes nine different tumor types: leukemia, colon, lung, CNS, renal, melanoma, ovarian, breast and prostate. The protocols used for one-dose and five-dose assays are reported in the Experimental section 1.4.3.

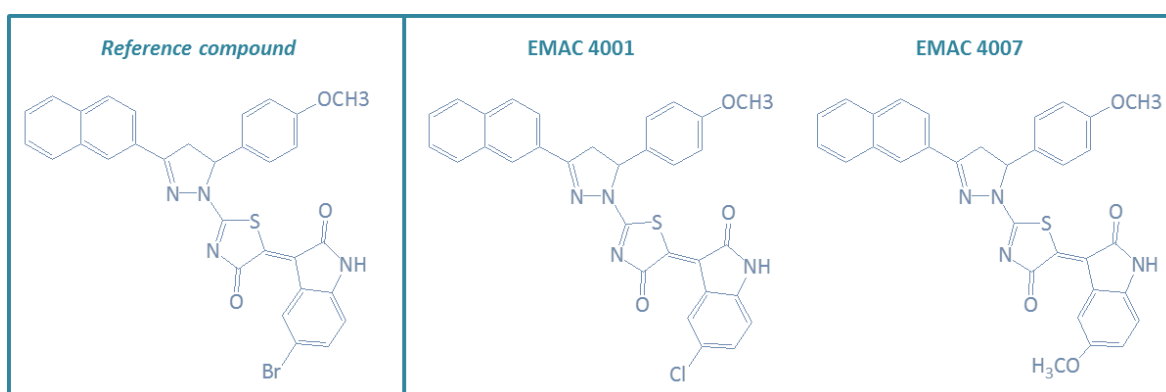


**Figure 1.3.** Compounds selected and tested by the NCI for antitumor activity.

Both **EMAC4001** and **EMAC4007** display a significant activity when tested in a single-dose assay. In this case the data are reported as a mean graph of the percent growth of cells, treated with 10  $\mu$ M concentration of analyzed compound. The growth value is compared to an untreated control and referred to a number of cells at time zero. This allows the detection of both growth inhibition and lethality: the growth inhibition percentage is reported in the left side of graph as positive values, while the lethality is reported in the right side of the graph as negative values. Figure 1.4 shows, as an example, the one-dose mean graph of **EMAC4001**.

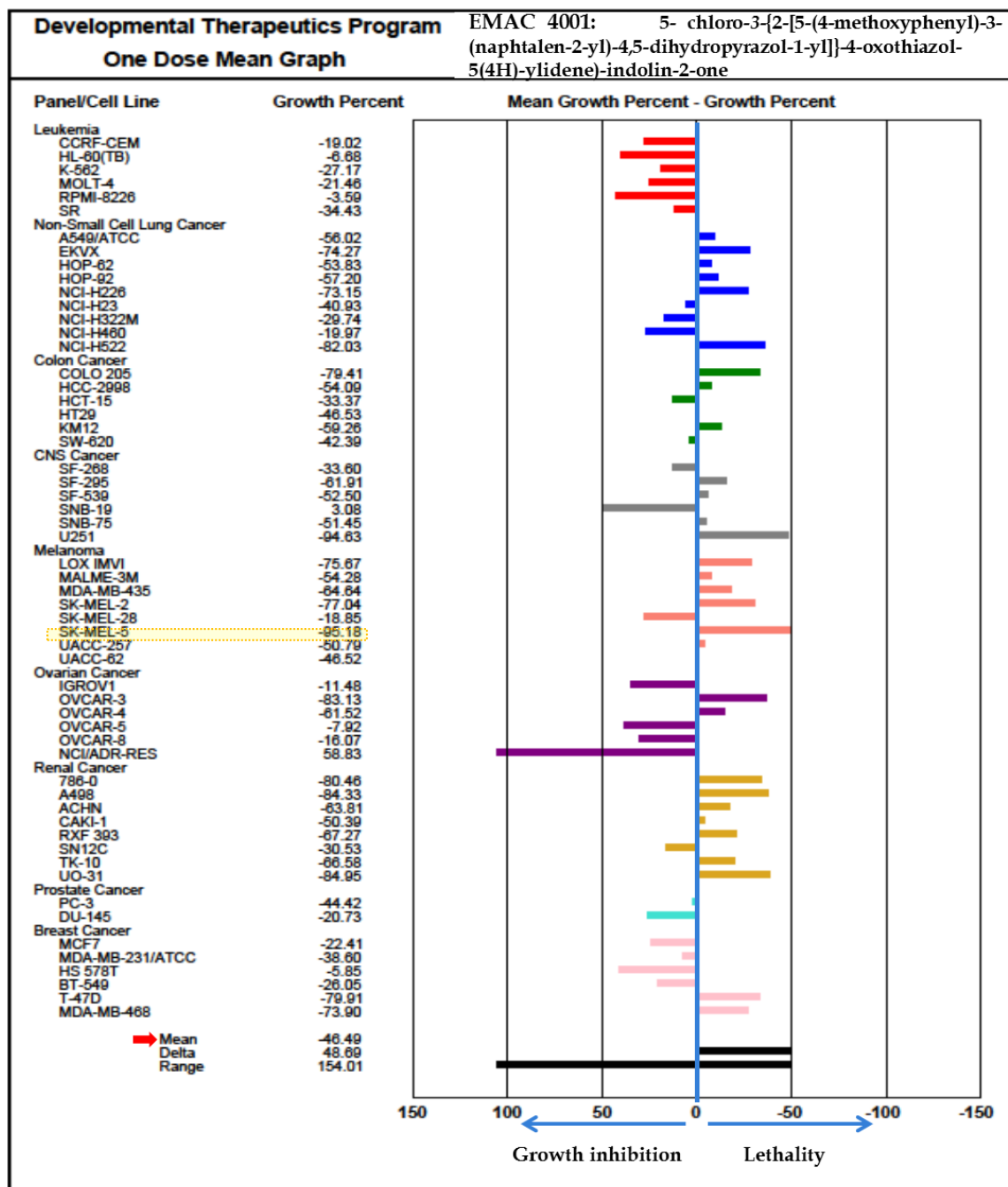


Figure 1.4. One dose results of EMAC4001.

In particular, the mean growth value, averaged over the different cancer subpopulation, is -46.49 and -45.87 for **EMAC4001** and **EMAC4007**, respectively. These compounds show a similar broad range of activities (154.01 **EMAC4001** and 150.30 **EMAC4007**) that highlight a not uniform activity toward the different cell lines. In both cases the most sensitive cancer subtype is SK-MEL-5, a melanoma cell-line, with values of -95.18 and -93.26 for **EMAC4001** and **EMAC4007**, respectively. In addition, significant results have been found also for other solid tumor subtypes. For example, **EMAC4001**

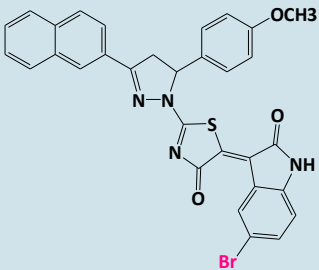
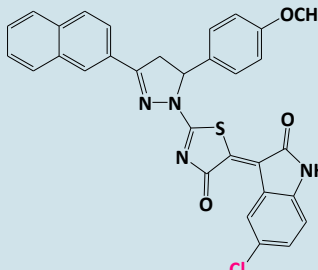
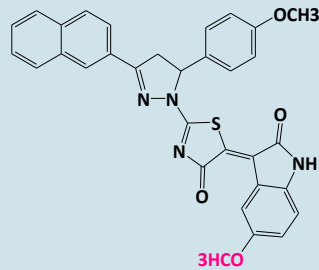
exhibits interesting growth percentage values for some renal cancer (786-0; A498; UO-31), ovarian cancer (OVCAR-3), CNS cancer (U251), Non-small Cell lung cancer (NCI-H522), for which these values range between -80.46 and -94.63. It is worth noting that both **EMAC4001** and **EMAC4007** have similar behavior, in terms of activity, with respect to the reference compound<sup>18</sup> but both of them show a worse mean growth percentage and, consequently, they result less active when considering the whole cell panel.

However, considering their good performance, these compounds have been selected, by the NCI, for a second screening, performed at ten-fold dilution of five concentrations. In this case the resulting activities are reported as dose-response curves in which three parameters can be found. More in detail, the Growth Inhibition,  $GI_{50}$ , is the molar concentration of the analyzed compound that inhibits the 50% of total growth; the Total Growth Inhibition, TGI, is the molar concentration leading the total inhibition and, finally, the Lethal Concentration,  $LC_{50}$ , is the molar concentration of tested compound able to determine a lethal effect on the 50% of cells. These values are tabulated for each cancer type and plotted in a dose-response graph. Furthermore, a mean graph midpoints, similar to the one-dose mean growth percent, is reported for each parameter.

The  $GI_{50}$ , TGI and  $LC_{50}$  mean value are reported in Table 1.2 and compared with the corresponding data of the reference compound.<sup>18</sup>



**Table 1.2.** Biological results obtained by the NCI screening.

Biological results	Reference compound	EMAC 4001	EMAC 4007
			
<b>One-dose mean graph:</b>			
Mean growth, % SK-MEL-5 (most sensitive cell-line)	-59.81 ----	-46.49 -95.18	-45.87 -93.26
<b>Five-dose mean graph:</b>			
GI <sub>50</sub> (μM)	0.071	0.028	0.071
TGI (μM)	0.76	0.11	0.53
LC <sub>50</sub> (μM)	19.76	0.46	8.1

The obtained data confirm that the substituent in position C-5 in the isatin portion is crucial for the hybrid activity and show that the variation of the substituent in this position has a strong impact on the potency of analysed compounds. As part of this triad of compounds, **EMAC4001** shows the best values for each parameter considered with a mean GI<sub>50</sub> equal to 0.028 μM, a mean TGI equal to 0.11 μM and mean LC<sub>50</sub> equal to 0.46 μM. Even though the potency of tested compounds increase in the order Cl>OCH<sub>3</sub>>Br, the data so far available are not sufficient to provide an adequate analysis on the features of the substituent in this position.

### 1.3 CONCLUSIONS

This work involves the synthesis of several derivatives whose scaffold has been built upon a hybrid pharmacophore model.<sup>18</sup> The synthetic method reported in literature has been optimized, obtaining the final compounds with quantitative yields.

All the Series 1 derivatives (**EMAC4000-4009**) have been submitted to the NCI, but among these only **EMAC4001** and **EMAC4007** have been selected for the biological screening. The preliminary data confirm that the synthesized compounds possess anti-proliferative activity toward the solid cancers and that the substitution pattern proposed for the indolinone portion enhances the potency of compounds with respect to the reference derivative *Errore. L'origine riferimento non è stata trovata.*<sup>18</sup>

However, further investigations are needed to elucidate the biological target/s of synthesized compounds and their mechanism of action. In particular, a more deep analysis of these data will enable to:

1. establish whether the employed approach may actually be validated as a method for the synthesis of molecular hybrids;
2. optimize the potency on the bases of computational and SARs studies.

Finally, since the adopted conditions for the pyrazoline synthesis are not enantioselective, each compound has been obtained as a couple of enantiomers (Figure 1.2). Considering the importance of enantiomers in the activity and toxicity of several drugs, the chiral separation and the subsequent analysis of biological data could provide an interesting way to obtain anticancer drugs with a larger therapeutic window.

### 1.4 EXPERIMENTAL SECTION

#### 1.4.1 Materials and methods

All the materials, reagents and solvents, where not specified, were purchased from commercial suppliers and used without any further purification.

Each reaction and purification method were monitored using Thin Layer Chromatography (TLC), using precoated Merk Silica gel 60 254F plates and petroleum ether/ethyl acetate as eluent, with different ratios for intermediates and final products.

Purification methods were performed by crystallization from ethanol (chalcones and pyrazolines) or by chromatographic columns, when possible, for final compounds. Chromatographic columns were performed using Silica gel 70-240 mesh.

Melting points (Mp) were measured using a Stuart Melting Point SMP30 apparatus and are uncorrected.

The <sup>1</sup>HNMR spectra of synthesized compounds were recorded on a Varian Unity 500MHz spectrometer in DMSO-d<sub>6</sub>, chloroform-d or aceton-d<sub>6</sub>, using tetramethylsilane

(TMS) as internal standard. Chemical shifts are reported in ppm, with the use of a  $\delta$  scale, coupling constants (J) in Hz.

Biological assays have been performed at the National Cancer Institute, according to well-known protocols.

#### 1.4.2 Chemistry and structural characterization

The general method for the synthesis of 3,5-diaryl-1-thiocarbamoyl-2-pyrazolines and of final compounds has been discussed in the Section 1.2.3. In this paragraph a more detailed overview of the synthesis of the single compounds for each one of the series will be provided.

##### **Series 1: Synthesis of 3-{2-[5-(4-methoxyphenyl)-3-(naphthalen-2-yl)-4,5-dihydropyrazol-1-yl]}-4-oxothiazol-5(4H)-ylidene-indolin-2-one (EMAC 4000-4009)**

###### ***Synthesis of 3-(4-methoxy-phenyl)-1-(naphthalen-2-yl)-2-propen-1-one***

An aqueous solution of NaOH 10% (1.2 mmol; 480  $\mu$ L) was slowly added to a solution of 2-acetyl-naphthalene (1 mmol; 170 mg) in ethanol. The mixture was vigorously stirred, until to obtain a cloudy solution. Then, a solution in ethanol of 4-methoxy-benzaldehyde (1.2 mmol; 163 mg) is added dropwise, obtaining a light yellow suspension. The obtained solid was filtered, washed with water and ethanol to obtain a light yellow solid. This crude product was crystallized from ethanol. The whole reaction was carried out keeping the temperature around 0°C and its progression monitored with TLC, using ethyl acetate/petroleum ether 1:1 as eluent.

Yellow solid; Yield 88%; MW 288.34 g/mol; Mp 90-92°C

$^1\text{H}$  NMR (500 MHz, DMSO- $d_6$ ):  $\delta$  8.92 (s, 1H, -CH aromatic), 8.17 (d, 1H, -CH aromatic,  $J_o=8$ ), 8.14 (dd, 1H, -CH aromatic,  $J_o=8.5$ ;  $J_m=2$ ), 8.07 (d, 1H, -CH aromatic,  $J_o=8.5$ ), 8.03 (d, 1H, -CH aromatic,  $J_o=8$ ), 8.00 (d, 1H, -CH propen,  $J_E=15.5$ ), 7.91 (d, 2H, -CH aromatic,  $J_o=8.5$ ), 7.80 (d, 1H, -CH propen,  $J_E=15.5$ ), 7.70 (td, 1H, -CH aromatic,  $J_o=8.5$ ;  $J_m=2$ ), 7.66 (td, 1H, -CH aromatic,  $J_o=8.5$ ;  $J_m=2$ ), 7.06 (d, 2H, -CH aromatic,  $J_o=8.5$ ), 3.85 (s, 3H, -OCH<sub>3</sub>).

###### ***Synthesis of 5-(4-methoxyphenyl)-3-(naphthalen-2-yl)-4,5-dihydropyrazole-1-carbothioamide***

A freshly prepared solution of alcoholic KOH 5% (1.2 mmol; 1.3 mL) was added dropwise to a mixture of 3-(4-methoxy-phenyl)-1-(naphthalen-2-yl)-2-propenone (1 mmol, 288 mg) and thiosemicarbazide (1.2 mmol; 110 mg) in ethanol. This solution was refluxed until reaction completion, checking the progression with TLC. This solution was cooled at

room temperature, obtaining a yellow suspension. The solid was filtered out, washed with water and crystallized from ethanol.

Yellow solid; Yield 74%; MW 361.43 g/mol; Mp 210-211°C

<sup>1</sup>H NMR (500 MHz, CDCl<sub>3</sub>): δ 8.02 (d, 1H, -CH aromatic, J<sub>o</sub>=8.5), 7.98 (s, 1H, -CH aromatic), 7.89-7.84 (m, 3H, -CH aromatic), 7.58-7.52 (m, 2H, -CH aromatic), 7.20 (d, 2H, -CH aromatic, J<sub>o</sub>=8), 7.15 (bs, 1H, -NH thiocarbamoyl), 6.87 (d, 2H, -CH aromatic, J<sub>o</sub>=8), 6.06 (dd, 1H, -CH<sub>x</sub> pyrazoline, J<sub>AX</sub>=4; J<sub>MX</sub>=11), 3.94 (dd, 1H -CH<sub>M</sub> pyrazoline, J<sub>MA</sub>=18.5; J<sub>MX</sub>=11), 3.78 (s, 3H, -OCH<sub>3</sub>), 3.36 (dd, 1H, -CH<sub>A</sub> pyrazoline, J<sub>AM</sub>=18.5; J<sub>AX</sub>=4).

**Synthesis of 3-{2-[5-(4-methoxyphenyl)-3-(naphthalen-2-yl)-4,5-dihydropyrazol-1-yl]}-4-oxothiazol-5(4H)-ylidene-indolin-2-one**

A mixture of 5-(4-methoxyphenyl)-3-(naphthalen-2-yl)-1-thiocarbamoyl-2-pyrazoline (1.0 mmol), ethyl bromoacetate (1.0 mmol), appropriate isatin (1.2 mmol), and anhydrous sodium acetate (2.0 mmol) was refluxed in glacial acetic acid (5 mL) until reaction completion. The mixture was cooled at room temperature and the obtained precipitate was filtered off, washed with water and methanol.

**(EMAC 4000) 7-bromo-3-{2-[5-(4-methoxyphenyl)-3-(naphthalen-2-yl)-4,5-dihydropyrazol-1-yl]}-4-oxothiazol-5(4H)-ylidene-indolin-2-one**

Light orange solid; MW 609.49 g/mol; Mp 341-342°C

<sup>1</sup>H NMR (400 MHz, DMSO-d<sub>6</sub>): δ 11.47(s,1H, -NH isatin), 8.99 (d, 1H, -CH aromatic, J<sub>o</sub>=8.5), 8.46 (s, 1H, -CH aromatic), 8.17-8.04 (m, 4H, -CH aromatic), 7.70-7.63 (m, 2H, -CH aromatic), 7.58 (d, 1H, -CH aromatic, J<sub>o</sub>=8.5), 7.29 (d, 2H, -CH aromatic, J<sub>o</sub>=8.4), 7.04 (t, 1H, -CH aromatic, J<sub>o</sub>=8.5), 6.97 (d, 2H, -CH aromatic, J<sub>o</sub>=8.4), 6.01 (dd, 1H, -CH<sub>x</sub> pyrazoline, J<sub>AX</sub>=4; J<sub>MX</sub>=11), 4.30 (dd, 1H, -CH<sub>M</sub> pyrazoline, J<sub>MA</sub>=18.5; J<sub>MX</sub>=11), 3.75 (s, 3H, -OCH<sub>3</sub>), 3.67 (dd, 1H, -CH<sub>A</sub> pyrazoline, J<sub>AM</sub>=18.5; J<sub>AX</sub>=4).

**(EMAC 4001) 5-chloro-3-{2-[5-(4-methoxyphenyl)-3-(naphthalen-2-yl)-4,5-dihydropyrazol-1-yl]}-4-oxothiazol-5(4H)-ylidene-indolin-2-one**

Orange solid; MW 565.04 g/mol; Mp 314-317°C

<sup>1</sup>H NMR (500 MHz, DMSO-d<sub>6</sub>): δ 11.29 (s, 1H, -NH isatin), 8.97 (s, 1H, -CH aromatic), 8.42 (s, 1H, -CH aromatic), 8.11 (d, 1H, -CH aromatic, J<sub>o</sub>=9), 8.08-8.01 (m, 3H, -CH aromatic), 7.67-7.61 (m, 2H, -CH aromatic), 7.39 (dd, 1H, -CH aromatic, J<sub>o</sub>=8.5; J<sub>m</sub>=2), 7.28 (d, 2H, -CH aromatic, J<sub>o</sub>=8.5), 6.96 (s, 1H, -CH aromatic), 6.95 (d, 2H, -CH aromatic, J<sub>o</sub>=8.5), 5.98 (dd, 1H, -CH<sub>x</sub> pyrazoline, J<sub>AX</sub>=4; J<sub>MX</sub>=11), 4.28 (dd, 1H, -CH<sub>M</sub> pyrazoline, J<sub>MA</sub>=18.5; J<sub>MX</sub>=11), 3.74 (s, -3H, -OCH<sub>3</sub>), 3.67 (dd, 1H, -CH<sub>A</sub> pyrazoline, J<sub>AM</sub>=18.5; J<sub>AX</sub>=4).

**(EMAC 4003) 5,7-dimethyl-3-{2-[5-(4-methoxyphenyl)-3-(naphthalen-2-yl)-4,5-dihydropyrazol-1-yl]}-4-oxothiazol-5(4H)-ylidene-indolin-2-one**

Light orange solid; MW 558.65 g/mol; Mp 335-336°C

<sup>1</sup>H NMR (500 MHz, DMSO-d<sub>6</sub>): δ 11.07 (s, 1H, -NH isatin), 8.64 (s, 1H, -CH aromatic), 8.43 (s, 1H, -CH aromatic), 8.14 (d, 1H, -CH aromatic, J<sub>o</sub>=8.5), 8.09-8.02 (m, 3H, -CH

aromatic) 7.68- 7.62 (m, 2H, -CH aromatic), 7.28 (d, 2H, -CH aromatic,  $J_o=8.5$ ), 7.02 (s, 1H, -CH aromatic), 6.95 (d, 2H, -CH aromatic,  $J_o=8.5$ ), 5.98 (dd, 1H, -CH<sub>x</sub> pyrazoline,  $J_{AX}=4$ ;  $J_{MX}=11$ ), 4.28 (dd, 1H -CH<sub>M</sub> pyrazoline,  $J_{MA}=18.5$ ;  $J_{MX}=11$ ), 3.74 (s, 3H, -OCH<sub>3</sub>), 3.65 (dd, 1H, -CH<sub>A</sub> pyrazoline,  $J_{AM}=18.5$ ;  $J_{AX}=4$ ), 2.26 (s, 3H, -CH<sub>3</sub>), 2.21 (s, 3H, -CH<sub>3</sub>).

**(EMAC 4005) 7-fluoro-3-{2-[5-(4-methoxyphenyl)-3-(naphthalen-2-yl)-4,5-dihydropyrazol-1-yl]}-4-oxothiazol-5(4H)-ylidene)-indolin-2-one**

Light orange solid; MW 548.59 g/mol; Mp 308-309°C

<sup>1</sup>H NMR (500 MHz, DMSO-d<sub>6</sub>): δ 11.69 (s, 1H, -NH isatin), 8.79 (d, 1H, -CH aromatic,  $J_o=8$ ), 8.44 (s, 1H, -CH aromatic), 8.13 (d, 1H, -CH aromatic,  $J_o=8.5$ ), 8.10-8.02 (m, 3H, -CH aromatic), 7.68-7.62 (m, 2H, -CH aromatic), 7.31 (d, 1H, -CH aromatic,  $J_o=8.5$ ), 7.28 (d, 1H, -CH aromatic,  $J_o=8.5$ ), 7.09-7.05 (m, 1H, -CH aromatic), 6.95 (d, 1H, -CH aromatic,  $J_o=8.5$ ), 5.98 (dd, 1H, -CH<sub>x</sub> pyrazoline,  $J_{XA}=4$ ;  $J_{XM}=11$ ), 4.30 (dd, 1H, -CH<sub>M</sub> pyrazoline,  $J_{MA}=18.5$ ;  $J_{MX}=11$ ), 3.74 (s, 3H, -OCH<sub>3</sub>), 3.66 (dd, 1H, -CH<sub>A</sub> pyrazoline,  $J_{AM}=18.5$ ;  $J_{AX}=4$ ).

**(EMAC 4006) 5-iodo-3-{2-[5-(4-methoxyphenyl)-3-(naphthalen-2-yl)-4,5-dihydropyrazol-1-yl]}-4-oxothiazol-5(4H)-ylidene)-indolin-2-one**

Orange solid; MW 656.49 g/mol; Mp 288-290°C

<sup>1</sup>H NMR (500 MHz, DMSO-d<sub>6</sub>): δ 10.55 (s, 1H, -NH isatin), 8.36 (s, 1H, -CH aromatic), 8.11-8.01 (m, 4H, -CH aromatic), 7.84 (s, 1H, -CH aromatic), 7.66-7.60 (m, 2H, -CH aromatic), 7.56 (d, 1H, -CH aromatic,  $J_o=8.5$ ), 7.06 (d, 2H, -CH aromatic,  $J_o=8.5$ ), 6.99 (d, 2H, -CH aromatic,  $J_o=8.5$ ), 6.62 (d, 1H, -CH aromatic,  $J_o=8.5$ ), 5.79 (dd, 1H, -CH<sub>x</sub> pyrazoline,  $J_{XA}=4$ ;  $J_{XM}=11$ ), 4.20 (dd, 1H, -CH<sub>M</sub> pyrazoline,  $J_{MX}=11$ ;  $J_{MA}=18.5$ ), 3.73 (s, 3H, -OCH<sub>3</sub>), 3.48 (dd, 1H, -CH<sub>A</sub> pyrazoline,  $J_{AX}=4$ ;  $J_{AM}=18.5$ ).

**(EMAC 4007) 5-methoxy-3-{2-[5-(4-methoxyphenyl)-3-(naphthalen-2-yl)-4,5-dihydropyrazol-1-yl]}-4-oxothiazol-5(4H)-ylidene)-indolin-2-one**

Brown solid; MW 560.62 g/mol; Mp 303-305°C

<sup>1</sup>H NMR (500 MHz, DMSO-d<sub>6</sub>): δ 10.96 (s, 1H, -NH isatin), 8.67 (s, 1H, -CH aromatic), 8.43 (s, 1H, -CH aromatic), 8.13 (d, 1H, -CH aromatic,  $J_o=8.5$ ), 8.10-8.02 (m, 3H, -CH aromatic), 7.68-7.62 (m, 2H, -CH aromatic), 7.28 (d, 2H, -CH aromatic,  $J_o=8.5$ ), 6.98-6.94 (m, 3H, -CH aromatic), 6.84 (d, 1H, aromatic,  $J_o=8.5$ ), 5.97 (dd, 1H, -CH<sub>x</sub> pyrazoline,  $J_{XA}=4$ ;  $J_{XM}=11$ ), 4.29 (dd, 1H, -CH<sub>M</sub> pyrazoline,  $J_{MA}=18.5$ ;  $J_{MX}=11$ ), 3.75 (s, 3H, -OCH<sub>3</sub>), 3.74 (s, 3H, -OCH<sub>3</sub>), 3.66 (dd, 1H, -CH<sub>A</sub> pyrazoline,  $J_{AM}=18.5$ ;  $J_{AX}=4$ ).

**(EMAC 4008) 5-methyl-3-{2-[5-(4-methoxyphenyl)-3-(naphthalen-2-yl)-4,5-dihydropyrazol-1-yl]}-4-oxothiazol-5(4H)-ylidene)-indolin-2-one**

Orange solid; MW 544.62 g/mol; Mp 288-291°C

<sup>1</sup>H NMR (500 MHz, DMSO-d<sub>6</sub>): δ 11.05 (s, 1H, -NH isatin), 8.78 (s, 1H, -CH aromatic), 8.43 (s, 1H, -CH aromatic), 8.13 (d, 1H, -CH aromatic,  $J_o=8.5$ ), 8.09-8.02 (m, 3H, -CH aromatic), 7.67-7.62 (m, 2H, -CH aromatic), 7.28 (d, 2H, -CH aromatic,  $J_o=8.5$ ), 7.17 (d, 1H, -CH aromatic,  $J_o=8.5$ ), 6.95 (d, 2H, -CH aromatic,  $J_o=8.5$ ), 6.83 (d, 1H, -CH aromatic,  $J_o=8.5$ ), 5.98 (dd, 1H, -CH<sub>x</sub> pyrazoline,  $J_{XA}=4$ ;  $J_{XM}=11$ ), 4.28 (dd, 1H, -CH<sub>M</sub> pyrazoline,  $J_{MA}=18.5$ );

$J_{MX}=11$ ), 3.74 (s, 3H, -OCH<sub>3</sub>), 3.66 (dd, 1H, -CH<sub>A</sub> pyrazoline,  $J_{AM}=18.5$ ;  $J_{AX}=4$ ), 2.30 (s, 3H, -CH<sub>3</sub>).

**(EMAC 4009) 5-trifluoromethyl-3-{2-[5-(4-methoxyphenyl)-3-(naphthalen-2-yl)-4,5-dihydropyrazol-1-yl]-4-oxothiazol-5(4H)-ylidene)-indolin-2-one**

Orange solid; MW 598.59 g/mol; Mp 303-305 °C

<sup>1</sup>H NMR (500 MHz, DMSO-d<sub>6</sub>): δ 11.35 (s, 1H, -NH isatin), 8.98 (s, 1H, -CH aromatic), 8.44 (s, 1H, -CH aromatic), 8.13 (d, 1H, -CH aromatic,  $J_o=8.5$ ), 8.10-8.02 (m, 3H, -CH aromatic), 7.68-7.62 (m, 2H, -CH aromatic), 7.38 (d, 1H, -CH aromatic,  $J_o=8.5$ ), 7.29 (d, 2H, -CH aromatic,  $J_o=8.5$ ), 7.02 (d, 1H, -CH aromatic,  $J_o=8.5$ ), 6.95 (d, 2H, -CH aromatic,  $J_o=8.5$ ), 5.99 (dd, 1H, -CH<sub>X</sub> pyrazoline,  $J_{XA}=4$ ;  $J_{XM}=11$ ), 4.30 (dd, 1H, -CH<sub>M</sub> pyrazoline,  $J_{MA}=18.5$ ;  $J_{MX}=11$ ), 3.74 (s, 3H, -OCH<sub>3</sub>), 3.68 (dd, 1H, -CH<sub>A</sub> pyrazoline,  $J_{AM}=18.5$ ;  $J_{AX}=4$ ).

**Series 2: Synthesis of 3-{2-[5-(4-methoxyphenyl)-3-(thiophen-2-yl)-4,5-dihydropyrazol-1-yl]-4-oxothiazol-5(4H)-ylidene)-indolin-2-one (EMAC 4011-4020)**

***Synthesis of 3-(4-methoxyphenyl)-1-(thiophen-2-yl)-2-propen-1-one.***

An aqueous solution of NaOH 10% (1.2 mmol; 480 μL) was slowly added to a solution of 2-acetyl-thiophene (1 mmol; 130 mg) in ethanol. The mixture was vigorously stirred, until to obtain a cloudy solution. Then, a solution in ethanol of 4-methoxybenzaldehyde (1.2 mmol; 163 mg) is added dropwise, obtaining a light yellow solution. The whole reaction was carried out keeping the temperature around 0°C and its progression monitored with TLC, using ethyl acetate/petroleum ether 1:1 as eluent.

Since the reaction product is soluble in ethanol, the solution is concentrated in vacuum to halve the volume and poured in ~ 20 g of chipped ice, obtaining a yellow precipitate. The solid was filtered off and washed with water, obtaining a light yellow powder that crystallized from isopropanol.

Yellow solid; Yield 86%; MW 244.31 g/mol; Mp 70°C

<sup>1</sup>H NMR (500 MHz, chloroform-d): δ 7.87 (d, 1H, -CH<sub>5</sub> thioph.,  $J_{4-5}=3.5$ ), 7.85 (d, 1H, -CH propen,  $J_E=15.5$ ), 7.65 (d, 1H, -CH<sub>3</sub> thioph.,  $J_{3-4}=5$ ), 7.63 (d, 2H, -CH aromatic,  $J_o=8.5$ ), 7.33 (d, 1H, -CH propen,  $J_E=15.5$ ), 7.20 (t, 1H, -CH<sub>4</sub> thioph.,  $J_{4-5}=3.5$ ;  $J_{3-4}=5$ ), 6.97 (d, 2H, -CH aromatic,  $J_o=8.5$ ), 3.88 (s, 3H, -OCH<sub>3</sub>).

***Synthesis of 5-(4-methoxyphenyl)-3-(thiophen-2-yl)-4,5-dihydropyrazole-1-carbothioamide.***

To a mixture of 3-(4-methoxyphenyl)-1-(thiophen-2-yl)-2-propenone (1 mmol; 244 mg) and thiosemicarbazide (1.2 mmol; 110 mg) in ethanol a freshly prepared solution of alcoholic KOH 5% (1.2 mmol; 1.3 mL) was added dropwise at room temperature. After 1 h the temperature was gradually increased to 50°C and maintained at this level until

reaction completion. The reaction was monitored with TLC, using ethyl acetate/petroleum ether 1:1 as eluent.

For the synthesis of this pyrazoline the control of the temperature is absolutely required. In fact, both higher and lower temperatures than 50°C, are related to poor yields. In the first case, refluxing the reaction system the yield lowering is due to the formation of a mixture of products, in which the pyrazoline is the 38% of the total. On the other hand, reacting these compounds at room temperature does not lead to the final product, even if the reaction time is prolonged (>48 h). Also in this case a mixture of compounds have been obtained, in which the starting material is the prevalent one. The obtained pyrazoline was crystallized from ethanol, obtaining a light yellow solid.

Yellow solid; Yield 74%; MW 317.43 g/mol; Mp 150-152°C

<sup>1</sup>H NMR (500 MHz, chloroform-d): δ 7.50 (d, 1H, -CH<sub>5</sub> thioph., J<sub>4-5</sub>=5), 7.28 (solvent peak and -CH<sub>3</sub> thioph. signal), 7.19 (d, 2H, -CH aromatic, J<sub>o</sub>=8.5), 7.11 (t, 1H, -CH<sub>4</sub> thiph., J<sub>4-5</sub>=5; J<sub>3-4</sub>=4), 7.04 (bs, 1H, -NH<sub>2</sub> thiocarbamoil), 6.88 (d, 2H, -CH aromatic, J<sub>o</sub>=8.5), 6.01 (dd, 1H, -CH<sub>X</sub> pyrazoline, J<sub>XA</sub>=3.5; J<sub>XM</sub>=11.5), 3.86 (dd, 1H, -CH<sub>M</sub> pyrazoline, J<sub>MX</sub>=11.5; J<sub>MA</sub>=18.5), 3.80 (s, 3H, -OCH<sub>3</sub>), 3.20 (dd, 1H, -CH<sub>A</sub> pyrazoline, J<sub>AM</sub>=18.5; J<sub>AX</sub>=3.5).

***Synthesis of 3-{2-[5-(4-methoxyphenyl)-3-(thiophen-2-yl)-4,5-dihydropyrazol-1-yl]}-4-oxothiazol-5(4H)-ylidene)-indolin-2-one.***

A mixture of 5-(4-methoxyphenyl)-3-(thiophen-2-yl)-1-thiocarbamoyl-2-pyrazoline (1.0 mmol), ethyl bromoacetate (1.0 mmol), appropriate isatin (1.2 mmol), and anhydrous sodium acetate (2.0 mmol) was refluxed in glacial acetic acid (5 mL) until reaction completion. The mixture was cooled at room temperature and the obtained precipitate was filtered off, washed with water and methanol.

**(EMAC 4011) 7-bromo-3-{2-[5-(4-methoxyphenyl)-3-(thiophen-2-yl)-4,5-dihydropyrazol-1-yl]}-4-oxothiazol-5(4H)-ylidene)-indolin-2-one**

Orange solid; MW 565.46 g/mol; Mp 323-324°C

<sup>1</sup>H NMR (500 MHz, DMSO-d<sub>6</sub>): δ 11.43 (s, 1H, -NH isatin), 8.96 (d, 1H, -CH aromatic, J<sub>o</sub>=8), 7.97 (d, 1H, -CH<sub>5</sub> thioph., J<sub>4-5</sub>=5), 7.73 (d, 1H, -CH<sub>3</sub> thioph., J<sub>3-4</sub>=3), 7.55 (d, 1H, -CH aromatic, J<sub>o</sub>=8), 7.27 (t, 1H, -CH<sub>4</sub> thioph., J<sub>4-5</sub>=5; J<sub>3-4</sub>=3), 7.23 (d, 2H, -CH aromatic, J<sub>o</sub>=8), 7.02 (t, 1H, -CH aromatic, J<sub>o1,2</sub>=8), 6.94 (d, 2H, -CH aromatic, J<sub>o</sub>=8), 5.93 (dd, 1H, -CH<sub>X</sub> pyrazoline, J<sub>XA</sub>=3.5; J<sub>XM</sub>=11.5), 4.18 (dd, 1H, -CH<sub>M</sub> pyrazoline, J<sub>MX</sub>=11.5; J<sub>MA</sub>=18.5), 3.74 (s, 3H, -OCH<sub>3</sub>), 3.54 (dd, 1H, -CH<sub>A</sub> pyrazoline, J<sub>AM</sub>=18.5; J<sub>AX</sub>=3.5).

**(EMAC 4012) 5-chloro-3-{2-[5-(4-methoxyphenyl)-3-(thiophen-2-yl)-4,5-dihydropyrazol-1-yl]}-4-oxothiazol-5(4H)-ylidene)-indolin-2-one**

Red solid; MW 521.01 g/mol; Mp 307-309°C

<sup>1</sup>H NMR (500 MHz, DMSO-d<sub>6</sub>): δ 11.29 (s, 1H, -NH isatin), 8.98 (s, 1H, -CH aromatic), 7.97 (d, 1H, -CH<sub>5</sub> thioph., J<sub>4-5</sub>=4.5), 7.74 (d, 1H, -CH<sub>3</sub> thioph., J<sub>3-4</sub>=3), 7.41 (d, 1H, -CH aromatic, J<sub>o</sub>=8), 7.27 (t, 1H, -CH<sub>4</sub> thioph., J<sub>4-5</sub>=4.5; J<sub>3-4</sub>=3), 7.23 (d, 1H, -CH aromatic, J<sub>o</sub>=8.5), 6.95-6.94 (m, 3H, -CH aromatic), 5.94 (dd, 1H, -CH<sub>X</sub> pyrazoline, J<sub>XA</sub>=3.5; J<sub>XM</sub>=11.5),

4.17 (dd, 1H, -CH<sub>M</sub> pyrazoline, J<sub>MX</sub>=11.5; J<sub>MA</sub>=18.5), 3.74 (s, 3H, -OCH<sub>3</sub>), 3.54 (dd, 1H, -CH<sub>A</sub> pyrazoline, J<sub>AM</sub>=18.5; J<sub>AX</sub>=3.5).

**(EMAC 4014) 5,7-dimethyl-3-{2-[5-(4-methoxyphenyl)-3-(thiophen-2-yl)-4,5-dihydropyrazol-1-yl]}-4-oxothiazol-5(4H)-ylidene)-indolin-2-one**

Brown solid; MW 514.62 g/mol; Mp >350°C

<sup>1</sup>H NMR (500 MHz, DMSO-d<sub>6</sub>): δ 11.05 (s, 1H, -NH isatin), 8.62 (s, 1H, -CH aromatic), 7.96 (d, -1H, -CH<sub>5</sub> thioph., J<sub>4-5</sub>=5), 7.71 (d, 1H, -CH<sub>3</sub> thioph., J<sub>3-4</sub>=3), 7.26 (t, 1H, -CH<sub>4</sub> thioph., J<sub>4-5</sub>=5; J<sub>3-4</sub>=3), 7.23 (d, 1H, -CH aromatic, J<sub>o</sub>=8.5), 7.01 (s, 1H, -CH aromatic), 6.94 (d, 1H, -CH aromatic, J<sub>o</sub>=8.5), 5.94 (dd, 1H, -CH<sub>X</sub> pyrazoline, J<sub>XA</sub>=3.5; J<sub>XM</sub>=11.5), 4.17 (dd, 1H, -CH<sub>M</sub> pyrazoline, J<sub>MX</sub>=11.5; J<sub>MA</sub>=18.5), 3.74 (s, 3H, -OCH<sub>3</sub>), 3.54 (dd, 1H, -CH<sub>A</sub> pyrazoline, J<sub>AM</sub>=18.5; J<sub>AX</sub>=3.5), 2.25 (s, 3H, -CH<sub>3</sub>), 2.20 (s, 3H, -CH<sub>3</sub>).

**(EMAC 4015) 5-fluoro-3-{2-[5-(4-methoxyphenyl)-3-(thiophen-2-yl)-4,5-dihydropyrazol-1-yl]}-4-oxothiazol-5(4H)-ylidene)-indolin-2-one**

Red solid; MW 504.56 g/mol; Mp 318-320°C

<sup>1</sup>H NMR (500 MHz, DMSO-d<sub>6</sub>): δ 11.17 (s, 1H, -NH isatin), 8.74 (dd, 1H, -CH aromatic, J<sub>m</sub>=2.5; J<sub>OH-F</sub>=10), 7.97 (d, 1H, -CH thioph., J<sub>4-5</sub>=4.5), 7.73 (d, 1H, -CH thioph., J<sub>3-4</sub>=3), 7.27 (t, 1H, -CH thioph., J<sub>3-4</sub>=3; J<sub>4-5</sub>=4.5), 7.24 (d, 2H, -CH aromatic, J<sub>o</sub>=8.5), 7.22-7.20 (m, 1H, -CH aromatic), 6.95 (d, 2H, -CH aromatic, J<sub>o</sub>=8.5), 6.93-6.91 (m, 1H, -CH aromatic), 5.92 (dd, 1H, -CH<sub>X</sub> pyrazoline, J<sub>XA</sub>=3.5; J<sub>XM</sub>=11.5), 4.17 (dd, 1H, -CH<sub>M</sub> pyrazoline, J<sub>MX</sub>=11.5; J<sub>MA</sub>=18.5), 3.74 (s, 3H, -OCH<sub>3</sub>), 3.54 (dd, 1H, -CH<sub>A</sub> pyrazoline, J<sub>AM</sub>=18.5; J<sub>AX</sub>=3.5).

**(EMAC 4016) 7-fluoro-3-{2-[5-(4-methoxyphenyl)-3-(thiophen-2-yl)-4,5-dihydropyrazol-1-yl]}-4-oxothiazol-5(4H)-ylidene)-indolin-2-one**

Light orange; MW 504.56 g/mol; Mp 299-300°C

<sup>1</sup>H NMR (500 MHz, DMSO-d<sub>6</sub>): δ 11.43 (s, 1H, -NH isatin), 8.96 (d, 1H, -CH aromatic, J<sub>o</sub>=8), 7.97 (d, 1H, -CH thioph., J<sub>4-5</sub>=4.5), 7.73 (d, 1H, -CH thioph., J<sub>3-4</sub>=3), 7.55 (d, 1H, -CH aromatic, J<sub>o</sub>=8), 7.27 (t, 1H, -CH thioph., J<sub>3-4</sub>=3; J<sub>4-5</sub>=4.5), 7.23 (d, 2H, -CH aromatic, J<sub>o</sub>=8), 7.02 (t, 1H, -CH aromatic, J<sub>o</sub>=8), 6.95 (d, 2H, -CH aromatic, J<sub>o</sub>=8), 6.02 (dd, 1H, -CH<sub>X</sub> pyrazoline, J<sub>AX</sub>=4; J<sub>MX</sub>=11), 4.32 (dd, 1H, -CH<sub>M</sub> pyrazoline, J<sub>MA</sub>=18; J<sub>MX</sub>=11), 3.74 (s, 3H, -OCH<sub>3</sub>), 3.54 (dd, 1H, -CH<sub>A</sub> pyrazoline, J<sub>AM</sub>=18; J<sub>AX</sub>=4).

**(EMAC 4017) 5-iodo-3-{2-[5-(4-methoxyphenyl)-3-(thiophen-2-yl)-4,5-dihydropyrazol-1-yl]}-4-oxothiazol-5(4H)-ylidene)-indolin-2-one**

Orange solid; MW 512.46 g/mol; Mp 307-308°C

<sup>1</sup>H NMR (500 MHz, DMSO-d<sub>6</sub>): δ 11.27 (s, 1H, -NH isatin), 9.28 (s, 1H, -CH aromatic), 7.97 (d, 1H, -CH thioph., J<sub>4-5</sub>=4.5), 7.73 (d, 1H, -CH thioph., J<sub>3-4</sub>=3), 7.67 (d, 1H, -CH aromatic, J<sub>o</sub>=8), 7.27 (t, 1H, -CH thioph., J<sub>3-4</sub>=3; J<sub>4-5</sub>=4.5), 7.24 (d, 2H, -CH aromatic, J<sub>o</sub>=8.5), 6.95 (d, 2H, -CH aromatic, J<sub>o</sub>=8.5), 6.79 (d, 1H, -CH aromatic, J<sub>o</sub>=8), 5.93 (dd, 1H, -CH<sub>X</sub> pyrazoline, J<sub>XA</sub>=3.5; J<sub>XM</sub>=11.5), 4.17 (dd, 1H, -CH<sub>M</sub> pyrazoline, J<sub>MX</sub>=11.5; J<sub>MA</sub>=18.5), 3.74 (s, 3H, -OCH<sub>3</sub>), 3.54 (dd, 1H, -CH<sub>A</sub> pyrazoline, J<sub>AM</sub>=18.5; J<sub>AX</sub>=3.5).

**(EMAC 4018) 5-methoxy-3-{2-[5-(4-methoxyphenyl)-3-(thiophen-2-yl)-4,5-dihydropyrazol-1-yl]}-4-oxothiazol-5(4H)-ylidene)-indolin-2-one**



Brown solid; MW 516.59 g/mol; Mp 283-284°C

<sup>1</sup>H NMR (500 MHz, DMSO-d<sub>6</sub>): δ 10.95 (s, 1H, -NH isatin), 8.65 (d, 1H, -CH aromatic, J<sub>m</sub>=2.5), 7.97 (d, 1H, -CH thioph., J<sub>4-5</sub>=4.5), 7.73 (d, 1H, -CH thioph., J<sub>3-4</sub>=3), 7.27 (t, 1H, -CH thioph., J<sub>3-4</sub>=3; J<sub>4-5</sub>=4.5), 7.23 (d, 2H, -CH aromatic, J<sub>o</sub>=8.5), 6.97 (m, 1H, -CH aromatic), 6.95 (d, 2H, -CH aromatic, J<sub>o</sub>=8.5), 6.84 (d, 1H, -CH aromatic, J<sub>o</sub>=8), 5.91 (dd, 1H, -CH<sub>x</sub> pyrazoline, J<sub>xA</sub>=3.5; J<sub>xM</sub>=11.5), 4.17 (dd, 1H, -CH<sub>M</sub> pyrazoline, J<sub>MX</sub>=11.5; J<sub>MA</sub>=18.5), 3.74 (s, 6H, -OCH<sub>3</sub>), 3.53 (dd, 1H, -CH<sub>A</sub> pyrazoline, J<sub>AM</sub>=18.5; J<sub>AX</sub>=3.5).

**(EMAC 4019) 5-methyl- 3-{2-[5-(4-methoxyphenyl)-3-(thiophen-2-yl)-4,5-dihydropyrazol-1-yl]}-4-oxothiazol-5(4H)-ylidene)-indolin-2-one**

Red solid; MW 500.59 g/mol; Mp 285-286°C

<sup>1</sup>H NMR (500 MHz, DMSO-d<sub>6</sub>): δ 11.04 (s, 1H, -NH isatin), 8.76 (s, 1H, -CH isatin), 7.96 (d, 1H, -CH<sub>5</sub> thioph., J<sub>4-5</sub>=5), 7.72 (d, 1H, -CH<sub>3</sub> thioph., J<sub>3-4</sub>=3.5), 7.26 (t, 1H, -CH<sub>4</sub> thioph., J<sub>4-3</sub>=3.5; J<sub>4-5</sub>=5), 7.23 (dd, 2H, -CH aromatic, J<sub>o</sub>=8.5), 7.17 (d, 1H, -CH isatin, J<sub>o</sub>=8), 6.94 (d, 2H, -CH aromatic, J<sub>o</sub>=8.5), 6.82 (d, 1H, -CH isatin, J<sub>o</sub>=8), 5.92 (dd, 1H, -CH<sub>x</sub> pyrazoline, J<sub>AX</sub>=4; J<sub>MX</sub>=11), 4.16 (dd, 1H, -CH<sub>M</sub> pyrazoline, J<sub>MA</sub>=18.5; J<sub>MX</sub>=11), 3.74 (s, -3H, -OCH<sub>3</sub>), 3.52 (dd, 1H, -CH<sub>A</sub> pyrazoline, J<sub>AM</sub>=18.5; J<sub>AX</sub>=4), 3.29 (s, 1H, -CH<sub>3</sub>).

**(EMAC 4020) 5-trifluoromethyl- 3-{2-[5-(4-methoxyphenyl)-3-(thiophen-2-yl)-4,5-dihydropyrazol-1-yl]}-4-oxothiazol-5(4H)-ylidene)-indolin-2-one**

Orange solid; MW 554.56 g/mol; Mp 302-303°C

<sup>1</sup>H NMR (500 MHz, DMSO-d<sub>6</sub>): δ 11.34 (s, 1H, -NH isatin), 8.96 (s, 1H, -CH aromatic), 7.97 (d, 1H, -CH<sub>5</sub> thioph., J<sub>4-5</sub>=5), 7.74 (d, 1H, -CH<sub>3</sub> thioph., J<sub>3-4</sub>=3.5), 7.37 (t, 1H, -CH<sub>4</sub> thioph., J<sub>4-3</sub>=3.5; J<sub>4-5</sub>=5), 7.27-7.23 (m, 3H, -CH aromatic), 7.02 (d, 1H, -CH aromatic, J<sub>o</sub>=8.5), 6.94 (d, 1H, -CH aromatic, J<sub>o</sub>=8), 5.93 (dd, 1H, -CH<sub>x</sub> pyrazoline, J<sub>AX</sub>=4; J<sub>MX</sub>=11), 4.18 (dd, 1H, -CH<sub>M</sub> pyrazoline, J<sub>MA</sub>=18.5; J<sub>MX</sub>=11), 3.74 (s, -3H, -OCH<sub>3</sub>), 3.54 (dd, 1H, -CH<sub>A</sub> pyrazoline, J<sub>AM</sub>=18.5; J<sub>AX</sub>=4).

**Series 3: Synthesis of 3-{2-[5-(4-fluorophenyl)-3-(naphthalen-2-yl)-4,5-dihydropyrazol-1-yl]}-4-oxothiazol-5(4H)-ylidene)-indolin-2-one (EMAC 4022-4031)**

***Synthesis of 3-(4-fluorophenyl)-1-(naphthalen-2-yl)-2-propen-1-one***

An aqueous solution of NaOH 10% (1.2 mmol; 480 μL) was slowly added to a solution of 2-acetyl-naphthalene (1 mmol; 170 mg) in ethanol. The mixture was vigorously stirred, until a cloudy solution was obtained. Then, a solution in ethanol of 4-fluorobenzaldehyde (1.2 mmol; 149 mg) is added dropwise and a light yellow suspension is formed. The obtained solid was filtered, washed with water and ethanol to give a light yellow solid. This crude product was crystallized from ethanol. The whole reaction was carried out keeping the temperature around 0°C and its progression monitored with TLC, using ethyl acetate/petrol ether 1:1 as eluent.

Yellow solid; Yield 79%; MW 276.3 g/mol; Mp 135-137°C

<sup>1</sup>H NMR (500 MHz, chloroform-d): δ 8.55 (s, 1H, -CH aromatic), 8.12 (d, 2H, -CH aromatic, J<sub>o</sub>=8.5), 8.03 (d, 1H, -CH aromatic, J<sub>o</sub>=8), 7.97 (d, 1H, -CH aromatic, J<sub>o</sub>=8.5), 7.93 (d, 1H, -CH aromatic, J<sub>o</sub>=8), 7.87 (d, 1H, -CH propen, J<sub>E</sub>=16), 7.71 (dd, 2H, -CH aromatic, J<sub>H-H</sub>=8.5; J<sub>H-F</sub>=6), 7.66-7.58 (m, 3H, -CH aromatic and propen, J=nd), 7.17-7.14 (m, 2H, -CH aromatic).

**Synthesis of 5-(4-fluorophenyl)-3-(naphthalen-2-yl)-4,5-dihydropyrazole-1-carbothioamide**

A freshly prepared solution of alcoholic KOH 5% (1.2 mmol; 1.3 mL) was added dropwise to a mixture of 3-(4-fluoro-phenyl)-1-(naphthalen-2-yl)-2-propenone (1 mmol, 288 mg) and thiosemicarbazide (1.2 mmol; 110 mg) in ethanol. This solution was refluxed until reaction completion, checking the progression with TLC. This solution was cooled at room temperature, obtaining a yellow suspension. The solid was filtered out, washed with water and crystallized from ethanol.

Yellow solid; Yield 80%; MW 349.42 g/mol; Mp 243-245°C

<sup>1</sup>H NMR (500 MHz, chloroform-d): δ 8.03 (d, 1H, -CH aromatic, J<sub>o</sub>=8.5), 7.99 (s, 1H, -CH aromatic), 7.88 (m, 3H, -CH aromatic), 7.53 (m, 2H, -CH aromatic), 7.27 (dd, 2H, -CH aromatic, J<sub>H-H</sub>=8.5; J<sub>H-F</sub>=6), 7.16 (bs, 2H, -NH<sub>2</sub> thiocarbamoyl), 7.04 (t, 2H, -CH aromatic, J<sub>H-H</sub>=8.5; J<sub>H-F</sub>=6), 6.10 (dd, 1H, -CH<sub>X</sub> pyrazoline, J<sub>AX</sub>=4; J<sub>MX</sub>=11), 3.99 (dd, 1H, -CH<sub>M</sub> pyrazoline, J<sub>MA</sub>=18.5; J<sub>MX</sub>=11), 3.35 (dd, 1H, -CH<sub>A</sub> pyrazoline, J<sub>AM</sub>=18.5; J<sub>AX</sub>=4).

**Synthesis of 3-{2-[5-(4-fluorophenyl)-3-(naphthalen-2-yl)-4,5-dihydropyrazol-1-yl]}-4-oxothiazol-5(4H)-ylidene)-indolin-2-one**

A mixture of 5-(4-fluorophenyl)-3-(naphthalen-2-yl)-1-thiocarbamoyl-2-pyrazoline (1.0 mmol), ethyl bromoacetate (1.0 mmol), appropriate isatin (1.2 mmol), and anhydrous sodium acetate (2.0 mmol) was refluxed in glacial acetic acid (5 mL) until reaction completion. The mixture was cooled at room temperature and the obtained precipitate was filtered off, washed with water and methanol.

**(EMAC 4022) 7-bromo-dichloro-3-{2-[5-(4-fluorophenyl)-3-(naphthalen-2-yl)-4,5-dihydropyrazol-1-yl]}-4-oxothiazol-5(4H)-ylidene)-indolin-2-one**

Light orange; MW 597.46 g/mol; Mp *nd*

<sup>1</sup>H NMR (500 MHz, DMSO-d<sub>6</sub>): δ 11.45 (s, H, -NH isatin), 8.96 (d, 1H, -CH aromatic, J<sub>o</sub>=8), 8.43 (s, 1H, -CH aromatic), 8.13 (d, 1H, -CH aromatic, J<sub>o</sub>=8.5), 8.10-8.02 (m, 3H, -CH aromatic), 7.68-7.62 (m, 2H, -CH aromatic), 7.56 (d, 1H, -CH aromatic, J<sub>o</sub>=8), 7.42 (dd, 2H, -CH aromatic, J<sub>mH-F</sub>=5.5; J<sub>oH-H</sub>=8.5), 7.24 (t, 2H, -CH aromatic, J<sub>o</sub>=8.5), 7.03 (t, 1H, -CH aromatic, J<sub>o</sub>=8), 6.06 (dd, , 1H, -CH<sub>X</sub> pyrazoline, J<sub>AX</sub>=4; J<sub>MX</sub>=11), 4.33 (dd, 1H, -CH<sub>M</sub> pyrazoline, J<sub>MA</sub>=18; J<sub>MX</sub>=11), 3.69 (dd, 1H, -CH<sub>A</sub> pyrazoline, J<sub>AM</sub>=18; J<sub>AX</sub>=4).

**(EMAC 4023) 5-chloro-3-{2-[5-(4-fluorophenyl)-3-(naphthalen-2-yl)-4,5-dihydropyrazol-1-yl]}-4-oxothiazol-5(4H)-ylidene)-indolin-2-one**

Orange solid; MW 553.01 g/mol; Mp 346-348°C

<sup>1</sup>H NMR (500 MHz, DMSO-d<sub>6</sub>): δ 11.31 (s, 1H, -NH isatin), 8.99 (s, 1H, -CH aromatic), 8.44 (s, 1H, -CH aromatic), 8.13 (d, 1H, -CH aromatic, J<sub>o</sub>=8.5), 8.10-8.03 (m, 3H, -CH aromatic), 7.68-7.62 (m, 2H, -CH aromatic), 7.43-7.41 (m, 3H, -CH aromatic), 7.24 (t, 2H, -CH aromatic, J<sub>o</sub>=8.5), 6.96 (d, 1H, -CH aromatic, J<sub>o</sub>=8), 6.07 (dd, , 1H, -CH<sub>x</sub> pyrazoline, J<sub>AX</sub>=4; J<sub>MX</sub>=11), 4.33 (dd, 1H, -CH<sub>M</sub> pyrazoline, J<sub>MA</sub>=18; J<sub>MX</sub>=11), 3.69 (dd, 1H, -CH<sub>A</sub> pyrazoline, J<sub>AM</sub>=18; J<sub>AX</sub>=4).

**(EMAC 4024) 4,7-dichloro-3-{2-[5-(4-fluorophenyl)-3-(naphtalen-2-yl)-4,5-dihydropyrazol-1-yl]}-4-oxothiazol-5(4H)-ylidene)-indolin-2-one**

Light orange solid; MW 587.45 g/mol; Mp 280-282°C

<sup>1</sup>H NMR (500 MHz, DMSO-d<sub>6</sub>): δ 11.70 (s, 1 H, -NH isatin), 8.42 (s, 1H, -CH aromatic), 8.11 (dd, 1H, -CH aromatic, J<sub>o</sub>=8.5; J<sub>m</sub>=1.5), 8.09-8.06 (m, 2H, -CH aromatic), 8.03 (d, 1H, -CH aromatic, J<sub>o</sub>=8.5), 7.67-7.61 (m, 2H, -CH aromatic), 7.45-7.38 (m, 3H, -CH aromatic), 7.25-7.22 (m, 2H, -CH pyrazoline, J<sub>AX</sub>=4; J<sub>MX</sub>=11), 4.32 (dd, 1H, -CH<sub>M</sub> pyrazoline, J<sub>MA</sub>=18; J<sub>MX</sub>=11), 3.68 (dd, 1H, -CH<sub>A</sub> pyrazoline, J<sub>AM</sub>=18; J<sub>AX</sub>=4).

**(EMAC 4025) 5,7-dimethyl-3-{2-[5-(4-fluorophenyl)-3-(naphtalen-2-yl)-4,5-dihydropyrazol-1-yl]}-4-oxothiazol-5(4H)-ylidene)-indolin-2-one**

Orange solid; MW 546.61 g/mol; Mp 355-356°C

<sup>1</sup>H NMR (500 MHz, DMSO-d<sub>6</sub>): δ 11.08 (s, 1 H, -NH isatin), 8.63 (s, 1H, -CH aromatic), 8.42 (s, 1H, -CH aromatic), 8.13 (d, 1H, -CH aromatic, J<sub>o</sub>=8.5), 8.09-8.02 (m, 3H, -CH aromatic), 7.68-7.62 (m, 2H, -CH aromatic), 7.41 (dd, 2H, -CH aromatic, J<sub>OH-H</sub>=8; J<sub>OH-F</sub>=6), 7.23 (t, 2H, -CH aromatic, J<sub>o</sub>=8), 7.02 (s, 1H, -CH aromatic), , 6.06 (dd, 1H, -CH<sub>x</sub> pyrazoline, J<sub>AX</sub>=4; J<sub>MX</sub>=11), 4.32 (dd, 1H, -CH<sub>M</sub> pyrazoline, J<sub>MA</sub>=18; J<sub>MX</sub>=11), 3.68 (dd, 1H, -CH<sub>A</sub> pyrazoline, J<sub>AM</sub>=18; J<sub>AX</sub>=4), 2.26 (s, 3H, -CH<sub>3</sub>), 2.21 (s, 3H, -CH<sub>3</sub>).

**(EMAC 4026) 5-fluoro-3-{2-[5-(4-fluorophenyl)-3-(naphtalen-2-yl)-4,5-dihydropyrazol-1-yl]}-4-oxothiazol-5(4H)-ylidene)-indolin-2-one**

Orange solid; MW 536.55 g/mol; Mp 315-317°C

<sup>1</sup>H NMR (500 MHz, DMSO-d<sub>6</sub>): δ 11.20 (s, 1 H, -NH isatin), 8.74 (dd, 1H, -CH aromatic, J<sub>o</sub>=8.5; J<sub>m</sub>=2.5), 8.43 (s, 1H, -CH aromatic), 8.13 (d, 1H, -CH aromatic, J<sub>o</sub>=8.5), 8.09-8.02 (m, 3H, -CH aromatic), 7.68-7.61 (m, 2H, -CH aromatic), 7.42 (dd, 2H, -CH aromatic, J<sub>OH-H</sub>=8; J<sub>OH-F</sub>=6), 7.25-7.20 (m, 3H, -CH aromatic), 6.94 (dd, 1H, -CH aromatic, J<sub>OH-H</sub>=8; J<sub>OH-F</sub>=6), 6.06 (dd, 1H, -CH<sub>x</sub> pyrazoline, J<sub>AX</sub>=4; J<sub>MX</sub>=11), 4.32 (dd, 1H, -CH<sub>M</sub> pyrazoline, J<sub>MA</sub>=18; J<sub>MX</sub>=11), 3.68 (dd, 1H, -CH<sub>A</sub> pyrazoline, J<sub>AM</sub>=18; J<sub>AX</sub>=4).

**(EMAC 4027) 7-fluoro-3-{2-[5-(4-fluorophenyl)-3-(naphtalen-2-yl)-4,5-dihydropyrazol-1-yl]}-4-oxothiazol-5(4H)-ylidene)-indolin-2-one**

Light orange solid; MW 536.55 g/mol; Mp 327-329°C

<sup>1</sup>H NMR (500 MHz, DMSO-d<sub>6</sub>): δ 11.69 (s, 1 H, -NH isatin), 8.78 (d, 1H, -CH aromatic, J<sub>o</sub>=8), 8.42 (s, 1H, -CH aromatic), 8.13 (d, 1H, -CH aromatic, J<sub>o</sub>=8.5), 8.09-8.02 (m, 3H, -CH aromatic), 7.68-7.61 (m, 2H, -CH aromatic), 7.41 (dd, 2H, -CH aromatic, J<sub>OH-H</sub>=8; J<sub>OH-F</sub>=6), 7.30 (t, 1H, -CH aromatic, J<sub>o1,2</sub>=8), 7.23 (t, 2H, -CH aromatic, J<sub>o</sub>=8), 7.09-7.05 (m, 1H, -CH

aromatic), 6.06 (dd, 1H, -CH<sub>X</sub> pyrazoline, J<sub>AX</sub>=4; J<sub>MX</sub>=11), 4.32 (dd, 1H, -CH<sub>M</sub> pyrazoline, J<sub>MA</sub>=18; J<sub>MX</sub>=11), 3.68 (dd, 1H, -CH<sub>A</sub> pyrazoline, J<sub>AM</sub>=18; J<sub>AX</sub>=4).

**(EMAC 4029) 5-methoxy-3-{2-[5-(4-fluorophenyl)-3-(naphthalen-2-yl)-4,5-dihydropyrazol-1-yl]}-4-oxothiazol-5(4H)-ylidene)-indolin-2-one**

Brown solid; MW 548.59 g/mol; Mp *nd*

<sup>1</sup>H NMR (500 MHz, DMSO-d<sub>6</sub>): δ 10.99 (s, 1H, -NH isatin), 8.66 (d, 1H, -CH aromatic, J<sub>m</sub>=2.5), 8.43 (s, 1H, -CH aromatic), 8.13 (d, 1H, -CH aromatic, J<sub>o</sub>=8.5), 8.10-8.02 (m, 3H, -CH aromatic), 7.68-7.61 (m, 2H, -CH aromatic), 7.43-7.40 (m, 2H, -CH aromatic), 7.23 (t, 2H, -CH aromatic, J<sub>o</sub>=8.5), 6.97 (dd, 1H, -CH aromatic, J<sub>m</sub>=2.5; J<sub>o</sub>=8), 6.85 (d, 1H, -CH aromatic, J<sub>o</sub>=8), 6.05 (dd, 1H, -CH<sub>X</sub> pyrazoline, J<sub>AX</sub>=4; J<sub>MX</sub>=11), 4.32 (dd, 1H, -CH<sub>M</sub> pyrazoline, J<sub>MA</sub>=18; J<sub>MX</sub>=11), 3.74 (s, 3H, -OCH<sub>3</sub>), 3.68 (dd, 1H, -CH<sub>A</sub> pyrazoline, J<sub>AM</sub>=18; J<sub>AX</sub>=4).

**(EMAC 4030) 5-methyl-3-{2-[5-(4-fluorophenyl)-3-(naphthalen-2-yl)-4,5-dihydropyrazol-1-yl]}-4-oxothiazol-5(4H)-ylidene)-indolin-2-one**

<sup>1</sup>H NMR (500 MHz, DMSO-d<sub>6</sub>): δ 11.06 (s, 1H, -NH isatin), 8.77 (s, 1H, -CH aromatic), 8.42 (s, 1H, -CH aromatic), 8.13 (d, 1H, -CH aromatic, J<sub>o</sub>=8.5), 8.09-8.02 (m, 3H, -CH aromatic), 7.68-7.61 (m, 2H, -CH aromatic), 7.41 (dd, 2H, -CH aromatic, J<sub>oH-H</sub>=8; J<sub>oH-F</sub>=6), 7.23 (t, 2H, -CH aromatic, J<sub>o</sub>=8), 7.18 (d, 1H, -CH aromatic, J<sub>o</sub>=8), 6.83 (d, 1H, -CH aromatic, J<sub>o</sub>=8), 6.05 (dd, 1H, -CH<sub>X</sub> pyrazoline, J<sub>AX</sub>=4; J<sub>MX</sub>=11), 4.31 (dd, 1H, -CH<sub>M</sub> pyrazoline, J<sub>MA</sub>=18; J<sub>MX</sub>=11), 3.68 (dd, 1H, -CH<sub>A</sub> pyrazoline, J<sub>AM</sub>=18; J<sub>AX</sub>=4), 2.29 (s, 3H, -CH<sub>3</sub>).

Orange solid; MW 532.59 g/mol; Mp 310-311°C

**(EMAC 4031) 5-trifluoromethyl-3-{2-[5-(4-fluorophenyl)-3-(naphthalen-2-yl)-4,5-dihydropyrazol-1-yl]}-4-oxothiazol-5(4H)-ylidene)-indolin-2-one**

Red solid; MW 586.56 g/mol; Mp 318-320°C

<sup>1</sup>H NMR (500 MHz, DMSO-d<sub>6</sub>): δ 11.36 (s, 1H, -NH isatin), 8.97 (s, 1H, -CH aromatic), 8.43 (s, 1H, -CH aromatic), 8.13 (d, 1H, -CH aromatic, J<sub>o</sub>=8.5), 8.09-8.02 (m, 3H, -CH aromatic), 7.69-7.61 (m, 2H, -CH aromatic), 7.42 (dd, 2H, -CH aromatic, J<sub>oH-H</sub>=8; J<sub>oH-F</sub>=6), 7.38 (d, 1H, -CH aromatic, J<sub>o</sub>=8.5), 7.23 7.23 (t, 2H, -CH aromatic, J<sub>o</sub>=8.5), 7.02 (d, 1H, -CH aromatic, J<sub>o</sub>=8.5), 6.06 (dd, 1H, -CH<sub>X</sub> pyrazoline, J<sub>AX</sub>=4; J<sub>MX</sub>=11), 4.32 (dd, 1H, -CH<sub>M</sub> pyrazoline, J<sub>MA</sub>=18; J<sub>MX</sub>=11), 3.69 (dd, 1H, -CH<sub>A</sub> pyrazoline, J<sub>AM</sub>=18; J<sub>AX</sub>=4).

**Series 4: Synthesis of 3-{2-[5-(4-methoxyphenyl)-3-(4-biphenyl)-4,5-dihydropyrazol-1-yl]}-4-oxothiazol-5(4H)-ylidene)-indolin-2-one (EMAC 4033-4042)**

***Synthesis of 3-(4-methoxy-phenyl)-1-(4-biphenyl)-2-propen-1-one***

An aqueous solution of NaOH 10% (1.2 mmol; 480 μL) was slowly added to a solution of 4-acetyl-biphenyl (1 mmol; 196 mg) in ethanol. The mixture was vigorously stirred, until to obtain a cloudy solution. Then, a solution in ethanol of 4-methoxy-benzaldehyde (1.2 mmol; 163 mg) is added dropwise, obtaining a light yellow suspension. The obtained solid was filtered, washed with water and ethanol to give a light yellow

solid. This crude product was crystallized from ethanol. The whole reaction was carried out keeping the temperature around 0°C and its progression monitored with TLC, using ethyl acetate/petrol ether 1:1 as eluent.

Light yellow solid; Yield 80%; MW 314.38 g/mol; Mp 105°C

<sup>1</sup>H NMR (500 MHz, chloroform-d): δ 8.11 (d, 2H, -CH aromatic, J<sub>o</sub>=8), 7.84 (d, 1H, -CH propen, J<sub>E</sub>=16), 7.74 (d, 2H, -CH aromatic, J<sub>o</sub>=8), 7.67 (d, 2H, -CH aromatic, J<sub>o</sub>=8), 7.64 (d, 2H, -CH aromatic, J<sub>o</sub>=8), 7.52-7.47 (m, 3H, -CH aromatic and -CH propen, J<sub>aromatic</sub>=nd; J<sub>E</sub>=16), 7.42 (t, 2H, -CH aromatic, J<sub>o</sub>=8), 6.97 (d, 2H, -CH aromatic, J<sub>o</sub>=8).

### **Synthesis of 5-(4-methoxyphenyl)-3-(4-biphenyl)-4,5-dihydropyrazole-1-carbothioamide**

A freshly prepared solution of alcoholic KOH 5% (1.2 mmol; 1.3 mL) was added dropwise to a mixture of 3-(4-methoxy-phenyl)-1-(4-biphenyl)-2-propenone (1 mmol, 314 mg) and thiosemicarbazide (1.2 mmol; 110 mg) in ethanol. This solution was refluxed until reaction completion, checking the progression with TLC. This solution was cooled at room temperature and a yellow suspension is formed. The solid was filtered out, washed with water and crystallized from ethanol.

Light yellow solid; Yield 70%; MW 387.5 g/mol; Mp 130-132°C

<sup>1</sup>H NMR (500 MHz, chloroform-d): δ 7.83 (d, 2H, -CH aromatic, J<sub>o</sub>=8), 7.69 (d, 2H, -CH aromatic, J<sub>o</sub>=8), 7.61 (d, 2H, -CH aromatic, J<sub>o</sub>=8), 7.45 (d, 2H, -CH aromatic, J<sub>o</sub>=8), 7.41 (t, 1H, -CH aromatic, J<sub>o</sub>=8), 7.21 (d, 2H, -CH aromatic, J<sub>o</sub>=8), 7.12 (bs, 2H, -NH<sub>2</sub> thiocarbamoil); 6.89 (d, 2H, -CH aromatic, J<sub>o</sub>=8), 6.03 (dd, 1H, -CH<sub>x</sub> pyrazoline, J<sub>AX</sub>=4; J<sub>MX</sub>=11), 3.87 (dd, 1H -CH<sub>M</sub> pyrazoline, J<sub>MA</sub>=18.5; J<sub>MX</sub>=11), 3.80 (s, 3H, -OCH<sub>3</sub>), 3.26 (dd, 1H, -CH<sub>A</sub> pyrazoline, J<sub>AM</sub>=18.5; J<sub>AX</sub>=4).

### **Synthesis of 3-{2-[5-(4-methoxyphenyl)-3-(4-biphenyl)-4,5-dihydropyrazol-1-yl]}-4-oxothiazol-5(4H)-ylidene)-indolin-2-one**

A mixture of 5-(4-methoxyphenyl)-3-(4-biphenyl)-1-thiocarbamoyl-2-pyrazoline (1.0 mmol), ethyl bromoacetate (1.0 mmol), appropriate isatin (1.2 mmol), and anhydrous sodium acetate (2.0 mmol) was refluxed in glacial acetic acid (5 mL) until reaction completion. The mixture was cooled at room temperature and the obtained precipitate was filtered off, washed with water and methanol.

### **(EMAC 4033) 7-bromo-3-{2-[5-(4-methoxyphenyl)-3-(4-biphenyl)-4,5-dihydropyrazol-1-yl]}-4-oxothiazol-5(4H)-ylidene)-indolin-2-one**

Light orange solid; MW 635.53 g/mol; Mp 331-334°C

<sup>1</sup>H NMR (500 MHz, DMSO-d<sub>6</sub>): δ 11.43 (s, 1H, -NH isatin), 8.97 (d, 1H, -CH aromatic, J<sub>o</sub>=8), 8.03 (d, 2H, -CH aromatic, J<sub>o</sub>=8.5), 7.88 (d, 2H, -CH aromatic, J<sub>o</sub>=8.5), 7.77 (d, 2H, -CH aromatic, J<sub>o</sub>=8.5), 7.55 (d, 1H, -CH aromatic, J<sub>o</sub>=8), 7.53 (d, 2H, -CH aromatic, J<sub>o</sub>=8.5), 7.45 (t, 1H, -CH aromatic, J<sub>o1,2</sub>=8.5), 7.26 (d, 2H, -CH aromatic, J<sub>o</sub>=8.5), 7.02 (t, 1H, -CH aromatic, J<sub>o1,2</sub>=8), 6.95 (d, 2H, -CH aromatic, J<sub>o</sub>=8.5), 5.95 (dd, 1H, -CH<sub>x</sub> pyrazoline, J<sub>AX</sub>=4;

$J_{MX}=11$ ), 4.21 (dd, 1H, -CH<sub>M</sub> pyrazoline,  $J_{MA}=18$ ;  $J_{MX}=11$ ), 3.74 (s, 3H, -OCH<sub>3</sub>), 3.57 (dd, 1H, -CH<sub>A</sub> pyrazoline,  $J_{AM}=18$ ;  $J_{AX}=4$ ).

**(EMAC 4034) 5-chloro-3-{2-[5-(4-methoxyphenyl)-3-(4-biphenyl)-4,5-dihydropyrazol-1-yl]}-4-oxothiazol-5(4H)-ylidene)-indolin-2-one**

Orange solid; MW 591.08 g/mol; Mp 340-342°C

<sup>1</sup>H NMR (500 MHz, DMSO-d<sub>6</sub>): δ 11.28 (s, 1H, -NH isatin), 8.99 (s, 1H, -CH aromatic), 8.03 (d, 2H, -CH aromatic,  $J_o=8.5$ ), 7.88 (d, 2H, -CH aromatic,  $J_o=8.5$ ), 7.77 (d, 2H, -CH aromatic,  $J_o=8.5$ ), 7.53 (t, 2H, -CH aromatic,  $J_{o1,2}=8.5$ ), 7.46-7.40 (m, 2H, -CH aromatic), 7.27 (d, 2H, -CH aromatic,  $J_o=8.5$ ), 6.95 (d, 3H, -CH aromatic,  $J_o=8.5$ ), 5.95 (dd, 1H, -CH<sub>X</sub> pyrazoline,  $J_{AX}=4$ ;  $J_{MX}=11$ ), 4.21 (dd, 1H, -CH<sub>M</sub> pyrazoline,  $J_{MA}=18$ ;  $J_{MX}=11$ ), 3.75 (s, 3H, -OCH<sub>3</sub>), 3.57 (dd, 1H, -CH<sub>A</sub> pyrazoline,  $J_{AM}=18$ ;  $J_{AX}=4$ ).

**(EMAC 4037) 5-fluoro-3-{2-[5-(4-methoxyphenyl)-3-(4-biphenyl)-4,5-dihydropyrazol-1-yl]}-4-oxothiazol-5(4H)-ylidene)-indolin-2-one**

Orange solid; MW 574.62 g/mol; Mp *nd*

<sup>1</sup>H NMR (500 MHz, DMSO-d<sub>6</sub>): δ 11.17 (s, 1H, -NH isatin), 8.75 (d, 1H, -CH aromatic,  $J_o=9$ ), 8.03 (d, 2H, -CH aromatic,  $J_o=8.5$ ), 7.88 (d, 2H, -CH aromatic,  $J_o=8.5$ ), 7.77 (d, 2H, -CH aromatic,  $J_o=8.5$ ), 7.53 (t, 2H, -CH aromatic,  $J_{o1,2}=8.5$ ), 7.44 (t, 1H, -CH aromatic,  $J_{o1,2}=8.5$ ), 7.27 (d, 2H, -CH aromatic,  $J_o=8.5$ ), 7.22 (t, 1H, -CH aromatic,  $J_{o1,2}=8.5$ ), 6.96-6.91 (m, 3H, -CH aromatic), 5.95 (dd, 1H, -CH<sub>X</sub> pyrazoline,  $J_{AX}=4$ ;  $J_{MX}=11$ ), 4.21 (dd, 1H, -CH<sub>M</sub> pyrazoline,  $J_{MA}=18$ ;  $J_{MX}=11$ ), 3.74 (s, 3H, -OCH<sub>3</sub>), 3.57 (dd, 1H, -CH<sub>A</sub> pyrazoline,  $J_{AM}=18$ ;  $J_{AX}=4$ ).

**(EMAC 4038) 7-fluoro-3-{2-[5-(4-methoxyphenyl)-3-(4-biphenyl)-4,5-dihydropyrazol-1-yl]}-4-oxothiazol-5(4H)-ylidene)-indolin-2-one**

Orange solid; Mw 574.62 g/mol; Mp 311-313°C

<sup>1</sup>H NMR (500 MHz, DMSO-d<sub>6</sub>): δ 11.67 (s, 1H, -NH isatin), 8.79 (d, 1H, -CH aromatic,  $J_o=8$ ), 8.03 (d, 2H, -CH aromatic,  $J_o=8.5$ ), 7.88 (d, 2H, -CH aromatic,  $J_o=8.5$ ), 7.77 (d, 2H, -CH aromatic,  $J_o=8.5$ ), 7.53 (t, 2H, -CH aromatic,  $J_{o1,2}=8.5$ ), 7.45 (t, 1H, -CH aromatic,  $J_{o1,2}=8.5$ ), 7.32-7.26 (m, 3H, -CH aromatic), 7.09-7.05 (m, 1H, -CH aromatic), 6.95 (d, 2H, -CH aromatic,  $J_o=8.5$ ), 5.95 (dd, 1H, -CH<sub>X</sub> pyrazoline,  $J_{AX}=4$ ;  $J_{MX}=11$ ), 4.21 (dd, 1H, -CH<sub>M</sub> pyrazoline,  $J_{MA}=18$ ;  $J_{MX}=11$ ), 3.74 (s, 3H, -OCH<sub>3</sub>), 3.57 (dd, 1H, -CH<sub>A</sub> pyrazoline,  $J_{AM}=18$ ;  $J_{AX}=4$ ).

**(EMAC 4039) 5-iodo-3-{2-[5-(4-methoxyphenyl)-3-(4-biphenyl)-4,5-dihydropyrazol-1-yl]}-4-oxothiazol-5(4H)-ylidene)-indolin-2-one**

Orange solid; MW 682.53 g/mol; Mp *nd*

<sup>1</sup>H NMR (500 MHz, DMSO-d<sub>6</sub>): δ 11.27 (s, 1H, -NH isatin), 9.29 (s, 1H, -CH aromatic), 8.03 (d, 2H, -CH aromatic,  $J_o=8.5$ ), 7.88 (d, 2H, -CH aromatic,  $J_o=8.5$ ), 7.77 (d, 2H, -CH aromatic,  $J_o=8.5$ ), 7.68 (d, 1H, -CH aromatic,  $J_o=8.5$ ), 7.53 (t, 2H, -CH aromatic,  $J_{o1,2}=8.5$ ), 7.45 (t, 1H, -CH aromatic,  $J_{o1,2}=8.5$ ), 7.27 (d, 2H, -CH aromatic,  $J_o=8.5$ ), 6.95 (d, 2H, -CH aromatic,  $J_o=8.5$ ), 6.79 (d, 1H, -CH aromatic,  $J_o=8.5$ ), 5.95 (dd, 1H, -CH<sub>X</sub> pyrazoline,  $J_{AX}=4$ ;

$J_{MX}=11$ ), 4.21 (dd, 1H, -CH<sub>M</sub> pyrazoline,  $J_{MA}=18$ ;  $J_{MX}=11$ ), 3.74 (s, 3H, -OCH<sub>3</sub>), 3.57 (dd, 1H, -CH<sub>A</sub> pyrazoline,  $J_{AM}=18$ ;  $J_{AX}=4$ ).

**(EMAC 4040) 5-methoxy-3-{2-[5-(4-methoxyphenyl)-3-(4-biphenyl)-4,5-dihydropyrazol-1-yl]}-4-oxothiazol-5(4H)-ylidene)-indolin-2-one**

Red solid; MW 586.66 g/mol; Mp 322-323°C

<sup>1</sup>H NMR (500 MHz, DMSO-d<sub>6</sub>): δ 10.96 (s, 1H, -NH isatin), 8.66 (d, 1H, -CH aromatic,  $J_m=2.5$ ), 8.03 (d, 2H, -CH aromatic,  $J_o=8.5$ ), 7.88 (d, 2H, -CH aromatic,  $J_o=8.5$ ), 7.77 (d, 2H, -CH aromatic,  $J_o=8.5$ ), 7.53 (d, 2H, -CH aromatic,  $J_o=8.5$ ), 7.45 (t, 1H, -CH aromatic,  $J_{o1,2}=8.5$ ), 7.26 (d, 2H, -CH aromatic,  $J_o=8.5$ ), 6.98-6.94 (m, 3H, -CH aromatic), 6.84 (d, 1H, -CH aromatic,  $J_o=8.5$ ), 5.94 (dd, 1H, -CH<sub>X</sub> pyrazoline,  $J_{AX}=4$ ;  $J_{MX}=11$ ), 4.21 (dd, 1H, -CH<sub>M</sub> pyrazoline,  $J_{MA}=18$ ;  $J_{MX}=11$ ), 3.75 (s, 6H, -OCH<sub>3</sub>), 3.57 (dd, 1H, -CH<sub>A</sub> pyrazoline,  $J_{AM}=18$ ;  $J_{AX}=4$ ).

**(EMAC 4041) 5-methyl-3-{2-[5-(4-methoxyphenyl)-3-(4-biphenyl)-4,5-dihydropyrazol-1-yl]}-4-oxothiazol-5(4H)-ylidene)-indolin-2-one**

Orange solid; MW 570.66 g/mol; Mp 336-338°C

<sup>1</sup>H NMR (500 MHz, DMSO-d<sub>6</sub>): δ 11.04 (s, 1H, -NH isatin), 8.77 (s, 1H, -CH aromatic), 8.03 (d, 2H, -CH aromatic,  $J_o=8.5$ ), 7.88 (d, 2H, -CH aromatic,  $J_o=8.5$ ), 7.77 (d, 2H, -CH aromatic,  $J_o=8.5$ ), 7.53 (d, 2H, -CH aromatic,  $J_o=8.5$ ), 7.44 (t, 1H, -CH aromatic,  $J_{o1,2}=8.5$ ), 7.26 (d, 2H, -CH aromatic,  $J_o=8.5$ ), 7.18 (d, 1H, -CH aromatic,  $J_o=8.5$ ), 6.95 (d, 2H, -CH aromatic,  $J_o=8.5$ ), 6.83 (d, 1H, -CH aromatic,  $J_o=8.5$ ), 5.94 (dd, 1H, -CH<sub>X</sub> pyrazoline,  $J_{AX}=4$ ;  $J_{MX}=11$ ), 4.21 (dd, 1H, -CH<sub>M</sub> pyrazoline,  $J_{MA}=18$ ;  $J_{MX}=11$ ), 3.74 (s, 3H, -OCH<sub>3</sub>), 3.57 (dd, 1H, -CH<sub>A</sub> pyrazoline,  $J_{AM}=18$ ;  $J_{AX}=4$ ), 2.29 (s, 3H, -CH<sub>3</sub>).

**(EMAC 4042) 5-trifluoromethyl-3-{2-[5-(4-methoxyphenyl)-3-(4-biphenyl)-4,5-dihydropyrazol-1-yl]}-4-oxothiazol-5(4H)-ylidene)-indolin-2-one**

Orange solid; MW 624.14 g/mol; Mp 343-344°C

<sup>1</sup>H NMR (500 MHz, DMSO-d<sub>6</sub>): δ 11.34 (s, 1H, -NH isatin), 8.98 (s, 1H, -CH aromatic), 8.03 (d, 2H, -CH aromatic,  $J_o=8.5$ ), 7.88 (d, 2H, -CH aromatic,  $J_o=8.5$ ), 7.77 (d, 2H, -CH aromatic,  $J_o=8.5$ ), 7.53 (d, 2H, -CH aromatic,  $J_o=8.5$ ), 7.45 (t, 1H, -CH aromatic,  $J_{o1,2}=8.5$ ), 7.38 (d, 2H, -CH aromatic,  $J_o=8.5$ ), 7.27 (d, 1H, -CH aromatic,  $J_o=8.5$ ), 7.02 (d, 2H, -CH aromatic,  $J_o=8.5$ ), 6.95 (dd, 1H, -CH<sub>X</sub> pyrazoline,  $J_{AX}=4$ ;  $J_{MX}=11$ ), 4.22 (dd, 1H, -CH<sub>M</sub> pyrazoline,  $J_{MA}=18$ ;  $J_{MX}=11$ ), 3.75 (s, 3H, -OCH<sub>3</sub>), 3.58 (dd, 1H, -CH<sub>A</sub> pyrazoline,  $J_{AM}=18$ ;  $J_{AX}=4$ ).

**Series 5: Synthesis of 3-{2-[5-(4-chlorophenyl)-3-(naphthalen-2-yl)-4,5-dihydropyrazol-1-yl]}-4-oxothiazol-5(4H)-ylidene)-indolin-2-one (EMAC 4066-4075)**

***Synthesis of 3-(4-chlorophenyl)-1-(naphthalen-2-yl)-2-propen-1-one***

An aqueous solution of NaOH 10% (1.2 mmol; 480 μL) was slowly added to a solution of 2-acetyl-naphthalene (1 mmol; 170 mg) in ethanol. The mixture was vigorously stirred, until to obtain a cloudy solution. Then, a solution in ethanol of 4-methoxy-

benzaldehyde (1.2 mmol; 163 mg) is added dropwise and a light yellow suspension is formed. The obtained solid was filtered, washed with water and ethanol to give a light yellow solid. This crude product was crystallized from ethanol. The whole reaction was carried out keeping the temperature around 0°C and its progression monitored with TLC, using ethyl acetate/petroleum ether 1:1 as eluent.

Light yellow solid; Yield 63%; MW 292.76 g/mol; Mp 147-148 °C

<sup>1</sup>H NMR (500 MHz, chloroform-d): δ 8.56 (s, 1H, -CH aromatic), 8.12 (d, 1H, -CH aromatic, J<sub>o</sub>=8.5), 8.03 (d, 1H, -CH aromatic, J<sub>o</sub>=8.5), 7.97 (d, 1H, -CH aromatic, J<sub>o</sub>=8.5), 7.93 (d, 1H, -CH aromatic, J<sub>o</sub>=8.5), 7.85 (d, 1H, -CH propen, J<sub>E</sub>=15.5), 7.69 (d, 1H, -CH propen, J<sub>E</sub>=15.5), 7.66-7.59 (m, 4H, -CH aromatic), 7.44 (dd, 2H, -CH aromatic, J<sub>o</sub>=8.5; J<sub>m</sub>=2).

#### ***Synthesis of 5-(4-chlorophenyl)-3-(naphthalen-2-yl)-4,5-dihydropyrazole-1-carbothioamide***

A freshly prepared solution of alcoholic KOH 5% (1.2 mmol; 1.3 mL) was added dropwise to a mixture of 3-(4-chloro-phenyl)-1-(naphthalen-2-yl)-2-propenone (1 mmol, 293 mg) and thiosemicarbazide (1.2 mmol; 110 mg) in ethanol. This solution was refluxed until reaction completion, checking the progression with TLC. This solution was cooled at room temperature, obtaining a yellow suspension. The solid was filtered out, washed with water and crystallized from ethanol.

Yellow solid; Yield 81%; MW 365.88 g/mol; Mp 203-204°C

<sup>1</sup>H NMR (500 MHz, chloroform-d): δ 8.03 (d, 1H, -CH aromatic, J<sub>o</sub>=8.5), 7.99 (s, 1H, -CH aromatic), 7.92-7.86 (m, 3H, -CH aromatic), 7.60-7.54 (m, 2H, -CH aromatic), 7.33 (d, 2H, -CH aromatic, J<sub>o</sub>=8.5), 7.23 (d, 2H, -CH aromatic, J<sub>o</sub>=8.5), 6.09 (dd, 1H, -CH<sub>x</sub> pyrazoline, J<sub>AX</sub>=4; J<sub>MX</sub>=11), 4.00 (dd, 1H, -CH<sub>M</sub> pyrazoline, J<sub>MA</sub>=18; J<sub>MX</sub>=11), 3.35 (dd, 1H, -CH<sub>A</sub> pyrazoline, J<sub>AM</sub>=18; J<sub>AX</sub>=4).

#### ***Synthesis of 3-{2-[5-(4-chlorophenyl)-3-(naphthalen-2-yl)-4,5-dihydropyrazol-1-yl]}-4-oxothiazol-5(4H)-ylidene)-indolin-2-one***

A mixture of 5-(4-chlorophenyl)-3-(naphthalen-2-yl)-1-thiocarbamoyl-2-pyrazoline (1.0 mmol), ethyl bromoacetate (1.0 mmol), appropriate isatin (1.2 mmol), and anhydrous sodium acetate (2.0 mmol) was refluxed in glacial acetic acid (5 mL) until reaction completion. The mixture was cooled at room temperature and the obtained precipitate was filtered off, washed with water and methanol.

#### **(EMAC 4066) 7-bromo-3-{2-[5-(4-chlorophenyl)-3-(naphthalen-2-yl)-4,5-dihydropyrazol-1-yl]}-4-oxothiazol-5(4H)-ylidene)-indolin-2-one**

Light orange solid; MW 613.91 g/mol; Mp 347-348°C

<sup>1</sup>H NMR (500 MHz, DMSO-d<sub>6</sub>): δ 11.45 (s, 1H, -NH isatin), 8.96 (d, 1H, -CH aromatic, J<sub>o</sub>=8), 8.42 (s, 1H, -CH aromatic), 8.12 (d, 1H, -CH aromatic, J<sub>o</sub>=8.5), 8.09-8.02 (m, 3H, -CH aromatic), 7.68-7.61 (m, 2H, -CH aromatic), 7.56 (d, 1H, -CH aromatic, J<sub>o</sub>=8), 7.47 (d, 2H, -



CH aromatic,  $J_o=8$ ), 7.39 (d, 2H, -CH aromatic,  $J_o=8$ ), 7.03 (t, 1H, -CH aromatic,  $J_{o1}=J_{o2}=8$ ), 6.06 (dd, 1H, -CH<sub>X</sub> pyrazoline,  $J_{XA}=4$ ;  $J_{XM}=11$ ), 4.31 (dd, 1H, -CH<sub>M</sub> pyrazoline,  $J_{MA}=18$ ;  $J_{MX}=11$ ), 3.68 (dd, 1H, -CH<sub>A</sub> pyrazoline,  $J_{AM}=18$ ;  $J_{AX}=4$ ).

**(EMAC 4067) 5-chloro-3-{2-[5-(4-chlorophenyl)-3-(naphthalen-2-yl)-4,5-dihydropyrazol-1-yl]}-4-oxothiazol-5(4H)-ylidene)-indolin-2-one**

Orange solid; MW 569.49 g/mol; Mp 359-360°C

<sup>1</sup>H NMR (500 MHz, DMSO-d<sub>6</sub>): δ 11.31 (s, 1H, -NH isatin), 8.97 (s, 1H, -CH aromatic), 8.41 (s, 1H, -CH aromatic), 8.11 (d, 1H, -CH aromatic,  $J_o=8.5$ ), 8.08-8.01 (m, 3H, -CH aromatic), 7.67-7.61 (m, 2H, -CH aromatic), 7.47 (d, 2H, -CH aromatic,  $J_o=8$ ), 7.41-7.39 (m, 3H, -CH aromatic), 6.97 (d, 1H, -CH aromatic,  $J_o=8$ ), 6.06 (dd, 1H, -CH<sub>X</sub> pyrazoline,  $J_{XA}=4$ ;  $J_{XM}=11$ ), 4.32 (dd, 1H, -CH<sub>M</sub> pyrazoline,  $J_{MA}=18$ ;  $J_{MX}=11$ ), 3.69 (dd, 1H, -CH<sub>A</sub> pyrazoline,  $J_{AM}=18$ ;  $J_{AX}=4$ ).

**(EMAC 4069) 5,7-dimethyl-3-{2-[5-(4-chlorophenyl)-3-(naphthalen-2-yl)-4,5-dihydropyrazol-1-yl]}-4-oxothiazol-5(4H)-ylidene)-indolin-2-one**

Orange solid; MW 563.07 g/mol; Mp 365-366°C

<sup>1</sup>H NMR (500 MHz, DMSO-d<sub>6</sub>): δ 11.08 (s, 1H, -NH isatin), 8.63 (s, 1H, -CH aromatic), 8.41 (s, 1H, -CH aromatic), 8.13 (d, 1H, -CH aromatic  $J_o=8.5$ ), 8.09-8.02 (m, 3H, -CH aromatic), 7.68-7.61 (m, 2H, -CH aromatic), 7.47 (d, 2H, -CH aromatic,  $J_o=8$ ), 7.38 (d, 2H, -CH aromatic,  $J_o=8$ ), 7.02 (s, 1H, -CH aromatic), 6.06 (dd, 1H, -CH<sub>X</sub> pyrazoline,  $J_{XA}=4$ ;  $J_{XM}=11$ ), 4.31 (dd, 1H, -CH<sub>M</sub> pyrazoline,  $J_{MA}=18$ ;  $J_{MX}=11$ ), 3.68 (dd, 1H, -CH<sub>A</sub> pyrazoline,  $J_{AM}=18$ ;  $J_{AX}=4$ ), 2.26 (s, 3H, -CH<sub>3</sub>), 2.21 (s, 3H, -CH<sub>3</sub>).

**(EMAC 4070) 5-fluoro-3-{2-[5-(4-chlorophenyl)-3-(naphthalen-2-yl)-4,5-dihydropyrazol-1-yl]}-4-oxothiazol-5(4H)-ylidene)-indolin-2-one**

Orange solid; MW 553.01 g/mol; Mp 367-368°C

<sup>1</sup>H NMR (500 MHz, DMSO-d<sub>6</sub>): δ 11.20 (s, 1H, -NH isatin), 8.74 (dd, 1H, -CH isatin,  $J_{oH-F}=10.5$ ;  $J_{mH-H}=2.5$ ), 8.41 (s, 1H, -CH aromatic), 8.11 (d, 1H, -CH aromatic,  $J_o=8.5$ ), 8.09-8.02 (m, 3H, -CH aromatic), 7.67-7.61 (m, 2H, -CH aromatic), 7.47 (d, 2H, -CH aromatic,  $J_o=8.5$ ), 7.39 (d, 2H, -CH aromatic,  $J_o=8.5$ ), 7.22 (td, 1H, -CH isatin,  $J_{oH-H}=8.5$ ;  $J_{oH-F}=10.5$ ;  $J_{mH-H}=2.5$ ), 6.93 (dd, 1H, -CH isatin,  $J_{oH-H}=8.5$ ;  $J_{mH-F}=5$ ), 6.05 (dd, 1H, -CH<sub>X</sub> pyrazoline,  $J_{XA}=4$ ;  $J_{XM}=11$ ), 4.33 (dd, 1H, -CH<sub>M</sub> pyrazoline,  $J_{MA}=18$ ;  $J_{MX}=11$ ), 3.70 (dd, 1H, -CH<sub>A</sub> pyrazoline,  $J_{AM}=18$ ;  $J_{AX}=4$ ).

**(EMAC 4071) 7-fluoro-3-{2-[5-(4-chlorophenyl)-3-(naphthalen-2-yl)-4,5-dihydropyrazol-1-yl]}-4-oxothiazol-5(4H)-ylidene)-indolin-2-one**

Red solid; MW 553.01 g/mol; Mp 336-338°C

<sup>1</sup>H NMR (500 MHz, DMSO-d<sub>6</sub>): δ 11.69 (s, 1H, -NH isatin), 8.77 (d, 1H, -CH isatin,  $J_o=8$ ), 8.40 (s, 1H, -CH aromatic), 8.11 (d, 1H, -CH aromatic,  $J_o=8.5$ ), 8.09 (d, 1H, -CH aromatic,  $J_o=8.5$ ), 8.07 (d, 1H, -CH aromatic,  $J_o=8.5$ ), 8.05 (d, 1H, -CH aromatic,  $J_o=8.5$ ), 8.02 (d, 1H, -CH aromatic,  $J_o=8.5$ ), 7.67-7.60 (m, 2H, -CH aromatic), 7.47 (d, 2H, -CH aromatic,  $J_o=8.5$ ), 7.39 (d, 2H, -CH aromatic,  $J_o=8.5$ ), 7.29 (t, 1H, -CH isatin,  $J_{oH-H}=8.5$ ), 7.06

(dt, 1H, -CH isatin,  $J_{\text{OH-H}}=8.5$ ;  $J_{\text{MH-F}}=5.5$ ), 6.05 (dd, 1H, -CH<sub>X</sub> pyrazoline,  $J_{\text{AX}}=4$ ;  $J_{\text{MX}}=11$ ), 4.31 (dd, 1H, -CH<sub>M</sub> pyrazoline,  $J_{\text{MA}}=18$ ;  $J_{\text{MX}}=11$ ), 3.67 (dd, 1H, -CH<sub>A</sub> pyrazoline,  $J_{\text{AM}}=18$ ;  $J_{\text{AX}}=4$ ).

**(EMAC 4072) 5-iodo-3-{2-[5-(4-chlorophenyl)-3-(naphthalen-2-yl)-4,5-dihydropyrazol-1-yl]}-4-oxothiazol-5(4H)-ylidene)-indolin-2-one**

Orange solid; MW 660.91 g/mol; Mp 338-340°C

<sup>1</sup>HNMR (500 MHz, DMSO-d<sub>6</sub>): δ 11.92 (s, 1H, -N=C-OH isatin, enolic tautomer), 11.29 (s, 1H, -NH isatin), 9.27 (s, 1H, -CH isatin), 8.41 (s, 1H, aromatic), 8.11 (d, 1H, -CH aromatic,  $J_{\text{o}}=8.5$ ), 8.09-8.05 (m, 2H, -CH aromatic), 8.02 (d, 1H, -CH aromatic,  $J_{\text{o}}=8.5$ ), 7.67-7.61 (m, 3H, -CH aromatic and -CH isatin), 7.47 (d, 2H, -CH aromatic,  $J_{\text{o}}=8.5$ ), 7.39 (d, 2H, -CH aromatic,  $J_{\text{o}}=8.5$ ), 6.79 (d, 1H, -CH isatin,  $J_{\text{o}}=8$ ), 6.06 (dd, 1H, -CH<sub>X</sub> pyrazoline,  $J_{\text{AX}}=4$ ;  $J_{\text{MX}}=11$ ), 4.32 (dd, 1H, -CH<sub>M</sub> pyrazoline,  $J_{\text{MA}}=18$ ;  $J_{\text{MX}}=11$ ), 3.69 (dd, 1H, -CH<sub>A</sub> pyrazoline,  $J_{\text{AM}}=18$ ;  $J_{\text{AX}}=4$ ).

**(EMAC 4073) 5-methoxy-3-{2-[5-(4-chlorophenyl)-3-(naphthalen-2-yl)-4,5-dihydropyrazol-1-yl]}-4-oxothiazol-5(4H)-ylidene)-indolin-2-one**

Brown solid; MW 565.04 g/mol; Mp 313-314°C

<sup>1</sup>HNMR (500 MHz, DMSO-d<sub>6</sub>): δ 10.97 (s, 1H, -NH isatin), 8.65 (s, 1H, -CH isatin), 8.41 (s, 1H, aromatic), 8.11 (d, 1H, -CH aromatic,  $J_{\text{o}}=8.5$ ), 8.09-8.05 (m, 2H, -CH aromatic), 8.02 (d, 1H, -CH aromatic,  $J_{\text{o}}=8.5$ ), 7.67-7.60 (m, 2H, -CH aromatic), 7.47 (d, 2H, -CH aromatic,  $J_{\text{o}}=8.5$ ), 7.39 (d, 2H, -CH aromatic,  $J_{\text{o}}=8.5$ ), 6.98 (dd, 1H, -CH isatin,  $J_{\text{o}}=8.5$ ;  $J_{\text{m}}=2$ ), 6.84 (d, 1H, -CH isatin,  $J_{\text{o}}=8.5$ ), 6.04 (dd, 1H, -CH<sub>X</sub> pyrazoline,  $J_{\text{AX}}=4$ ;  $J_{\text{MX}}=11$ ), 4.31 (dd, 1H, -CH<sub>M</sub> pyrazoline,  $J_{\text{MA}}=18$ ;  $J_{\text{MX}}=11$ ), 3.74 (s, 3H, -OCH<sub>3</sub>), 3.68 (dd, 1H, -CH<sub>A</sub> pyrazoline,  $J_{\text{AM}}=18$ ;  $J_{\text{AX}}=4$ ).

**(EMAC 4074) 5-methyl-3-{2-[5-(4-chlorophenyl)-3-(naphthalen-2-yl)-4,5-dihydropyrazol-1-yl]}-4-oxothiazol-5(4H)-ylidene)-indolin-2-one**

Red solid; MW 549.04 g/mol; Mp 348°C

<sup>1</sup>HNMR (500 MHz, DMSO-d<sub>6</sub>): δ 11.05 (s, 1H, -NH isatin), 8.75 (s, 1H, -CH isatin), 8.40 (s, 1H, aromatic), 8.11 (d, 1H, -CH aromatic,  $J_{\text{o}}=8.5$ ), 8.08-8.04 (m, 2H, -CH aromatic), 8.02 (d, 1H, -CH aromatic,  $J_{\text{o}}=8.5$ ), 7.67-7.60 (m, 2H, -CH aromatic), 7.47 (d, 2H, -CH aromatic,  $J_{\text{o}}=8.5$ ), 7.39 (d, 2H, -CH aromatic,  $J_{\text{o}}=8.5$ ), 7.16 (d, 1H, -CH isatin,  $J_{\text{o}}=8.5$ ), 6.82 (d, 1H, -CH isatin,  $J_{\text{o}}=8.5$ ), 6.04 (dd, 1H, -CH<sub>X</sub> pyrazoline,  $J_{\text{AX}}=4$ ;  $J_{\text{MX}}=11$ ), 4.30 (dd, 1H, -CH<sub>M</sub> pyrazoline,  $J_{\text{MA}}=18$ ;  $J_{\text{MX}}=11$ ), 3.67 (dd, 1H, -CH<sub>A</sub> pyrazoline,  $J_{\text{AM}}=18$ ;  $J_{\text{AX}}=4$ ), 3.31 (s, 3H, -CH<sub>3</sub>).

**(EMAC 4075) 5-trifluoromethyl-3-{2-[5-(4-chlorophenyl)-3-(naphthalen-2-yl)-4,5-dihydropyrazol-1-yl]}-4-oxothiazol-5(4H)-ylidene)-indolin-2-one**

Red solid; MW 603.01 g/mol; Mp 328-330°C

<sup>1</sup>HNMR (500 MHz, DMSO-d<sub>6</sub>): δ 11.92 (s, 1H, -N=C-OH isatin, enolic tautomer), 11.36 (s, 1H, -NH isatin), 8.96 (s, 1H, -CH isatin), 8.42 (s, 1H, aromatic), 8.12 (d, 1H, -CH aromatic,  $J_{\text{o}}=8.5$ ), 8.09-8.05 (m, 2H, -CH aromatic), 8.02 (d, 1H, -CH aromatic,  $J_{\text{o}}=8.5$ ), 7.67-7.61 (m, 3H, -CH aromatic and -CH isatin), 7.47 (d, 2H, -CH aromatic,  $J_{\text{o}}=8.5$ ), 7.39 (d, 2H, -CH aromatic,  $J_{\text{o}}=8.5$ ), 7.38 (d, 1H, -CH isatin,  $J_{\text{o}}=8.5$ ), 7.02 (d, 1H, -CH isatin,  $J_{\text{o}}=8.5$ ),

6.06 (dd, , 1H, -CH<sub>X</sub> pyrazoline, J<sub>AX</sub>=4; J<sub>MX</sub>=11), 4.32 (dd, 1H, -CH<sub>M</sub> pyrazoline, J<sub>MA</sub>=18; J<sub>MX</sub>=11), 3.69 (dd, 1H, -CH<sub>A</sub> pyrazoline, J<sub>AM</sub>=18; J<sub>AX</sub>=4).

### 1.4.3 Biological assays

Biological assays have been performed in the National Cancer Institute on the bases of specific protocols. NCI-60 screening is carried out in two parts ([ntp.cancer.gov/discovery\\_development/nci-60](http://ntp.cancer.gov/discovery_development/nci-60)): at first a single concentration is tested in all 60 cell lines at a single dose of 10<sup>-5</sup> M or 15 µg/mL. If the results obtained meet the established criteria, the compound is tested again in all 60 cell lines in 5 10-fold dilutions. In this screening the highest dose is 10<sup>-4</sup> M or 150 µg/mL.

The human tumor cell lines of the cancer screening panel are grown in RPMI 1640 medium containing 5% fetal bovine serum and 2 mM L-glutamine. For a typical experiment, cells are inoculated into 96 well microtiter plates in 100 µL at plating densities ranging from 5,000 to 40,000 cells/well, depending on the cell line . After cell inoculation, the microtiter plates are incubated at 37°C, 5% CO<sub>2</sub>, 95% air and 100% relative humidity for 24 h prior to add the tested compound. After 24 h, two plates of each cell line are fixed *in situ* with TCA, to represent a measurement of the cell population for each cell line at the time of drug addiction (Tz). Experimental compounds are solubilized in dimethyl sulfoxide at 400-fold the desired final maximum test concentration and stored frozen prior to use. At the time of drug addition, an aliquot of frozen concentrate is thawed and diluted to twice the desired final maximum test concentration with complete medium containing 50 µg/mL gentamicin. Additional four, 10-fold or ½ log serial dilutions are made to provide a total of five drug concentrations plus control. Aliquots of 100 µL of these different drug dilutions are added to the appropriate microtiter wells already containing 100 µL of medium, resulting in the required final drug concentrations. Following drug addition, the plates are incubated for an additional 48 h at 37°C, 5% CO<sub>2</sub>, 95% air, and 100% relative humidity. For adherent cells, the assay is terminated by the addition of cold TCA. Cells are fixed *in situ* by the gentle addition of 50 µL of cold 50% (w/v) TCA (final concentration, 10% TCA) and incubated for 60 minutes at 4°C. The supernatant is discarded, and the plates are washed five times with tap water and air dried. Sulforhodamine B (SRB) solution (100 µL) at 0.4% (w/v) in 1% acetic acid is added to each well, and plates are incubated for 10 minutes at room temperature. After staining, unbound dye is removed by washing five times with 1% acetic acid and the plates are air dried. Bound stain is subsequently solubilized with 10 mM trizma base, and the absorbance is read on an automated plate reader at a wavelength of 515 nm. For suspension cells, the methodology is the same except that the assay is terminated by fixing settled cells at the bottom of the wells by gently adding 50 µL of 80% TCA (final concentration, 16% TCA). Using the seven absorbance measurements [time zero, (Tz), control growth, (C), and test growth in the presence of drug at the five concentration

levels (Ti)], the percentage growth is calculated at each of the drug concentrations levels. Percentage growth inhibition is calculated as:

$$[(Ti-Tz)/(C-Tz)] \times 100 \text{ for concentrations for which } Ti \geq Tz$$

$$[(Ti-Tz)/Tz] \times 100 \text{ for concentrations for which } Ti < Tz.$$

Three dose response parameters are calculated for each experimental agent. Growth inhibition of 50% ( $GI_{50}$ ) is calculated from  $[(Ti-Tz)/(C-Tz)] \times 100 = 50$ , which is the drug concentration resulting in a 50% reduction in the net protein increase (as measured by SRB staining) in control cells during the drug incubation. The drug concentration resulting in total growth inhibition (TGI) is calculated from  $Ti = Tz$ . The  $LC_{50}$  (concentration of drug resulting in a 50% reduction in the measured protein at the end of the drug treatment as compared to that at the beginning) indicating a net loss of cells following treatment is calculated from  $[(Ti-Tz)/Tz] \times 100 = -50$ . Values are calculated for each of these three parameters if the level of activity is reached; however, if the effect is not reached or is exceeded, the value for that parameter is expressed as greater or less than the maximum or minimum concentration tested.

#### 1.4 REFERENCES

1. Nepali, K.; Sharma, S.; Sharma, M.; Bedi, P. M.; Dhar, K. L., Rational approaches, design strategies, structure activity relationship and mechanistic insights for anticancer hybrids. *Eur. J. Med. Chem.* **2014**, *77*, 422-87.
2. Melisi, D.; Piro, G.; Tamburrino, A.; Carbone, C.; Tortora, G., Rationale and clinical use of multitargeting anticancer agents. *Curr. Opin. Pharmacol.* **2013**, *13*, 536-42.
3. Gediya, L. K.; Njar, V. C., Promise and challenges in drug discovery and development of hybrid anticancer drugs. *Expert Opin Drug Discov* **2009**, *4*, 1099-111.
4. Zimmermann, G. R.; Lehar, J.; Keith, C. T., Multi-target therapeutics: when the whole is greater than the sum of the parts. *Drug Discov. Today* **2007**, *12*, 34-42.
5. Frantz, S., The trouble with making combination drugs. *Nat. Rev. Drug Discov.* **2006**, *5*, 881-2.
6. Meunier, B., Hybrid molecules with a dual mode of action: dream or reality? *Acc. Chem. Res.* **2008**, *41*, 69-77.
7. Berube, G., An overview of molecular hybrids in drug discovery. *Expert Opin Drug Discov* **2016**, 1-25.
8. Srivastava, V.; Lee, H., Chloroquine-based hybrid molecules as promising novel chemotherapeutic agents. *Eur. J. Pharmacol.* **2015**, *762*, 472-86.
9. Descoteaux, C.; Brasseur, K.; Leblanc, V.; Asselin, E.; Berube, G., Exploring the Synthesis and Anticancer Potential of L-Tyrosine-Platinum(II) Hybrid Molecules. *Med. Chem.* **2015**, *11*, 717-24.
10. Loch-Neckel, G.; Bicca, M. A.; Leal, P. C.; Mascarello, A.; Siqueira, J. M.; Calixto, J. B., In vitro and in vivo anti-glioma activity of a chalcone-quinoxaline hybrid. *Eur. J. Med. Chem.* **2015**, *90*, 93-100.
11. Vilanova, C.; Diaz-Oltra, S.; Murga, J.; Falomir, E.; Carda, M.; Redondo-Horcajo, M.; Diaz, J. F.; Barasoain, I.; Marco, J. A., Design and synthesis of pironetin analogue/colchicine hybrids and study of their cytotoxic activity and mechanisms of interaction with tubulin. *J. Med. Chem.* **2014**, *57*, 10391-403.
12. Wang, L.; Switalska, M.; Wang, N.; Du, Z. J.; Fukumoto, Y.; Diep, N. K.; Kiguchi, R.; Nokami, J.; Wietrzyk, J.; Inokuchi, T., Design, synthesis, and biological evaluation of

artemisinin-indoloquinoline hybrids as potent antiproliferative agents. *Molecules* **2014**, *19*, 19021-35.

13. Kamal, A.; Balakrishna, M.; Nayak, V. L.; Shaik, T. B.; Faazil, S.; Nimbarte, V. D., Design and synthesis of imidazo[2,1-b]thiazole-chalcone conjugates: microtubule-destabilizing agents. *ChemMedChem* **2014**, *9*, 2766-80.

14. Vine, K. L.; Matesic, L.; Locke, J. M.; Ranson, M.; Skropeta, D., Cytotoxic and anticancer activities of isatin and its derivatives: a comprehensive review from 2000-2008. *Anticancer Agents Med. Chem.* **2009**, *9*, 397-414.

15. Vine, K. L.; Matesic, L.; Locke, J. M.; Skropeta, D. Recent highlights in the development of isatin-based anticancer agents. 2013; Bentham Science Publishers Ltd.: 2013; Vol. 2; pp 254-312.

16. Kaminsky, D.; Khylyuk, D.; Vasylenko, O.; Zaprutko, L.; Lesyk, R., A Facile Synthesis and Anticancer Activity Evaluation of Spiro[Thiazolidinone-Isatin] Conjugates. *Scientia Pharmaceutica* **2011**, *79*, 763-777.

17. Sharma, M.; Sharma, S.; Buddhiraja, A.; Saxena, A. K.; Nepali, K.; Bedi, P. M. S., Synthesis and cytotoxicity studies of 3,5-diaryl N-acetyl pyrazoline-isatin hybrids. *Med. Chem. Res.* **2014**, *23*, 4337-4344.

18. Havrylyuk, D.; Zimenkovsky, B.; Vasylenko, O.; Gzella, A.; Lesyk, R., Synthesis of new 4-thiazolidinone-, pyrazoline-, and isatin-based conjugates with promising antitumor activity. *J. Med. Chem.* **2012**, *55*, 8630-41.

19. Yusuf, M.; Jain, P., Synthetic and biological studies of pyrazolines and related heterocyclic compounds. *Arabian Journal of Chemistry* **2014**, *7*, 553-596.

20. Devinyak, O.; Havrylyuk, D.; Avdieiev, S.; Chumak, V.; Panchuk, R.; Stoika, R.; Kavsan, V.; Lesyk, R., Virtual Screening and its Experimental Validation Reveal Novel Compounds with Promising Anticancer Activity Among 4-Thiazolidinone- Pyrazoline- and Isatin-Based Conjugates. *Austin Journal of Bioorganic & Organic Chemistry* **2014**, *1*, 1-6.

21. Altintop, M. D.; Ozdemir, A.; Turan-Zitouni, G.; Ilgin, S.; Atli, O.; Demirel, R.; Kaplancikli, Z. A., A novel series of thiazolyl-pyrazoline derivatives: synthesis and evaluation of antifungal activity, cytotoxicity and genotoxicity. *Eur. J. Med. Chem.* **2015**, *92*, 342-52.

## **2 DESIGN AND SYNTHESIS OF PSORALEN DERIVATIVES AS DNA G-QUADRUPLEX STABILISERS**

### **2.1 INTRODUCTION**

From a molecular point of view, tumours can be defined as a consequence of impaired functions of DNA. Considering the complexity of the events related to cancer development, this definition could appear simplistic, however it shows immediately the reason why DNA has been the main target of anticancer therapy and research for several decades. The continuous advances in molecular biology and in the correlated fields provide a better knowledge of the physio-pathological processes and expand the number of potential targets for the antitumour therapy. In particular, a deeper appreciation of DNA functions arises from the recognition of its plasticity and its consequent ability to form a variety of conformations.<sup>1</sup>

These non-conventional forms of DNA, including Z-DNA, triplex, cruciform and quadruplexes, were originally individuated *in vitro* using biophysical methods, such as circular dichroism. Their existence has been confirmed *in vivo* using structure-specific antibodies and structure-binding ligands.<sup>2</sup> Among these possible DNA conformations, increasing attention has been focused toward G-quadruplex secondary structures. These structures are found in some repetitive genome sequences, in which guanine rich motifs are present, having relevant functions in the regulation of DNA metabolic processes, such as transcription and replication. More in detail, these sequences are found at the telomeric ends of chromosomes and in the transcriptional regulatory regions of several important oncogenes. Because both telomeric regions and activation of oncogenes are very important targets for anti-cancer drug design, G-quadruplex sequences are more and more attractive molecular targets in the anticancer drug development.<sup>1,3</sup>

The high potential of the quadruplexes-interacting molecules is related to the privileged position of these structures in the over-activated regions of the malignancy genome. Therefore, the selective stabilization of these structures in cancer cells could pave the way for high selective targeted antitumour therapies.

### **2.2 G-QUADRUPLEX: STRUCTURE AND CONFORMATIONS**

Generally, DNA is thought as a double-helix in which the two self-complementary strands are held together by Watson-Crick base pairs. Actually, DNA is a polymorphic and dynamic macromolecule that exhibits a number of structures, which significantly differ from canonical B-form. In particular, certain DNA sequences containing purine rich tracts (guanine runs) can form non-canonical four-strand architectures, named G-quadruplexes. The elemental skeleton of a DNA G-quadruplex structure is formed by at least two

contiguous stacked tetrads, in physiological ionic conditions. Each tetrad, also named G-quartet, stems from the planar association of four guanines in a cyclic Hoogsteen hydrogen bonding arrangement.<sup>1, 4</sup> G-tetrads are linked each other by short sequences, indicated as loops, whose nucleotides are not usually included in the tetrads.

These structures can be composed of one, two or four different strands of a nucleic acid. Therefore, the combination of different structural parameters, as the number of stacked tetrads, the strand polarity and the loop sequence, size and localization explain the high conformation variability of G-quadruplex topologies.<sup>5, 6</sup> G-quadruplex architecture can be also described in terms of grooves, whose dimensions (depth and width) and accessibility are a direct consequence of both tetrad arrangements and loop conformation.<sup>7</sup>

Monovalent cations, such as  $K^+$  and  $Na^+$ , further stabilize these structures coordinating the eight carbonyl oxygen atoms (in the position 6 of guanine) included among following tetrads. In fact, as a result of Hoogsteen bond formation, these groups are oriented toward the inner side of the G-quartet, creating a strong negative electrostatic potential. As a consequence, a channel is formed into the tetrads, that can accommodate monovalent cations (Figure 2.1).<sup>8</sup>

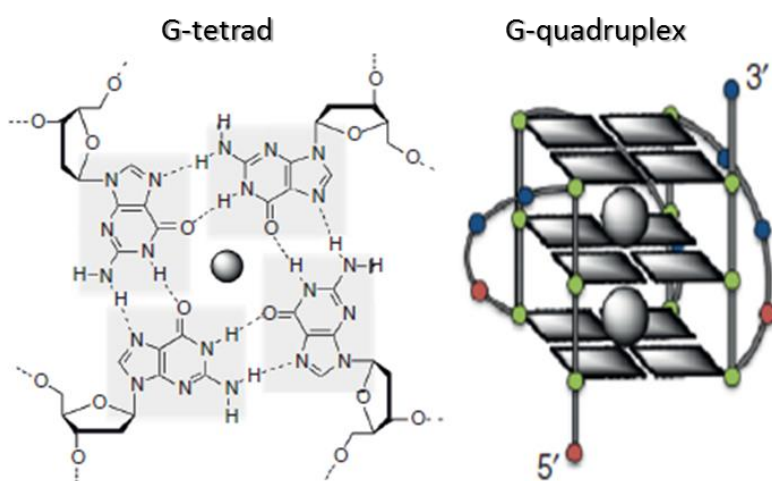


**Figure 2.1.** Illustration of a G-4 structure: G-4 architecture (on the right) are formed by the association of tetrads. Each tetrad (on the left) stem from the planar association of four guanines, stabilized by monovalent cations.<sup>8</sup>

Thus, the cation-dependent stability of G-quadruplexes is associated to the ability of these positive charged species to minimize this electrostatic potential. The effective location of dehydrated cations between tetrads depends on the nature of the ion. For example, the different size of  $K^+$  and  $Na^+$  influences their positioning and, in particular,  $Na^+$  ions are mainly located in the plane formed by G-tetrads whilst  $K^+$  can be found between G-tetrad planes. Therefore,  $K^+$  ions are always equidistant from the two subsequent G-tetrad planes and form a symmetric tetragonal bi-pyramidal configuration



with the eight oxygen atoms of tetrads. In general  $K^+$  is a better stabilizer of G-quadruplexes compared to  $Na^+$  and this probably reflects, in part, a much greater energetic penalty for  $Na^+$  dehydration. Finally, as shown by NMR analysis, the same sequence can adopt different G-quadruplex conformations in  $Na^+$  or  $K^+$  solutions. Thus, the nature of cation affects both stability and architecture of quadruplex DNA.<sup>5-7</sup>

As above mentioned, the highly polymorphic nature of G-quadruplex structures is strictly related to the association of different factors, including: the strand orientation, the *syn/anti* glycosidic conformation of guanines and the loop features (Figure 2.2).

First, the different strand directionalities are function of the glycosidic conformation of the guanines. In this regard, four possibilities are known:

1. the four strands are oriented in the same direction and the glycosidic angles are *anti-anti-anti-anti* and occasionally *syn-syn-syn-syn*;
2. three strands are oriented in the same direction and one is oriented in the opposite direction: the glycosidic angles can be *syn-anti-anti-anti* or *anti-syn-syn-syn*;
3. two adjacent strands are oriented in one direction and the others are oriented in the opposite manner: in this way each strand has as neighbours both parallel and anti-parallel strands and the glycosidic angles are *syn-syn-anti-anti*;
4. the last possibility is the geometry *anti-syn-anti-syn*, in which all the strands have anti-parallel neighbours.<sup>7</sup>

Finally, the loops can also affect the structural variability of G-quadruplex depending on their size and sequence, and are classified in four main families:

1. edge-wise or lateral loops connect two adjacent anti-parallel strands and are generally composed by at least two residues;
2. diagonal loops connect two opposing anti-parallel strands and are generally composed by three or more residues;
3. double-chain reversal or propeller loops connect adjacent parallel strands and can be very small (only one residue) or large (six or more residues). When the single residue double-chain reversal loop is an adenine that bridges two G-tetrads planes, there is the probability that this residue forms hydrogen bonds with one edge of G-tetrad, forming an A-(G-G-G-G) pentad.
4. V-shaped loops connect two corners of a G-tetrad core characterized by a missing support column.

In addition, loop residues can form base pairing alignments, which stack with terminal G-tetrads, further stabilizing quadruplex DNA.<sup>7</sup>

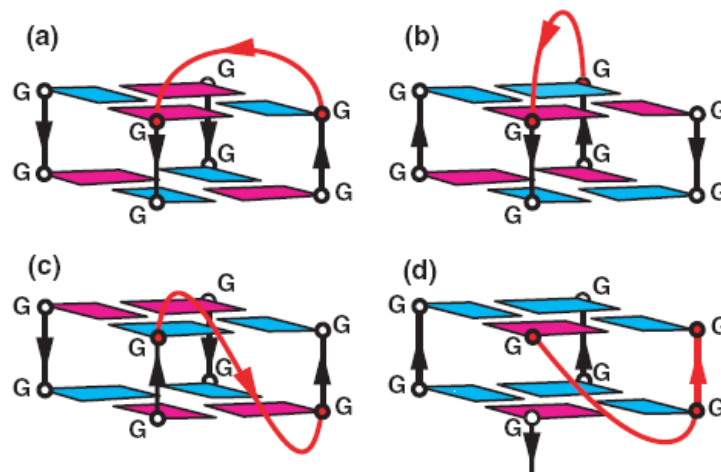


**Figure 2.2.** Schematic representation of loops and glycosidic conformations: a) edge-wise; b) diagonal; c) double chain reversal and d) V-shaped loops; glycosidic conformation are indicated as blue (*anti*) and magenta (*sin*).<sup>7</sup>

It is worth noting that each element of a tetraplex provides a possible target in the design of anticancer therapeutics. For example, the different topologies assumed by loops or grooves make them a target for small molecule-based ligand recognition. In addition, the conformation specificity in diverse genome sequences, arising from the mutual association of the possible structural features, complicates significantly the scenario. However, these differences could be exploited to confer high selectivity in the ligand-substrate recognition process, making possible the differentiation between two G-quadruplex forms (e.g. telomeric vs oncogene promoting region).<sup>7</sup>

### 2.3 DNA G-QUADRUPLEX: GENOMIC LOCALIZATION AND BIOLOGICAL ROLE

The presence of putative G-quadruplexes in the human genome has been dissected by predictive algorithms, resulting in more than 370.000 potential quadruplex structures.<sup>8</sup> The actual presence of these structures *in vivo* was confirmed by the discovery of G-quadruplex interacting proteins, including both stabilizing proteins as well as helicases and nucleases, that display G-quadruplex specificity. These findings indicate that each cell may be able to stabilize, form and remove quadruplex motifs and, most importantly, that G-quadruplexes might be routinely assembled and disassembled from duplex DNA during favourable physiologic conditions. Moreover, during the replication, recombination, transcription and telomeric elongation, the two strands of the ordinary B-form are transiently unpaired, providing an opportunity for the G-rich strand to form quadruplex structures.<sup>4,5</sup>

According to these considerations, potential quadruplex sequences have been identified in G-rich eukaryotic telomeres and in non-telomeric genomic DNA such as nuclease-hypersensitive promoter regions.<sup>6,8</sup>

### 2.3.1 DNA G-quadruplex in telomeric ends

Telomeres are nucleoprotein complexes located at the ends of linear eukaryotic chromosomes, to promote chromosomal stability and genetic stability. In addition, telomeric ends provide sites for recombination events and transcriptional silencing, and are crucial in cellular aging and tumorigenesis. Telomeric ends are composed by double strands and guanine rich 3'-overhang segments. Telomeric overhangs can be elongated by the telomerase, a ribonucleoprotein complex endowed with reverse transcriptase activity. Since this enzyme is expressed in the majority of cancer cells, the maintaining of the telomere length that leads to immortalization has been related to cancer pathogenesis.<sup>9</sup> The 3'-overhang G-rich sequence (TTAGGG)<sub>n</sub>, can exist both as single-strand and in a number of G-quadruplex folding variants. These forms are in equilibrium and telomeric quadruplexes have been found to block the telomerase activity, making inaccessible its target. Therefore, the stabilization of telomeric G-quadruplexes in cancer cells by rationally designed small-molecules may be a valid strategy in anticancer drug development. Nevertheless, since the telomeric shortening is also associated with several pathology states and premature cell aging, the unselective stabilization of these structures in healthy cells could be related to the onset of adverse effects.<sup>7</sup>

### 2.3.2 DNA G-quadruplex in oncogene promoter regions

The presence of G-quadruplex structures was also discovered in the promoter regions of genes generally involved in growth and proliferation. These genes are TATA-less and contain GC-rich motifs in the proximal regions of promoters. It has been demonstrated that the occurrence of these structures is more probable in oncogene promoters rather than in onco-suppressor genes and have been reported for *human c-MYC*, *human-BCL-2*, *human* and *mouse KRAS*, *human VEGF*, *human c-KIT*, *human HIF-1 $\alpha$*  and several other promoter regions. The G-rich sequences of gene promoters present different and peculiar structures with respect to telomeric quadruplexes. More in detail, promoter sequences may contain more than four G-motifs and each of them is unique for number and length of the G-tracts, as well as for the number of intervening bases. Different combinations of these parameter are possible, and thus multiple G-rich promoter sequences topologies were found. The GC-rich region in the proximal region of these promoters is usually hypersensitive to nucleases and may form an altered structure with a single-stranded character, which is often a feature of transcriptionally active genes. Promoter regions of *c-MYC*, *VEGF*, *HIF-1  $\alpha$* , *c-KIT*, *KRAS*, and *Bcl-2*, form three-tetrads G-quadruplex geometries. The comparison of the G-quadruplex-forming motifs among these genes reveals a sequence similarity, leading to a unique transcriptional regulation mechanism that involves the interconversion between a G-quadruplex, unwound single-

stranded DNA, and duplex DNA. In addition, in the 3'-end of each one of these sequences, an identical motif ( $G_3NG_3$ ) is present, which forms a single-nucleotide double-chain-reversal loop. Since the  $G_3NG_3$  motif is widespread in the promoter intramolecular G-quadruplex structures, it has been proposed as the stable core around which the different intramolecular G-quadruplex structures can be assembled.<sup>10, 11</sup>

The most extensively studied system for the G-quadruplex formation in gene promoters is *c-MYC*, whose overexpression has been associated with a large number of human malignancies, including colon, breast, prostate, cervical, and small-cell lung carcinomas, osteosarcomas, glioblastomas, lymphomas and myeloid leukemia.<sup>12</sup> Considering the importance of *c-MYC* in cell proliferation, differentiation and apoptosis, it is not surprising that its transcriptional expression is tightly regulated by several promoters and start sites. A highly conserved 27-base-pair nuclease hypersensitivity element III1 (NHE III<sub>1</sub>), located in the proximal region of the *c-MYC* promoter, controls 80–90% of the transcriptional activity. The formation of a G-quadruplex structure in this portion is critical for *c-MYC* transcriptional silencing. Therefore, compounds that bind and stabilize G-quadruplex conformations, formed in NHE III<sub>1</sub>, may reduce *c-MYC* expression and, consequently, display antitumour activity.<sup>13</sup>

Similarly to *c-MYC*, the proximal promoters of other human oncogenes, such as *BCL-2*, *VEGF*, *HIF-1  $\alpha$* , *KRAS*, *PDGF-A* and *c-MYB* also contain poly-G regulatory elements and have been shown to form intramolecular G-quadruplex structures. These findings further confirm the high therapeutic potential of DNA G-quadruplex stabilizers.<sup>10</sup>

## **2.4 SMALL MOLECULES TARGETING G-QUADRUPLEX DNA**

The recognition of the biological significance of G-quadruplex architectures provided a novel approach to anticancer drug design and development. In the last decades, different families of small-molecule G-quadruplex interactive compounds have been proposed, with continuous improvements in affinity and specificity.

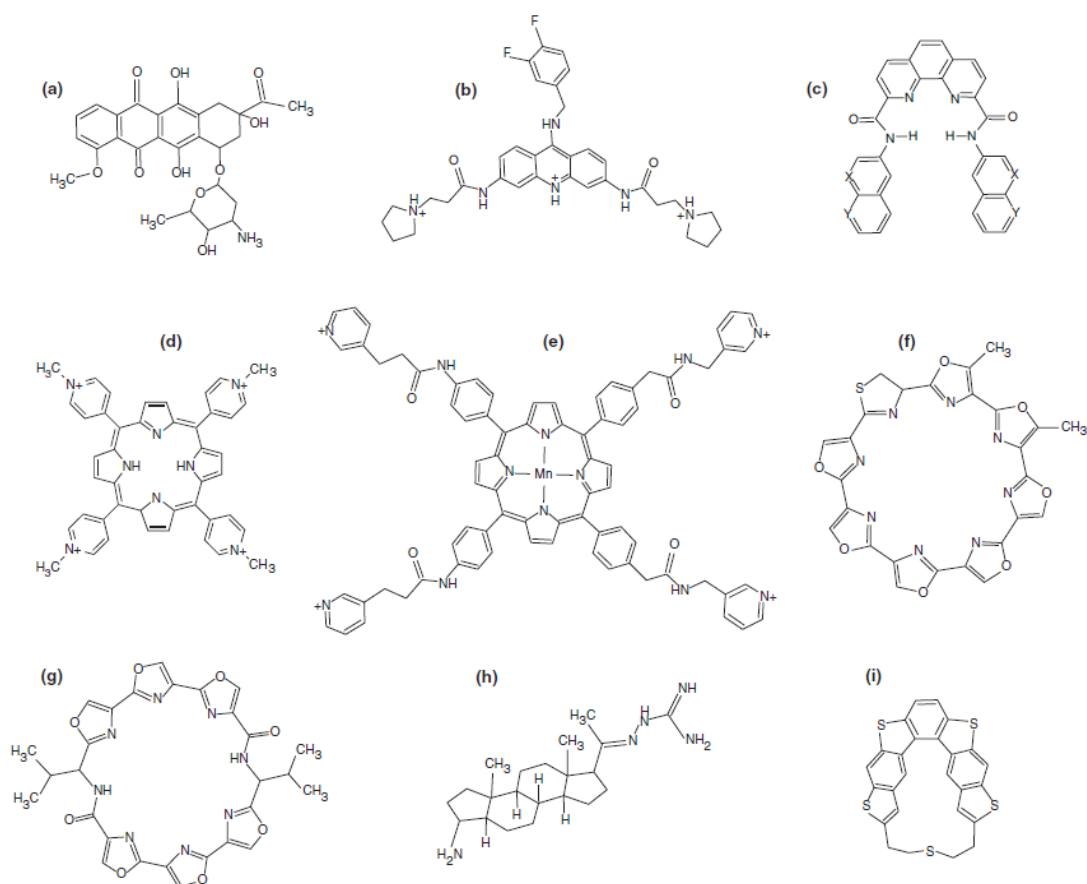


**Figure 2.3.** Chemical structures of G-quadruplex binders: a) daunomycin, b) 9-benzylamino-substituted acridine, c) bisquinolinium-substituted phenanthroline, d) 5,10,15,20-tetrakis-(N-methyl-4-pyridyl)porphyrin, e) Mn(III) porphyrin with flexible cationic arms, f) telomestatin, g) oxazole containing 24-membered macrocycle, h) steroid diamine funtumine and left-hend chiral cyclic helicene with a short linker.<sup>7</sup>

Among them, it is possible to observe some structural features commonly found in the G-quadruplex targeting-ligands. In particular, each compound exhibits a planar fused-ring system, which enables stacking interactions with terminal G-tetrads. The insertion of a lateral chain, in which a positive charge group can be present, increases the propensity of these molecules to interact with G-quadruplex grooves, leading a comprehensive tetraplex structure stabilization.<sup>10</sup>

Despite the continuing advancing in the understanding of the structural features necessary for an optimal interaction, none of the synthesized compounds passed the clinical trial so far. This unbalance between the SARs knowledges acquired and the lack of G-quadruplex binders in the market is related to a series of limitations inherent to these compounds, including the poor selectivity and druggability properties (poor water solubility, propensity to aggregate in aqueous media, chemical instability).<sup>14</sup>

## 2.5 RATIONAL DESIGN OF PSORALEN DERIVATIVES

### 2.5.1 Computational study

This work aims to the synthesis of different series of compounds, characterized by a psoralen scaffold, thought to interact and stabilise DNA G-quadruplex. Despite several examples reported in literature, only a restricted number of G-quadruplex ligands reached the clinical phase, but none of them is in the market. Therefore, to increase the success possibilities, the synthetic work of these psoralens was derived by a computational study in which ligand-based, structure-based, and *in silico* ADMET prediction approaches were combined.<sup>15</sup> The applied methods include fingerprints Molecular ACCess System (MACCS) MDL public Keys,<sup>16</sup> implemented in Pipeline Pilot<sup>17</sup> and Rapid Overlay of Chemical Structures (ROCS),<sup>18</sup> which aligns molecules according to their shape and chemical similarity. These similarity filters were combined with a tool able to predict molecular properties in order to discard, at an early stage, compounds with unfavourable ADMET profiles.<sup>19</sup> Then, ligand based selected compounds were submitted to ensemble docking simulations on all the four major structurally characterized conformations of the human telomeric sequence. The finally identified compounds were evaluated by biophysical methods to evaluate their G-quadruplex binding properties.<sup>15</sup>

In particular with this virtual screening around 2.7 million compounds from the ZINC database were screened, using RHPS4,<sup>20, 21</sup> CX-3543 (Quarfloxin),<sup>22, 23</sup> SYUIQ5,<sup>24, 25</sup> Triazine-115405,<sup>26</sup> Braco-19,<sup>27, 28</sup> Phen-DC3,<sup>29-31</sup> and BMVC<sup>32, 33</sup> as queries (Figure 2.4 a). These compounds were selected on the bases of their high affinity and selectivity toward G-quadruplex over duplex DNA, chemical diversity, *in vitro* activity in tumour cells, and, eventually, preclinical and clinical studies.

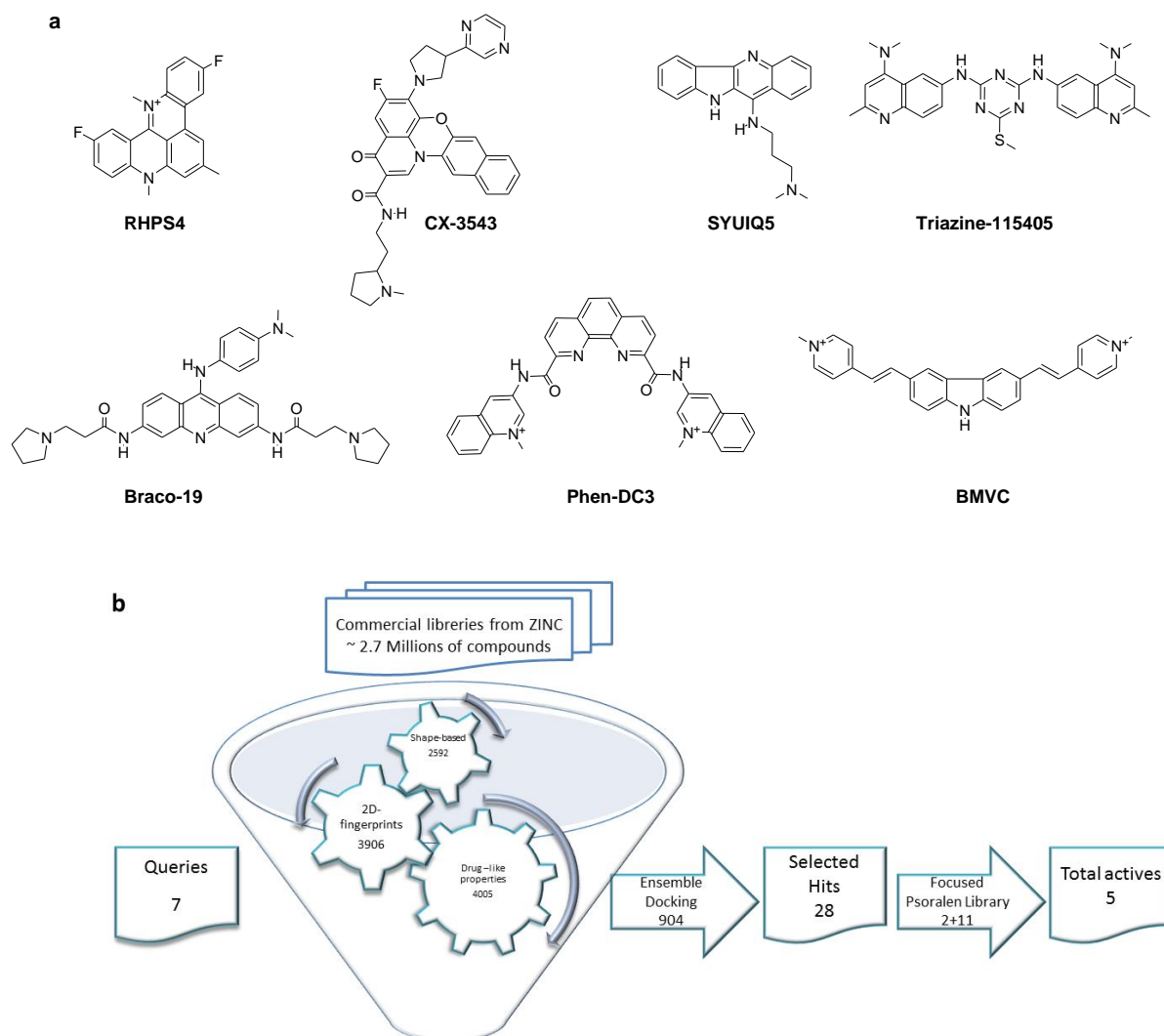


**Figure 2.4.** a) Chemical structures of the queries selected for the similarity VS ; b) Virtual screening workflow.<sup>15</sup>

The similarity of each molecule in the database was calculated with respect to each query, and the compounds were ranked according to their maximum similarity score, obtained using MACCS and ROCS. The best ranked molecules, identified for each query with the applied similarity approaches, were merged obtaining the so-called “data fusion”. This group fusion technique turned out to be more efficient in retrieving hits than searches performed using a single reference compound. In this way, 3906 compounds were selected with MACCS and 2592 compounds with ROCS. The two methods exhibited very low overlap because only 73 compounds were found in common. After discarding the duplicates, we ended up with 6425 compounds (Figure 2.4 b).<sup>15</sup> Moreover, as drug-likeness properties are a key factor in drug development, a further succession of filter were applied, based on the chemical-physical characteristics of drugs in the market. The

properties considered in this protocol included: molecular weight, number of rotatable bonds, hydrogen bond donors and acceptors, lipophilicity (by predicting ALogP), polar, molecular, and solvent accessible surface area, molecular volume, aqueous solubility (Log S), and number of atoms of each molecule.<sup>19</sup> Only 4005 compounds out of 6425 passed this multiple filter. The selected hits were submitted to ensemble docking experiments considering four quadruplex folds (Figure 2.5).

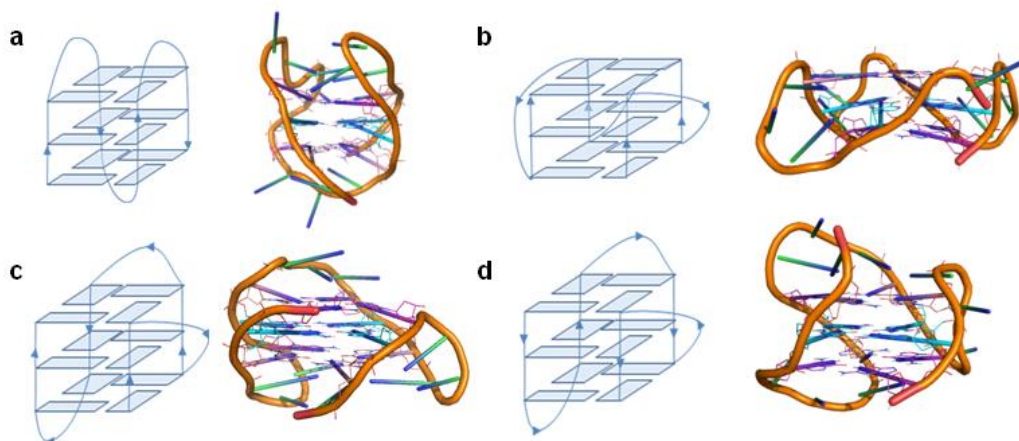


**Figure 2.5.** Schematic and 3D representation of the a) antiparallel or basket-type (pdb code 143d),<sup>34</sup> b) parallel or propeller-like (1kf1),<sup>35</sup> c) hybrid type-1 (2hy9)<sup>36</sup> and d) hybrid type-2 (2j pz)<sup>37</sup> DNA G-quadruplex conformations of d(AG<sub>3</sub>[T<sub>2</sub>AG<sub>3</sub>]<sub>3</sub>) sequence.

In fact, the human telomeric sequence has been shown to fold into at least four distinct structures. They derive from remarkably different arrays of guanine pairing, resulting in distinct strand orientations and loop arrangements. Hence, an efficient approach to overcome the polymorphism hitch is to consider multiple rigid receptor conformations. With ensemble docking, a single ligand library is docked to each target conformation. To properly compare the score energy of the complexes generated by the docking experiments, the receptors are required to have the same sequence. Consequently, the two additional nucleotides at the head and tail caps of the hybrid receptors were removed. We picked up the best compounds according to the highest docking consensus score ( $<-7,5$  kcal/mol). The threshold was chosen after the docking score comparison of active and decoys sets.

Following the described steps, we obtained 904 molecules: 540 were selected by MACCS fingerprints, 351 by ROCS only, and 13 by both. In addition, to take into account the reciprocal ligand-target flexibility, the best poses of the 904 compounds generated by the AutoDock Vina<sup>38</sup> docking were submitted to full energy minimization for each of the four G-quadruplex folds. Hence compounds containing unfavourable functional moieties (e.g., sulfonic ester, terminal vinyl, enol ether, more than one hydroxamic acid, too many



heteroatoms, and phosphonamide groups) were discarded. By sampling the diversity space of the clustered ligands, according to availability from the vendors, we reduced our data set to 28 compounds: 19 were selected from MACCS hit list, eight from ROCS, and one by both methods.

The potential efficiency of the selected compounds in binding G-quadruplex structures was assessed by fluorescence melting studies on a labelled sequence based on the human telomeric one (HTS), an approach extensively validated for screening of G-quadruplex ligand library and already applied to our queries. Most of our selected molecules were not able to increment the thermal stability of the telomeric G-quadruplex when used in the 0.5–10  $\mu\text{M}$  concentration range. Nevertheless, one compound induced a quite relevant shift of the G-quadruplex melting temperature ( $T_m \approx 14^\circ\text{C}$  at 10  $\mu\text{M}$  ligand concentration). This efficiency was reduced in comparison to those exerted by two queries ( $T_m \approx 32$  and  $30^\circ\text{C}$  at 10  $\mu\text{M}$  Braco-19 and RHPS4, respectively) in the same experimental conditions. This was not unexpected due to the selection procedure, thus we considered it worth of further investigation. This positive hit, labelled P1, was selected by MACCS fingerprints based on similarity with the reference query CX3543. This active compound P1 contained a psoralen moiety. Thus, all psoralen derivatives identified by the virtual screening were selected (P1–P7). The resulting new small library (Figure 2.6) was further incremented by “in house” available psoralens structurally related to the hit (P8–P13).

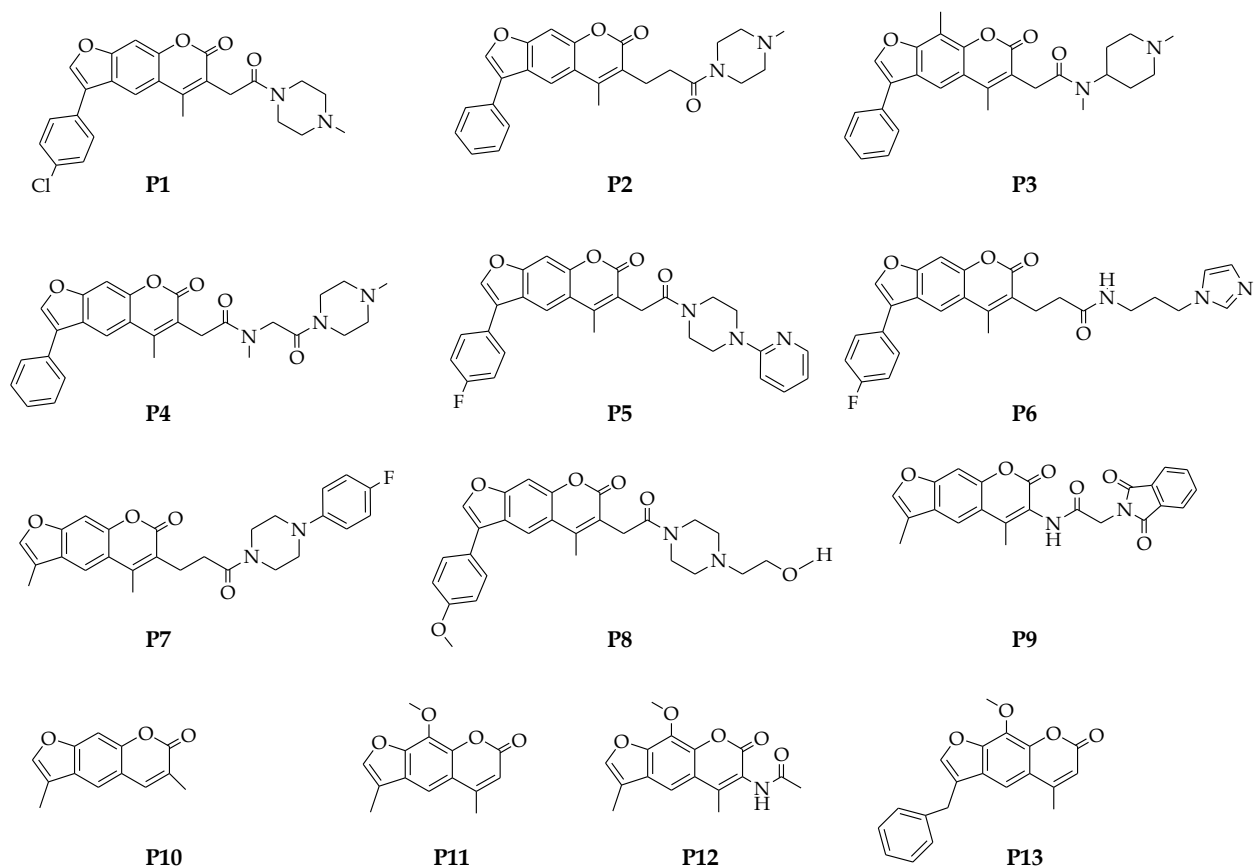


**Figure 2.6.** Chemical structure of psoralens resulting to VS workflow P1-7 and their “in house” structural analogues submitted to bio-physic assays.

All of them were tested in a wide concentration range to confirm the hit. Moreover, a short double-stranded DNA sequence was used as additional target in order to evaluate the ligands selectivity. This screening confirmed P1 and P3 as the most effective G-quadruplex stabilizers. Also P2, P6, and P8 were effective, although higher concentrations were required, with respect to P1 and P3, to achieve a similar effect. Interestingly, none of the selected ligands were able to stabilize the double helix. These results suggest phenyl-psoralen as the basic scaffold required to selectively stabilize the tested G-quadruplex and emphasize some structure-activity relationships:

1. the role of the aromatic ring at position 3 of the psoralen core is relevant: its presence was confirmed to be essential, as P7 and P9–P13 are inactive, and the bulkiness/electronic properties of the substituents are able to modulate the activity;
2. a strong influence of the side chain was highlighted: it should be not too rigid as in P5 and P7, and a small (P1, P2, P3) or a flexible chain (P6 and P8) is preferred;
3. the distance between the aromatic core and the amide group is also important: increasing the length of this linker a reduction in activity occurred. The most active compounds P1 e P3 have a methylene linker.

In addition, the opening of furan ring is detrimental for G-quadruplex recognition because the system loses its planarity, a key parameter to provide stability to the

complex. By analysing the energy minimized docking poses of the best compound P1, these considerations were sustained. In particular, the positively charged substituent was found to interact with the negatively charged phosphate backbone of the G-quadruplex within the grooves/loops, whereas the aromatic portion was alternatively involved in stacking with the bases.<sup>15</sup>

### 2.5.2 Synthetic strategy

On the bases of the SARs obtained by computational analysis the synthesis of different psoralen derivatives has been conceived.

Taken into account these features and combining some structural characteristics of most active compounds (P1 and P3), two series of compounds have been synthesized. Each compound is characterised by a phenyl-psoralen portion. In both series the aromatic ring is substituted with a chlorine atom, but the central core of second series differs from the one of the first series of derivatives, because of the introduction of a methyl group in the position 5 of psoralen. The lateral chain contains both amidic and tertiary amine groups that are spaced by a flexible ethyl- or propyl- group. The nitrogen of amine group is included in a six membered-ring. (Figure 2.7)

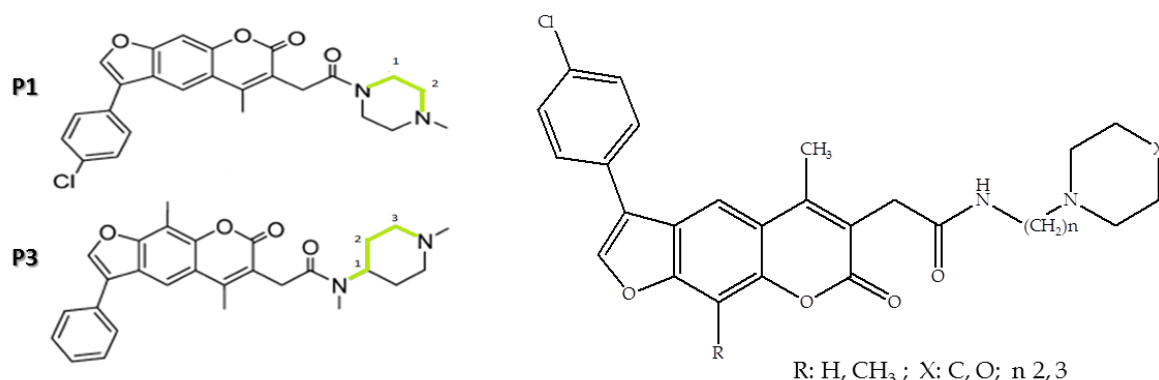
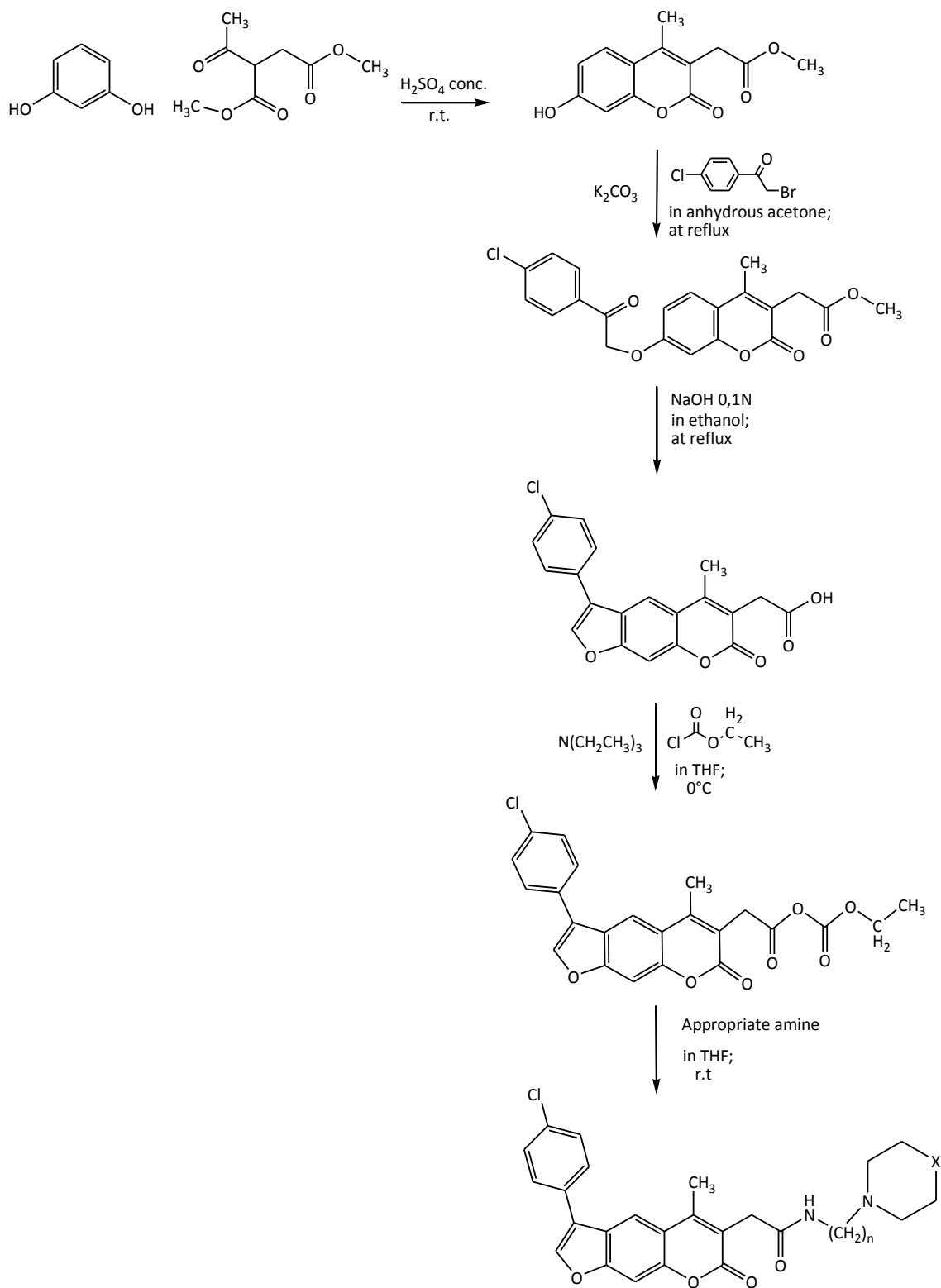


**Figure 2.7.** General structure of synthesized compounds (on the right) compared with the structure of the most active compounds (P1, P3), deriving from VS. The green lines highlight the length of the lateral chain.

Final compounds were obtained by a multi-step synthetic procedure, including:

- a. the synthesis of the psoralen moiety;
- b. the introduction of a lateral chain.

The general method of reaction is reported in Scheme 2.1.



**Scheme 2.1.** General scheme of reaction: in the last compound  $n$  indicates the length of the lateral chain ( $n=2, 2$ ) whilst  $X$  indicate the possibility to have different atoms in the cycle (oxygen or carbon).

The synthesis of substituted psoralen requires, in turn, a set of reactions. Methyl-2-(7-hydroxy-4-methyl-2-oxo-2*H*-3-chromenyl)acetate and methyl-2-(7-hydroxy-4,8-dimethyl-2-oxo-2*H*-3-chromenyl)acetate, that were necessary for further transformations, were prepared by Pechmann condensation of dimethylacetylsuccinate with resorcinol or 2-methylresorcinol, respectively. The reaction is performed in the presence of H<sub>2</sub>SO<sub>4</sub> concentrated as a condensing agent, at room temperature and without any solvent.<sup>39</sup>

Several approaches for the linear fusion of a furan ring to a coumarin core are known.<sup>40, 41</sup> In particular, psoralen systems were prepared by several methods, the majority of which involve numerous steps, low yields and limited possibilities to modify the coumarin and furan ring.<sup>39</sup> Since high flexibility in the synthetic method is required to achieve the final compounds, the method proposed by MacLeod for the total synthesis of psoralens was applied *Errore. L'origine riferimento non è stata trovata.*<sup>42</sup> Thus, the 7-hydroxy-cumarins, obtained in the first step, were reacted with an appropriate  $\alpha$ -halogeno-ketone (2-bromo-4'-chloroacetophenone) in acetone using potassium carbonate as proton scavenger, to obtain the correspondent substituted-oxoether. Then, the oxoether derivative was purified and further reacted to obtain psoralen with high yields in the following step. The cyclization of 7-(2-oxoethyl)coumarin in sodium hydroxide, leads the expected linear furocoumarin. In fact, the position 6 of the coumarin ring is less activated than the position 8. Therefore, the possible formation of the angular isomer is strongly un-favoured and its formation has never been observed. This assumption has been confirmed by <sup>1</sup>H-NMR spectra. In fact, a pattern of three expected singlets, definitely demonstrate that, in these conditions, only the psoralen system is formed (Figure 2.8).

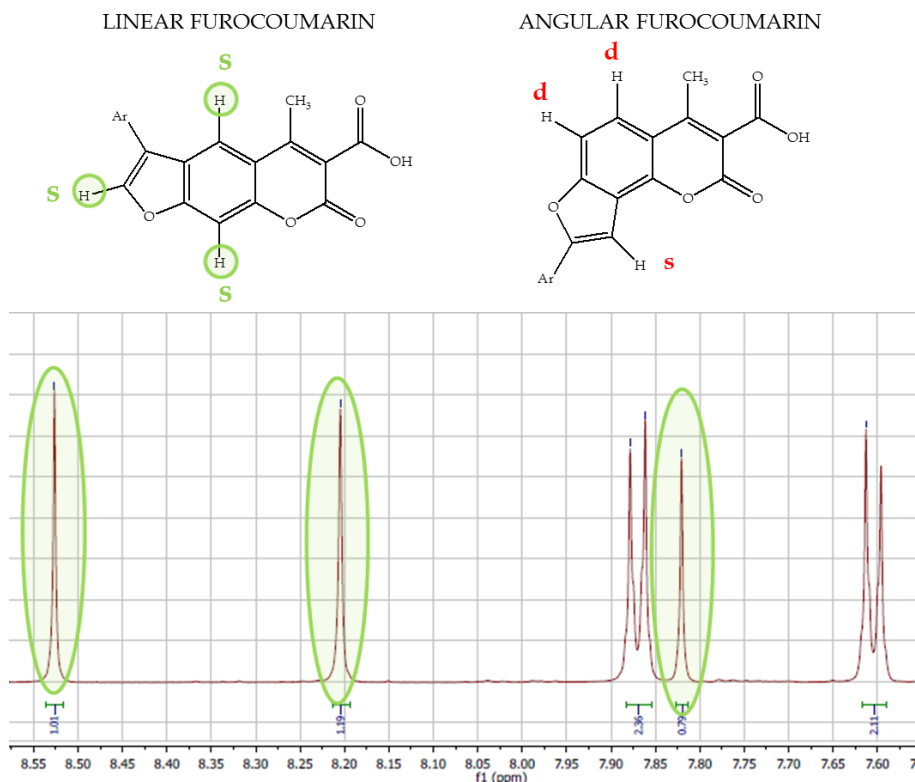


**Figure 2.8.** <sup>1</sup>H NMR spectrum: characteristic signal pattern of synthesized psoralen.

The insertion of the lateral chain involves an amidic bond formation via mixed carbonylic-carboxylic anhydride *Errone. L'origine riferimento non è stata trovata.*<sup>43</sup> The procedure involves separate preparation of the mixed anhydride (activation) and the relative amide derivative (aminolysis). Ethyl chloroformate is slowly added to a solution containing the obtained psoralen and a tertiary amine (triethylamine). The activation is rapid and the formation of mixed anhydride has been observed after 1-2 minutes by the addition of chloroformate. The reaction was performed using dry solvent, keeping the temperature around 0°C. Because of its instability, the mixed anhydride is directly used for the next step. Therefore, it was added dropwise in a solution of the appropriate amine. All stages of this reaction are performed at low temperatures to prevent side reactions.<sup>44</sup> The main side reaction associated with the mixed anhydride method is the aminolysis at the carbonyl of the carbonate moiety, giving a urethane (Figure 2.9).

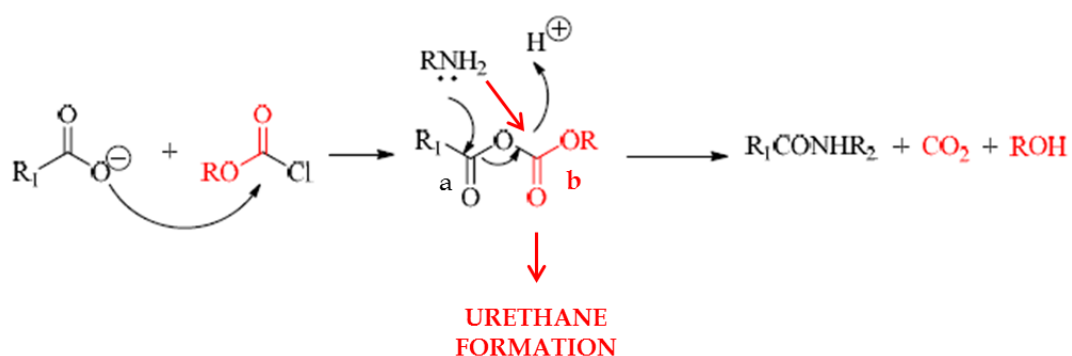


**Figure 2.9.** Urethane formation in the mixed anhydride synthesis.

In most cases, this reaction is not significant because the use of these mixed anhydrides guarantees an excellent regioselectivity, related to electronic effects. In fact, the carbonate electrophilic centre (a) is more reactive than the carboxylic site (b) as the reactive centre a is less stabilised by resonance. However, an additional source of urethane may result from the reaction of unconsumed reagent with the nucleophile. Aminolysis of chloroformate occurs when there is an excess of reagent or when the anhydride-forming reaction is incomplete. This side reaction can be prevented limiting the amount of chloroformate and extending the time of activation. In addition, the analysis of mass spectroscopy data deriving from a sample at the end of the activation reaction, subsequent supported by  $^{13}\text{C}$ -NMR, highlighted the presence of a ester, which formation could be related to an intramolecular reaction (Figure 2.10).

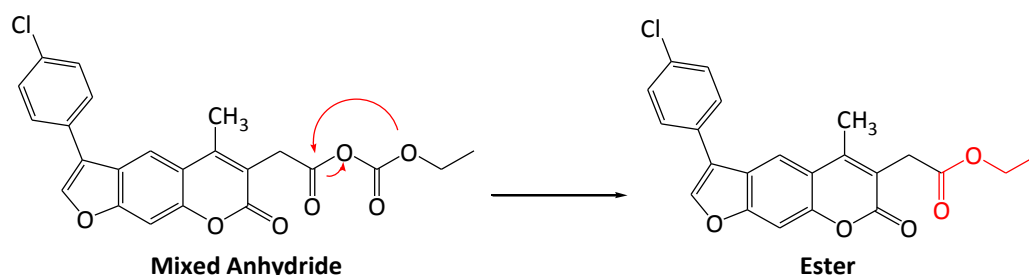


**Figure 2.10.** Proposed intramolecular reaction for the formation of a ester as side product during the activation reaction.

The success of mixed anhydride reactions is considered to be extremely dependent on the choice of conditions used. In particular, the use of dry solvents, like dry THF and DCM, is mandatory.

In order to find the best solvent different trials were done by using THF, DCM or mixtures of this solvents in various ratios. Since the mixture DCM/THF 1:3 provided the best result, the following procedure was applied. Firstly, during the activation, the obtained psoralen was suspended in the minimum amount of DCM. Once obtained, the

mixed anhydride is slowly added to a THF solution containing an excess of the appropriate amine. By using this method yields improvements, in the order of 15%, were obtained. The obtained compounds are reported in Figure 2.11.

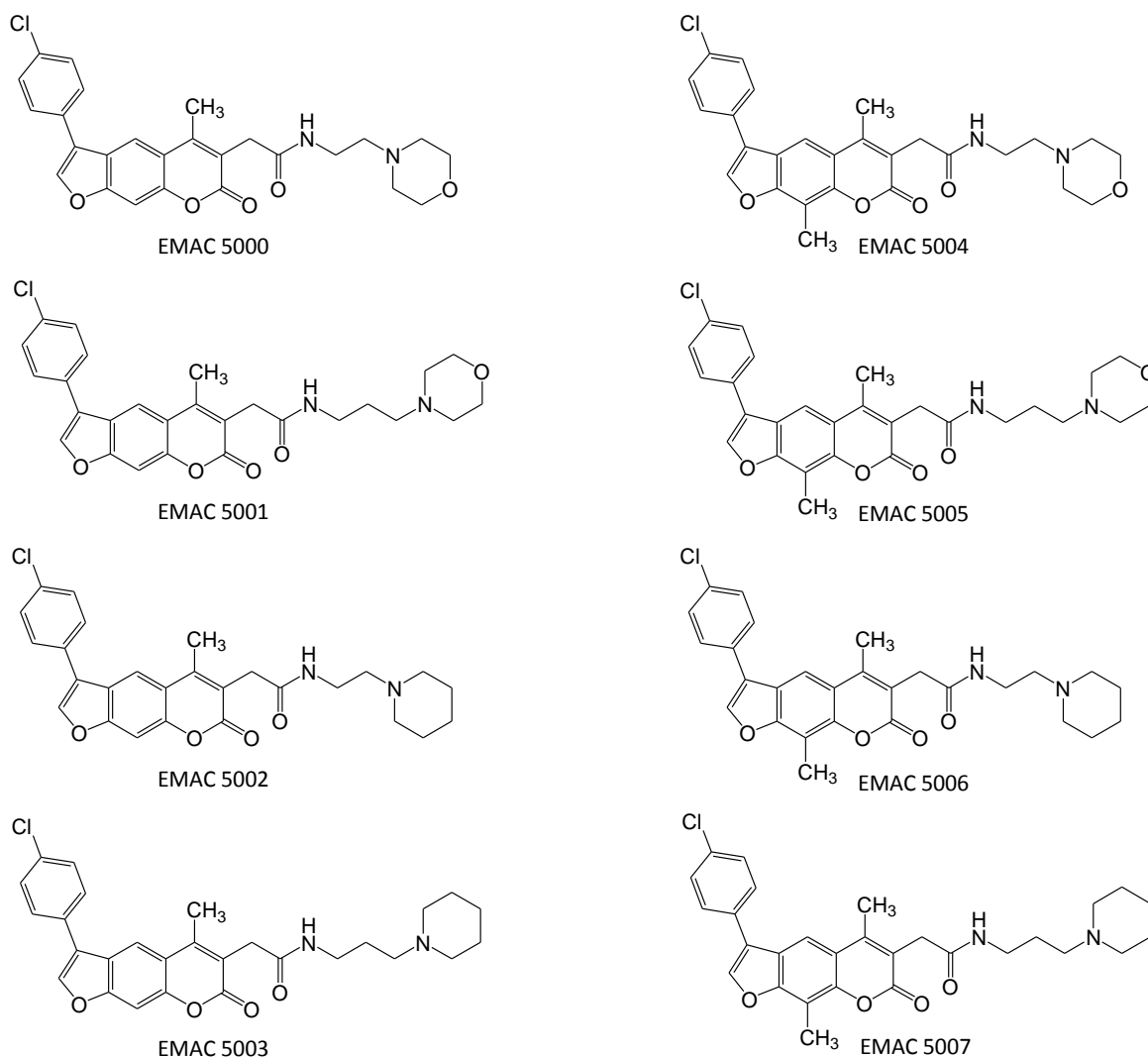


**Figure 2.11.** Chemical structure of synthesized compounds: series 1 (**EMAC5000-5004**) and series 2 (**EMAC5004-5007**).

## 2.6 EXPERIMENTAL SECTION

### 2.6.1 Materials and methods

All the materials, reagents and solvents, where not specified, were purchased from commercial suppliers and used without further purification.

Reactions were monitored using Thin Layer Chromatography (TLC), using precoated Merk Silica gel 60 254F plates and petroleum ether/ethyl acetate as eluent.



Purification methods were performed by crystallization from an appropriate solvent or by chromatographic columns for final compounds. Chromatographic columns were performed using Silica gel 70-240 mesh.

Melting points (Mp) were measured using a Stuart Melting Point SMP11 apparatus and are uncorrected.

<sup>1</sup>H NMR spectra were recorded on a Varian Unity 500MHz spectrometer in DMSO-d<sub>6</sub> or chloroform-d, using tetramethylsilane (TMS) as internal standard. Chemical shifts are reported in ppm, with the use of a  $\delta$  scale, coupling constants (J) in Hz.

## 2.6.2 Chemistry and structural characterization

In this paragraph a more detailed overview of the synthesis of each single compound is given.

### **Series 1: Synthesis of 2-(3-(4-chlorophenyl)-5-methyl-7-oxo-7H-furo[3,2-g]chromen-6-yl)-N-(substituted)acetamide (EMAC 5000-5007)**

#### ***Synthesis of methyl 2-(7-hydroxy-4-methyl-2-oxo-2H-chromen-3-yl)acetate***

A mixture of resorcinol (1 mmol), dimethylacetylsuccinate (1 mmol) and sulfuric acid 98% (2.8 mmol) was vigorously stirred at room temperature. The progression of the reaction was monitored by TLC, using ethyl acetate/n-hexane 2:1. After 30 minutes a homogeneous sticky solid was obtained which was dissolved in methanol and poured into ice. The mixture was stirred until ice melting and then filtered off to obtain a light yellow solid. The crude product was washed with ethyl ether giving a white powder which was re-crystallized from methanol.

White solid; Yield 68%; MW 248.23 g/mol; Mp 180-182°C

<sup>1</sup>H NMR (500 MHz, DMSO-d<sub>6</sub>):  $\delta$  10.56 (s, 1H, -OH phenol), 7.74 (d, 1H, -CH aromatic,  $J_o=8.5$ ), 6.89 (dd, 1H, -CH aromatic,  $J_o=8.5$ ;  $J_m=2$ ), 6.80 (d, 1H, -CH aromatic,  $J_m=2$ ), 3.73 (s, 2H, -CH<sub>2</sub>), 3.70 (s, 3H, -OCH<sub>3</sub>), 2.42 (s, 3H, -CH<sub>3</sub>).

#### ***Synthesis of methyl 2-{7-[2-(4-chlorophenyl)-2-oxoethyl]-4-methyl-2-oxo-2H-chromen-3-yl}acetate***

Methyl 2-(7-hydroxy-4-methyl-2-oxo-2H-chromen-3-yl)acetate (1 mmol) in anhydrous acetone was treated with potassium carbonate (1 mmol) and 2-bromo-4'-chloro acetophenone (1 mmol). The mixture was refluxed in acetone until reaction completion (4-5 hours). The reaction was monitored by TLC using ethyl acetate/n-hexane 2:1 as eluent. The reaction was stopped and the hot mixture filtered to remove the inorganic salt formed during the reaction. The solution was poured in H<sub>2</sub>SO<sub>4</sub> (15 mL, 0.01N) and a precipitate was formed which was filtered off and re-crystallized from aqueous methanol.

White solid; Yield 84%; MW 400.81 g/mol; Mp 177°C

<sup>1</sup>H NMR (500 MHz, DMSO-d<sub>6</sub>): δ 8.05 (d, 2H, -CH aromatic, J<sub>o</sub>=8.5), 7.77 (d, 1H, -CH aromatic, J<sub>o</sub>=8.5), 7.67 (d, 2H, -CH aromatic, J<sub>o</sub>=8.5), 7.12 (d, 1H, -CH aromatic, J<sub>m</sub>=2.5), 7.06 (dd, 1H, -CH aromatic, J<sub>o</sub>=8.5; J<sub>m</sub>=2.5), 5.73 (s, 2H, -CH<sub>2</sub>), 3.68 (s, 2H, -CH<sub>2</sub>), 3.63 (s, 3H, -OCH<sub>3</sub>), 2.40 (s, 3H, -CH<sub>3</sub>).

**Synthesis of 2-(3-(4-chlorophenyl)-5-methyl-7-oxo-7H-furo[3,2-g]chromen-6-yl)acetic acid**

A suspension of methyl 2-{7-[2-(4-chlorophenyl)-2-oxoethyl]-4-methyl-2-oxo-2H-chromen-3-yl}acetate in ethanol was refluxed until a clear solution was obtained. Then NaOH water solution (0.1 N) was added dropwise. The reaction mixture was heated for 3-4 hours, obtaining a dark solution. The solution was cooled at room temperature and concentrated under reduced pressure. The pH of this solution was acidified to 4-5 by the addition of concentrated HCl, obtaining a suspension that was cooled overnight. Then the precipitate was filtered off and re-crystallized from aqueous ethanol.

White solid; Yield 82%; MW 368.77 g/mol; Mp 246-247°C

<sup>1</sup>H NMR (500 MHz, DMSO-d<sub>6</sub>): δ 12.49 (s, 1H, -COOH), 8.53 (s, 1H, -CH aromatic), 8.21 (s, 1H, -CH aromatic), 7.87 (d, 2H, -CH aromatic, J<sub>o</sub>=8.5), 7.83 (s, 1H, aromatic), 7.61 (d, 2H, -CH aromatic, J<sub>o</sub>=8.5), 3.66 (s, 2H, -CH<sub>2</sub>), 2.55 (s, 3H, -CH<sub>3</sub>).

**Synthesis of 2-(3-(4-chlorophenyl)-5-methyl-7-oxo-7H-furo[3,2-g]chromen-6-yl)-N-(substituted)acetamide**

A suspension of 2-(3-(4-chlorophenyl)-5-methyl-7-oxo-7H-furo[3,2-g]chromen-6-yl)acetic acid (1 mmol) in DCM was treated with equimolar amounts of triethylamine. The suspension was stirred for 10 minutes at low temperature, using an ice bath. Then, ethyl chloroformate was added dropwise. The reaction was stirred until completion monitored by TLC, using as eluent ethyl acetate/n-hexane 2:1. Then, a light yellow mixture was obtained and added dropwise to a THF solution containing an appropriate ammine (2 mmol). The reaction was stirred for 1 hour, obtaining a white precipitate. The precipitate was filtered off and a white solid was obtained. The crude product was purified by column chromatography, using a ethyl acetate/n-hexane gradient and ethyl acetate/n-hexane/methanol.

**(EMAC 5000) 2-(3-(4-chlorophenyl)-5-methyl-7oxo-7H-furo[3,2-g]chromen-6-yl)-N-(2-morpholino ethyl)acetamide**

White solid; MW 480.94 g/mol; Mp 231-233°C

<sup>1</sup>H NMR (500 MHz, chloroform-d): δ 7.43 (s, 1H, -CH aromatic), 7.29 (s, 1H, -CH aromatic), 7.02 (d, 2H, -CH aromatic, J<sub>o</sub>=8.5), 6.98 (s, 1H, -CH aromatic), 6.96 (d, 2H, -CH aromatic, J<sub>o</sub>=8.5), 3.13-3.15 (m, 4H, -CH<sub>2</sub> morfoline), 3.10 (s, 2H, -CH<sub>2</sub>), 2.79 (q, 2H, -CH<sub>2</sub> lateral chain), 2.12 (s, 3H, -CH<sub>3</sub>), 1.95-1.89 (m, 6H, -CH<sub>2</sub>).

**(EMAC 5001) 2-(3-(4-chlorophenyl)-5-methyl-7oxo-7H-furo[3,2-g]chromen-6-yl)-N-(3-morpholino propyl)acetamide**

White solid; MW 494.97 g/mol; Mp 195-196°C

<sup>1</sup>H NMR (500 MHz, chloroform-d): δ 7.95 (s, 1H, -CH aromatic), 7.80 (s, 1H, -CH aromatic), 7.55 (d, 2H, -CH aromatic, J<sub>o</sub>=8.5), 7.79 (d, 2H, -CH aromatic, J<sub>o</sub>=8.5), 7.47 (s, 2H, -CH aromatic), 4.30 (bs, 2H, -CH<sub>2</sub>), 4.00 (bs, 2H, -CH<sub>2</sub>), 3.66 (s, 2H, -CH<sub>2</sub>), 3.56 (bs, 2H, -CH<sub>2</sub>), 3.45 (q, 4H, -CH<sub>2</sub> lateral chain), 3.16 (t, 2H, -CH<sub>2</sub> lateral chain), 2.87 (bs, 2H, -CH<sub>2</sub>), 2.56 (s, 3H, -CH<sub>3</sub>), 2.14 (q, 2H, -CH<sub>2</sub> lateral chain)

**(EMAC 5002) 2-(3-(4-chlorophenyl)-5-methyl-7oxo-7H-furo[3,2-g]chromen-6-yl)-N-(3-(piperidin-1-yl) ethyl)acetamide**

White solid; MW 478.97 g/mol; Mp 192-194°C

<sup>1</sup>H NMR (500 MHz, chloroform-d): δ 7.98 (s, 1H, -CH aromatic), 7.83 (s, 1H, -CH aromatic), 7.57 (d, 2H, -CH aromatic, J<sub>o</sub>=8.5), 7.53 (s, 1H, -CH aromatic), 7.52 (d, 2H, -CH aromatic), 3.66 (s, 2H, -CH<sub>2</sub>), 3.34 (s, 2H, -CH<sub>2</sub> lateral chain), 2.65 (s, 3H, -CH<sub>3</sub>), 2.46 (t, 2H, -CH<sub>2</sub> lateral chain), 2.40 (bs, 4H, -CH<sub>2</sub> piperidine), 1.57-1.55 (m, 4H, -CH<sub>2</sub> piperidine), 1.41 (bs, 2H, -CH<sub>2</sub> piperidine).

**(EMAC 5003) 2-(3-(4-chlorophenyl)-5-methyl-7oxo-7H-furo[3,2-g]chromen-6-yl)-N-(3-(piperidin-1-yl) propyl)acetamide**

White solid; MW 498.99 g/mol; Mp 173-174°C

<sup>1</sup>H NMR (500 MHz, DMSO-d<sub>6</sub>): δ 8.52 (s, 1H, -CH aromatic), 8.18 (s, 1H, -CH aromatic), 7.86 (d, 2H, -CH aromatic, J<sub>o</sub>=8.5), 7.81 (s, 1H, -CH aromatic), 7.60 (d, 2H, -CH aromatic, J<sub>o</sub>=8.5), 3.35 (s, 2H, -CH<sub>2</sub>), 3.13 (q, 2H, -CH<sub>2</sub> lateral chain), 2.98 (t, 2H, -CH<sub>2</sub> lateral chain), 2.90-2.81 (m, 6H, -CH<sub>2</sub> piperidine and lateral chain), 2.53 (s, 3H, -CH<sub>3</sub>), 1.80-1.74 (m, 6H, -CH<sub>2</sub> piperazine).

**Series 2: Synthesis of 2-(3-(4-chlorophenyl)-5,9-dimethyl-7-oxo-7H-furo[3,2-g]chromen-6-yl)-N-(substituted)acetamide (EMAC 5004-5007)**

***Synthesis of methyl 2-(7-hydroxy-4,8-dimethyl-2-oxo-2H-chromen-3-yl)acetate***

A mixture of 2-methyl-resorcinol (1 mmol), dimethylacetylsuccinate (1 mmol) and sulfuric acid 98% (2.8 mmol) was vigorously stirred at room temperature. The progression of the reaction was monitored by TLC, using ethyl acetate/n-hexane 2:1. After 30 minutes a homogeneous sticky solid was obtained. The solid was dissolved in methanol (minimum quantity) and poured into ice. The mixture was stirred until ice melting and then filtered off to obtain a light yellow solid. The crude product was washed with ethyl ether, achieving a white powder re-crystallized from methanol.

White solid; Yield 66%; MW 262.26 g/mol; Mp 174-176°C

<sup>1</sup>H NMR (500 MHz, DMSO-d<sub>6</sub>): δ 10.35 (s, 1H, -OH phenol), 7.51 (d, 1H, -CH aromatic, J<sub>o</sub>=8.5), 6.87 (d, 1H, -CH aromatic, J<sub>o</sub>=8.5), 3.64 (s, 2H, -CH<sub>2</sub>), 3.60 (s, 3H, -OCH<sub>3</sub>), 2.33 (s, 3H, -CH<sub>3</sub>), 2.15 (s, 3H, -CH<sub>3</sub>).

**Synthesis of Synthesis of methyl 2-{7-[2-(4-chlorophenyl)-2-oxoethyl]-4,8-dimethyl-2-oxo-2H-chromen-3-yl}acetate**

Methyl 2-(7-hydroxy-4,8-dimethyl-2-oxo-2H-chromen-3-yl)acetate (1 mmol) in anhydrous acetone was treated with potassium carbonate (1 mmol) and 2-bromo-4'-chloro acetophenone (1 mmol). The mixture was refluxed in acetone until reaction completion (4-5 hours) monitored with TLC using ethyl acetate/n-hexane 2:1 as eluent. The reaction was stopped and the hot mixture filtered to remove the inorganic salt formed during the reaction. The obtained solution was poured in H<sub>2</sub>SO<sub>4</sub> solution (15 mL, 0.01N). The resulting precipitate was filtered off and re-crystallized from aqueous methanol.

White solid; Yield 70%; MW 414.84 g/mol; Mp 173-176°C

<sup>1</sup>H NMR (500 MHz, DMSO-d<sub>6</sub>): δ 8.04 (d, 2H, -CH aromatic, J<sub>o</sub>=8.5), 7.66 (d, 2H, -CH aromatic, J<sub>o</sub>=8.5), 7.61 (d, 1H, -CH aromatic, J<sub>o</sub>=8.5), 7.05 (d, 2H, -CH aromatic, J<sub>o</sub>=8.5), 5.76 (s, 2H, -CH<sub>2</sub>), 3.67 (s, 2H, -CH<sub>2</sub>), 3.61 (s, 3H, -OCH<sub>3</sub>), 2.36 (s, 3H, -CH<sub>3</sub>), 2.27 (s, 3H, -CH<sub>3</sub>).

**Synthesis of 2-(3-(4-chlorophenyl)-5,9-dimethyl-7-oxo-7H-furo[3,2-g]chromen-6-yl)acetic acid**

A suspension of methyl 2-{7-[2-(4-chlorophenyl)-2-oxoethyl]-4,8-dimethyl-2-oxo-2H-chromen-3-yl}acetate in ethanol was refluxed until a clear solution was obtained. Then NaOH water solution (0.1 N) was added dropwise. The reaction mixture was heated for 3-4 hours, obtaining a dark solution. The solution was cooled at room temperature and concentrated under reduced pressure. The pH of this solution was acidified to 4-5 by the addition of concentrated HCl, obtaining a suspension that was cooled overnight. Then the precipitate was filtered off and re-crystallized from aqueous ethanol.

White solid; Yield 78%; MW 382.79 g/mol; Mp 241-243°C

<sup>1</sup>H NMR (500 MHz, DMSO-d<sub>6</sub>): δ 12.46 (bs, 1H, -COOH), 8.52 (s, 1H, -CH aromatic), 8.04 (s, 1H, -CH aromatic), 7.84 (d, 2H, -CH aromatic, J<sub>o</sub>=8.5), 7.58 (d, 2H, -CH aromatic, J<sub>o</sub>=8.5), 3.64 (s, 2H, -CH<sub>2</sub>), 2.55 (s, 3H, -CH<sub>3</sub>), 2.52 (s, 3H, -CH<sub>3</sub>).

**Synthesis of 2-(3-(4-chlorophenyl)-5,9-dimethyl-7-oxo-7H-furo[3,2-g]chromen-6-yl)-N-(substituted)acetamide**

A suspension of 2-(3-(4-chlorophenyl)-5,9-dimethyl-7-oxo-7H-furo[3,2-g]chromen-6-yl)acetic acid (1 mmol) in DCM is treated with equimolar amounts of triethylamine. The suspension was stirred for 10 minutes at low temperature, using an ice bath. Then, ethyl chloroformate was added dropwise. The reaction was stirred until completion end the progression was monitored by TLC, using as eluent ethyl acetate/n-hexane 2:1. Then, a light yellow mixture was obtained and added dropwise to a THF solution containing an appropriate ammine (2 mmol). The reaction was stirred for 1 hour, obtaining a white

precipitate. The precipitate was filtered off obtaining a white solid. The crude product was purified by chromatographic column, using a gradient of ethyl acetate/n-hexane and ethyl acetate/n-hexane/methanol.

The NMR data of compounds EMAC 5006 and 5007 are not available.

**(EMAC 5004) 2-(3-(4-chlorophenyl)-5,9-dimethyl-7oxo-7H-furo[3,2-g]chromen-6-yl)-N-(2-morpholino ethyl)acetamide**

White solid; MW 494.97 g/mol; Mp 254-255°C

<sup>1</sup>H NMR (500 MHz, chloroform-d): δ 7.85 (s, 1H, -CH aromatic), 7.84 (s, 1H, -CH aromatic), 7.57 (d, 2H, -CH aromatic, J<sub>o</sub>=8.5), 7.51 (d, 2H, -CH aromatic, J<sub>o</sub>=8.5), 3.68-3.66 (m, 6H, -CH<sub>2</sub> and -CH<sub>2</sub> morpholine), 3.34 (q, 2H, -CH<sub>2</sub> lateral chain), 2.66 (s, 6H, -CH<sub>3</sub>), 2.47 (t, 2H, -CH<sub>2</sub> lateral chain), 2.43 (bs, 4H, -CH<sub>2</sub> morpholine).

**(EMAC 5005) 2-(3-(4-chlorophenyl)-5,9-dimethyl-7oxo-7H-furo[3,2-g]chromen-6-yl)-N-(3-morpholino propyl)acetamide**

White solid; MW 508.18 g/mol; Mp 260-263°C

<sup>1</sup>H NMR (500 MHz, chloroform-d): δ 7.85 (s, 2H, -CH aromatic), 7.57 (d, 2H, -CH aromatic, J<sub>o</sub>=8.5), 7.51 (d, 2H, -CH aromatic, J<sub>o</sub>=8.5), 3.74-3.72 (m, 4H, -CH<sub>2</sub> morpholine), 3.62 (s, 2H, -CH<sub>2</sub>), 3.31 (q, 2H, -CH<sub>2</sub> lateral chain), 2.67 (s, 3H, -CH<sub>3</sub>), 2.66 (s, 3H, -CH<sub>3</sub>), 2.45 (bs, 4H, -CH<sub>2</sub> morpholine), 2.41 (t, 2H, -CH<sub>2</sub> lateral chain), 1.68 (q, 2H, -CH<sub>2</sub> lateral chain).

**(EMAC 5006) 2-(3-(4-chlorophenyl)-5,9-dimethyl-7oxo-7H-furo[3,2-g]chromen-6-yl)-N-(2-(piperidin-1-yl) ethyl)acetamide**

White solid; MW 492.18 g/mol

NMR data are not available.

**(EMAC 5007) 2-(3-(4-chlorophenyl)-5,9-dimethyl-7oxo-7H-furo[3,2-g]chromen-6-yl)-N-(2-(piperidin-1-yl) propyl)acetamide**

White solid; MW 507.02 g/mol

NMR data are not available.

## 2.7 CONCLUSIONS

In this work, different psoralen derivatives has been synthesized and the synthetic procedure optimized. The combination of synthetic effort with computational tools was exploited to provide more detailed information on structure-activity relationships, to design compounds characterized by high affinity and selectivity toward quadruplexes over duplex-DNA and, possibly able to distinguish among diverse G-quadruplex structures. All the synthesized compounds will be tested to gain insight into their mechanism of action and further optimize this scaffold.

Since the presence of a positive charge in the lateral chain give the possibility to better stabilize DNA G-quadruplex arrangements, on the bases of the obtained results will be evaluated the possibility to carried out a quaternization reaction, achieving a charged derivative for each final compound.

## 2.8 REFERENCES

1. Bochman, M. L.; Paeschke, K.; Zakian, V. A., DNA secondary structures: stability and function of structures. *Nat. Rev. Genet.* **2012**, *13*, 770-780.
2. Biffi, G.; Tannahill, D.; McCafferty, J.; Balasubramanian, S., Quantitative visualization of DNA G-quadruplex structures in human cells. *Nat Chem* **2013**, *5*, 182-186.
3. Balasubramanian, S.; Hurley, L. H.; Neidle, S., Targeting G-quadruplexes in gene promoters: a novel anticancer strategy? *Nature reviews. Drug discovery* **2011**, *10*, 261-275.
4. Han, H.; Hurley, L. H., G-quadruplex DNA: a potential target for anti-cancer drug design. *Trends in pharmacological sciences* **2000**, *21*, 136-42.
5. Phan, A. T.; Kuryavyi, V.; Patel, D. J., DNA architecture: from G to Z. *Current opinion in structural biology* **2006**, *16*, 288-98.
6. Burge, S.; Parkinson, G. N.; Hazel, P.; Todd, A. K.; Neidle, S., Quadruplex DNA: sequence, topology and structure. *Nucleic acids research* **2006**, *34*, 5402-15.
7. Patel, D. J.; Phan, A. T.; Kuryavyi, V., Human telomere, oncogenic promoter and 5'-UTR G-quadruplexes: diverse higher order DNA and RNA targets for cancer therapeutics. *Nucleic acids research* **2007**, *35*, 7429-55.
8. Murat, P.; Balasubramanian, S., Existence and consequences of G-quadruplex structures in DNA. *Current opinion in genetics & development* **2014**, *25*, 22-9.
9. Aubert, G.; Lansdorp, P. M., Telomeres and Aging. *Physiological Reviews* **2008**, *88*, 557-579.
10. Yang, D.; Okamoto, K., Structural insights into G-quadruplexes: towards new anticancer drugs. *Future medicinal chemistry* **2010**, *2*, 619-46.
11. Qin, Y.; Hurley, L. H., Structures, folding patterns, and functions of intramolecular DNA G-quadruplexes found in eukaryotic promoter regions. *Biochimie* **2008**, *90*, 1149-71.
12. Brooks, T. A.; Hurley, L. H., The role of supercoiling in transcriptional control of MYC and its importance in molecular therapeutics. *Nat Rev Cancer* **2009**, *9*, 849-861.
13. Gonzalez, V.; Guo, K.; Hurley, L.; Sun, D., Identification and characterization of nucleolin as a c-myc G-quadruplex-binding protein. *The Journal of biological chemistry* **2009**, *284*, 23622-35.

14. Ou, T. M.; Lu, Y. J.; Tan, J. H.; Huang, Z. S.; Wong, K. Y.; Gu, L. Q., G-quadruplexes: targets in anticancer drug design. *ChemMedChem* **2008**, 3, 690-713.
15. Alcaro, S.; Musetti, C.; Distinto, S.; Casatti, M.; Zagotto, G.; Artese, A.; Parrotta, L.; Moraca, F.; Costa, G.; Ortuso, F.; MacCioni, E.; Sissi, C., Identification and characterization of new DNA G-quadruplex binders selected by a combination of ligand and structure-based virtual screening approaches. *Journal of Medicinal Chemistry* **2013**, 56, 843-855.
16. Durant, J. L.; Leland, B. A.; Henry, D. R.; Nourse, J. G., Reoptimization of MDL Keys for Use in Drug Discovery. *Journal of Chemical Information and Computer Sciences* **2002**, 42, 1273-1280.
17. Accelrys inc *Pipeline Pilot 6.1.5*, San Diego, CA, 2007.
18. Nicholls, A.; McGaughey, G. B.; Sheridan, R. P.; Good, A. C.; Warren, G.; Mathieu, M.; Muchmore, S. W.; Brown, S. P.; Grant, J. A.; Haigh, J. A.; Nevins, N.; Jain, A. N.; Kelley, B., Molecular Shape and Medicinal Chemistry: A Perspective. *Journal of Medicinal Chemistry* **2010**, 53, 3862-3886.
19. Khanna, V.; Ranganathan, S., Physicochemical property space distribution among human metabolites, drugs and toxins. *BMC Bioinformatics* **2009**, 10, S10.
20. Heald, R. A.; Modi, C.; Cookson, J. C.; Hutchinson, I.; Laughton, C. A.; Gowan, S. M.; Kelland, L. R.; Stevens, M. F. G., Antitumor Polycyclic Acridines. 8.1 Synthesis and Telomerase-Inhibitory Activity of Methylated Pentacyclic Acridinium Salts. *Journal of Medicinal Chemistry* **2001**, 45, 590-597.
21. Leonetti, C.; Scarsella, M.; Riggio, G.; Rizzo, A.; Salvati, E.; D'Incalci, M.; Staszewsky, L.; Frapolli, R.; Stevens, M. F.; Stoppacciaro, A.; Mottolese, M.; Antoniani, B.; Gilson, E.; Zupi, G.; Biroccio, A., G-Quadruplex Ligand RHPS4 Potentiates the Antitumor Activity of Camptothecins in Preclinical Models of Solid Tumors. *Clinical Cancer Research* **2008**, 14, 7284-7291.
22. Drygin, D.; Siddiqui-Jain, A.; O'Brien, S.; Schwaebe, M.; Lin, A.; Bliesath, J.; Ho, C. B.; Proffitt, C.; Trent, K.; Whitten, J. P.; Lim, J. K. C.; Von Hoff, D.; Anderes, K.; Rice, W. G., Anticancer Activity of CX-3543: A Direct Inhibitor of rRNA Biogenesis. *Cancer Research* **2009**, 69, 7653-7661.

23. Rice, W. G.; Lim, J. K. C.; Schwaebe, M. K.; Siddiqui-Jain, A.; Streiner, N. H.; Trent, K. B.; Whitten, J. P.; Hurley, L. H.; Von Hoff, D. D., Design of CX-3543, a novel multi-targeting antitumor agent. *AACR Meeting Abstracts* **2005**, 2005, 594-.
24. Su, Q.-B.; He, F.; Wang, X.-D.; Guan, S.; Xie, Z.-Y.; Wang, L.-Y.; Lu, Y.-J.; Gu, L.-Q.; Huang, Z.-S.; Chen, X.; Huang, M.; Zhou, S.-F., Biotransformation and pharmacokinetics of the novel anticancer drug, SYUIQ-5, in the rat. *Investigational New Drugs* **2008**, 26, 119-137.
25. Zhou, J.-L.; Lu, Y.-J.; Ou, T.-M.; Zhou, J.-M.; Huang, Z.-S.; Zhu, X.-F.; Du, C.-J.; Bu, X.-Z.; Ma, L.; Gu, L.-Q.; Li, Y.-M.; Chan, A. S.-C., Synthesis and Evaluation of Quindoline Derivatives as G-Quadruplex Inducing and Stabilizing Ligands and Potential Inhibitors of Telomerase. *Journal of Medicinal Chemistry* **2005**, 48, 7315-7321.
26. Riou, J. F.; Guittat, L.; Mailliet, P.; Laoui, A.; Renou, E.; Petitgenet, O.; Mégnin-Chanet, F.; Hélène, C.; Mergny, J. L., Cell senescence and telomere shortening induced by a new series of specific G-quadruplex DNA ligands. *Proceedings of the National Academy of Sciences of the United States of America* **2002**, 99, 2672-2677.
27. Burger, A. M.; Dai, F.; Schultes, C. M.; Reszka, A. P.; Moore, M. J.; Double, J. A.; Neidle, S., The G-Quadruplex-Interactive Molecule BRACO-19 Inhibits Tumor Growth, Consistent with Telomere Targeting and Interference with Telomerase Function. *Cancer Research* **2005**, 65, 1489-1496.
28. Gowan, S. M.; Harrison, J. R.; Patterson, L.; Valenti, M.; Read, M. A.; Neidle, S.; Kelland, L. R., A G-Quadruplex-Interactive Potent Small-Molecule Inhibitor of Telomerase Exhibiting in Vitro and in Vivo Antitumor Activity. *Molecular Pharmacology* **2002**, 61, 1154-1162.
29. De Cian, A.; DeLemos, E.; Mergny, J.-L.; Teulade-Fichou, M.-P.; Monchaud, D., Highly Efficient G-Quadruplex Recognition by Bisquinolinium Compounds. *Journal of the American Chemical Society* **2007**, 129, 1856-1857.
30. Gomez, D.; Guédin, A.; Mergny, J.-L.; Salles, B.; Riou, J.-F.; Teulade-Fichou, M.-P.; Calsou, P., A G-quadruplex structure within the 5'-UTR of TRF2 mRNA represses translation in human cells. *Nucleic acids research* **2010**, 38, 7187-7198.



31. Monchaud, D.; Allain, C.; Bertrand, H.; Smargiasso, N.; Rosu, F.; Gabelica, V.; De Cian, A.; Mergny, J. L.; Teulade-Fichou, M. P., Ligands playing musical chairs with G-quadruplex DNA: A rapid and simple displacement assay for identifying selective G-quadruplex binders. *Biochimie* **2008**, 90, 1207-1223.
32. Chang, C.-C.; Kuo, I. C.; Lin, J.-J.; Lu, Y.-C.; Chen, C.-T.; Back, H.-T.; Lou, P.-J.; Chang, T.-C., A Novel Carbazole Derivative, BMVC: a Potential Antitumor Agent and Fluorescence Marker of Cancer Cells. *Chemistry & Biodiversity* **2004**, 1, 1377-1384.
33. Chang, C.-C.; Wu, J.-Y.; Chien, C.-W.; Wu, W.-S.; Liu, H.; Kang, C.-C.; Yu, L.-J.; Chang, T.-C., A Fluorescent Carbazole Derivative: High Sensitivity for Quadruplex DNA. *Analytical Chemistry* **2003**, 75, 6177-6183.
34. Wang, Y.; Patel, D. J., Solution structure of the human telomeric repeat d[AG<sub>3</sub>(T<sub>2</sub>AG<sub>3</sub>)<sub>3</sub>] G-tetraplex. *Structure* **1993**, 1, 263-282.
35. Parkinson, G. N.; Lee, M. P. H.; Neidle, S., Crystal structure of parallel quadruplexes from human telomeric DNA. *Nature* **2002**, 417, 876-880.
36. Dai, J.; Punchihewa, C.; Ambrus, A.; Chen, D.; Jones, R. A.; Yang, D., Structure of the intramolecular human telomeric G-quadruplex in potassium solution: a novel adenine triple formation. *Nucleic acids research* **2007**, 35, 2440-2450.
37. Dai, J.; Carver, M.; Punchihewa, C.; Jones, R. A.; Yang, D., Structure of the Hybrid-2 type intramolecular human telomeric G-quadruplex in K<sup>+</sup> solution: insights into structure polymorphism of the human telomeric sequence. *Nucleic acids research* **2007**, 35, 4927-4940.
38. Trott, O.; Olson, A. J., AutoDock Vina: Improving the speed and accuracy of docking with a new scoring function, efficient optimization, and multithreading. *Journal of Computational Chemistry* **2010**, 31, 455-461.
39. Garazd, Y. L.; Garazd, M. M.; Ogorodniichuk, A. S.; Khilya, V. P., Modified coumarins. 24. Synthesis of cycloheptane-annellated tetracyclic furocoumarins. *Chemistry of Natural Compounds* **2006**, 42, 656-664.
40. Jayaprakash, R. Y.; Chakravarthula, V., Combined Claisen Rearrangement and Oxidative Cyclization as a Route to Hydroxymethyl Dihydrofuran-Annulated Coumarins. *Journal of Heterocyclic Chemistry* **2015**, 52, 1014-1018.

41. Rajabi, M.; Hossaini, Z.; Khalilzadeh, M. A.; Datta, S.; Halder, M.; Mousa, S. A., Synthesis of a new class of furo[3,2-c]coumarins and its anticancer activity. *Journal of Photochemistry and Photobiology B: Biology* **2015**, 148, 66-72.
42. MacLeod, J. K.; Worth, B. R., Synthesis of benzofuranoid systems. I. Furocoumarins, benzofurans and dibenzofurans. *Tetrahedron Letters* **1972**, 13, 237-240.
43. Montalbetti, C. A. G. N.; Falque, V., Amide bond formation and peptide coupling. *Tetrahedron* **2005**, 61, 10827-10852.
44. El-Faham, A.; Albericio, F., Peptide Coupling Reagents, More than a Letter Soup. *Chemical Reviews* **2011**, 111, 6557-6602.

## SECTION II A2B ANTAGONISTS

### ADENOSINE RECEPTORS: STRUCTURE, DISTRIBUTION AND BIOLOGICAL FUNCTIONS

Adenosine is an endogenous purine nucleoside constitutively present at low concentrations in the extracellular space of several mammalian tissues.<sup>1</sup> In particular, extracellular adenosine acts as a local modulator both in physiological and pathophysiological conditions, in response to stress in organs and tissues, in both peripheral and central nervous system. In the brain, both neuronal and glial cell functions are regulated by adenosine.<sup>2</sup> Adenosine acts as a local modulator of the action of various other neurotransmitters, including biogenic amines and excitatory amino acids, attenuates the release of many stimulatory neurotransmitters and can counteract the excitotoxicity associated with excessive glutamate release in the brain. Adenosine can also modulate the interaction of neurotransmitters, such as dopamine, with their own receptors (Figure 1).<sup>3,4</sup>

In the periphery, adenosine has been shown to attenuate excessive inflammation, to promote wound healing, and to protect tissue against ischemic damage.<sup>5</sup> In the cardiovascular system, adenosine promotes vasodilation, vascular integrity, and angiogenesis and counteracts the lethal effects of prolonged ischemia on cardiac myocytes and skeletal muscle.<sup>2,6</sup>

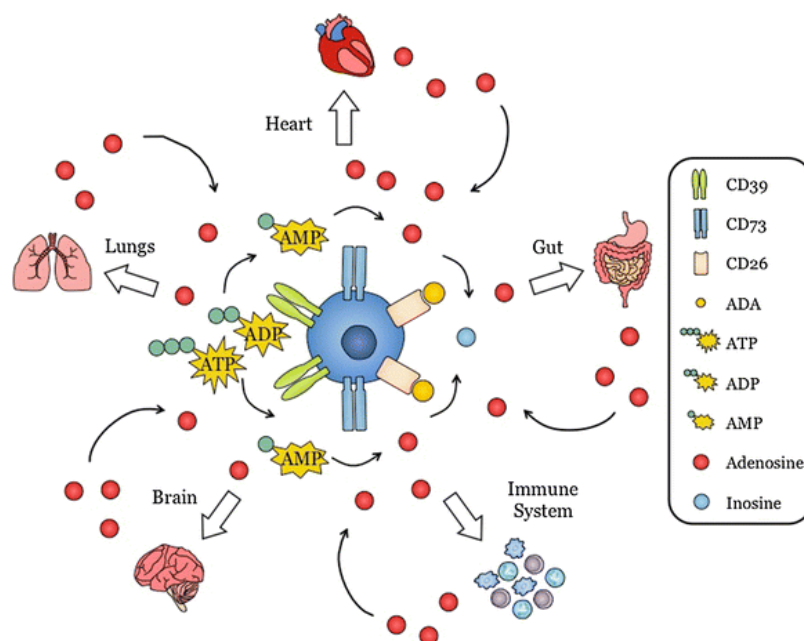


**Figure 1.** Schematic illustration of central and peripheral distribution of adenosine receptors.

The biological effects of adenosine are mediated by cell surface receptors coupled with intracellular signalling cascades. There are four known subtypes of adenosine receptors, ARs or AdoR, referred to as  $A_1$ ,  $A_{2A}$ ,  $A_{2B}$ , and  $A_3$ , each one with a unique pharmacological profile, tissue distribution and effector coupling.<sup>7</sup> All of them are members of the super-family of G-protein-coupled receptors, GPCRs, and are most closely related to the receptors for biogenic amines. Extracellular levels of adenosine are quite variable, depending on the tissue and the degree of stress experienced, and so the basal level of stimulation of these receptor subtypes by the endogenous agonist varies enormously.<sup>7,8</sup>

Different sources of adenosine are known. Notably, adenosine is not stored in vesicles and its extracellular release can be obtained through an equilibrative transporter or as a result of cell damage, or nucleotidase-mediated hydrolysis of extracellular adenine nucleotides (Figure 2), which have their own signal pathways mediated by purinergic P2 receptors.<sup>9</sup> Ectonucleotidases, including apyrase CD39 and the 5'-nucleotidase, are present on the extracellular surface of many tissues and are involved in numerous crucial functions.<sup>10,11</sup>

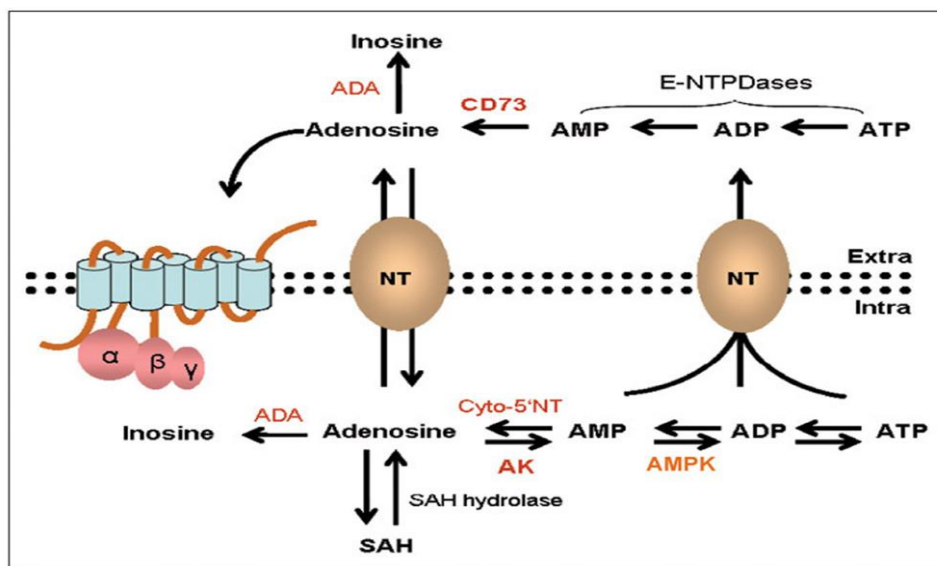
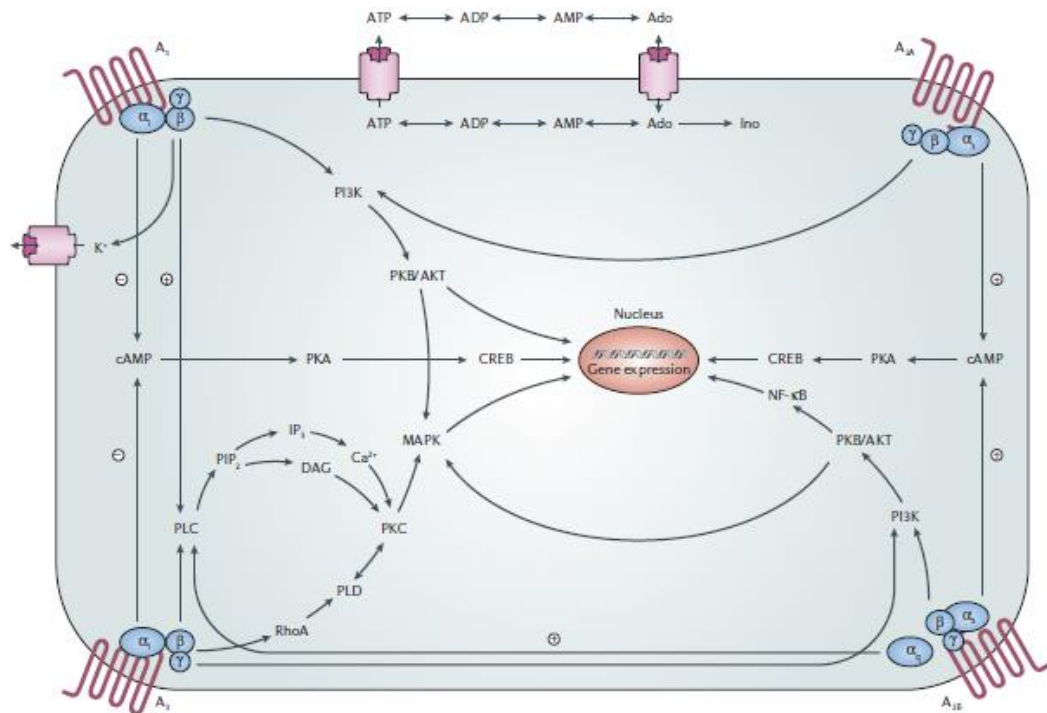


Figure 2. Biosynthesis and catabolism of adenosine.<sup>11</sup>

Adenosine receptor signalling is classically associated with the inhibition or the stimulation of adenylate cyclase but also other pathways, such as phospholipase C (PLC),  $Ca^{2+}$  and mitogen activated protein kinases (MAPK), are relevant.<sup>12</sup> Specifically,  $A_1$  and  $A_3$  are coupled with inhibitory G proteins, resulting in the inhibition of adenylate cyclase, while  $A_{2A}$  and  $A_{2B}$  are coupled with stimulatory G proteins, so that their activation increases the adenylate cyclase activity.<sup>13</sup>



**Figure 3.** Schematic representation of adenosine receptors signalling pathways.<sup>7</sup>

Activation of A<sub>1</sub> receptors inhibits adenylate cyclase activity through the activation of pertussis toxin-sensitive G<sub>i</sub> proteins with an increase of the PLC activity. In cardiac muscle and neurons A<sub>1</sub> receptors can activate also pertussis toxin sensitive K<sup>+</sup> channels, K<sub>ATP</sub> channels, as well as Q-, P- and N-type Ca<sup>2+</sup> channels. Activation of A<sub>2A</sub> receptor increases adenylate cyclase activity. G<sub>s</sub> and G<sub>olf</sub> are the proteins associated with this receptor subtype in the peripheral system and in the striatum, respectively.<sup>14</sup> Activation of A<sub>2A</sub> induces inositol phosphate to raise intracellular calcium and activates protein kinase C. A<sub>2B</sub> receptors are positively coupled with adenylate cyclase and PLC. In particular, the activation of PLC through G<sub>q</sub> proteins mediates many important functions of A<sub>2B</sub> receptors. The A<sub>3</sub>AR couples to classical second-messenger pathways that inhibit adenylate cyclase, stimulate PLC and calcium mobilization. Likewise to other ARs, A<sub>3</sub>ARs couple to MAPK, indicating their involvement in cell growth, survival, death and differentiation.<sup>13</sup>

All these receptors undergo agonist-induced regulation by desensitization and trafficking.<sup>15</sup> For all adenosine receptor subtypes, there is evidence to implicate arrest in agonist-induced desensitization and trafficking, but there is also evidences for other possible forms of regulation, including second messenger-dependent kinase regulation, heterologous effects involving G proteins, and the involvement of non-clathrin trafficking pathways.<sup>16</sup> The rapidity of this process is related to the receptor subtype. Moreover, since adenosine receptors couple to multiple signalling pathways, these pathways may desensitize differentially.<sup>13</sup> In addition to receptor desensitization, adenosine mediated-signalling is rapidly silenced by adenosine kinases and, to a lesser degree, by adenosine

deaminase that metabolizes the adenosine to AMP and inosine, respectively, which are both less active than adenosine at the ARs.<sup>10</sup>

The development of potent and selective agonists and antagonists of ARs has been a hot research topic in medicinal chemistry for more than three decades.<sup>1, 17, 18</sup> The main approach to discover AR agonists and antagonists has been the modification of adenosine itself and xanthines, like caffeine and theophylline, respectively. Selective agonists and antagonists have been found using both empirical and rational approaches, based on molecular modelling studies, supported by the knowledge derived from mutagenesis studies and the crystal structure of the seven transmembrane rhodopsin receptor. In addition, structural information for the ARs have been available since 2008<sup>19</sup> thanks to the high resolution X-ray structure of the human A<sub>2A</sub>AR in complex with the antagonist ZM241385 4-(2-[7-amino-2-(2-furyl)]1,2,4]triazolo[2,3-a][1,3,5]triazin-5-yl-amino]ethyl) phenol (Figure 4).<sup>20 21</sup>

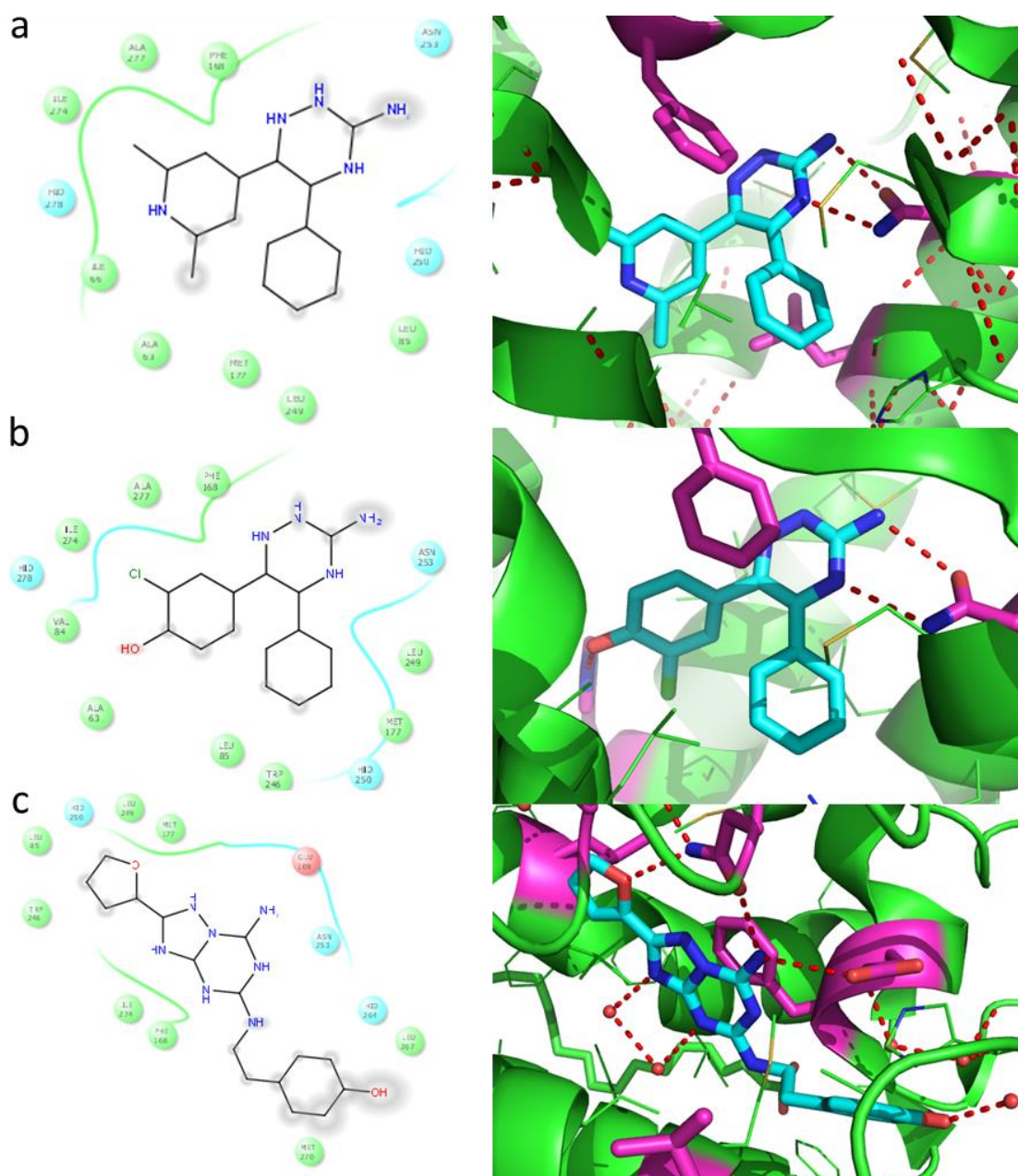


**Figure 4.** 2D and 3D representations of three crystal structures of Adenosine A<sub>2A</sub> in complex with the bound antagonists : a) PDB code: 3UZA, b) PDB code: 3UZC and c) 3EML.

The crystal structure of the A<sub>2A</sub>AR in its inactive conformation gave insight into the ligand recognition mechanism, showing the key residues involved in the ligand binding and the major interactions anchoring the antagonist to the binding site. Many of the site-directed mutagenesis data previously available for the ARs were structurally explained, and new mutational experiments were guided by the knowledge gained from the A<sub>2A</sub>AR structure, helping to further define the ligand binding cavity of this AR.<sup>22</sup> New crystal structures of the A<sub>2A</sub>AR in complex with different agonists provide a deeper comprehension about the activation mechanism and the conformational changes that

occur upon agonist binding to the A<sub>2A</sub>AR. These new crystal structures lack a coupled G protein, but are helpful to understand the function of the ARs, and they support the drug design approaches for the AR family, improving the quality of models for other AR subtypes.<sup>23</sup> A further contribution to the drug discovery process was the introduction of radioligands for adenosine receptors, including agonists and antagonists with high affinity and high selectivity for the human variants of each receptor.<sup>24</sup> Moreover, both agonist and antagonist ligands containing positron-emitting radio-isotopes have been developed to monitor the *in vivo* occupancy of adenosine receptors in humans.<sup>13, 25-27</sup> Such ligands for positron emission tomography (PET) can be useful for diagnostic as well as research purposes. Moreover, fluorescent ligands have been introduced for characterization of the ARs. Some of these spectroscopic probes are suitable for compound screening and avoid the use of radioisotopes.<sup>28-30</sup>

Due to the involvement of adenosine in various pathological conditions, the targeting of specific adenosine receptor subtypes, with selective agonists or antagonists, could potentially have significant therapeutic benefits. More in detail, several therapeutic indications were identified for cardiovascular<sup>31</sup> and neurological<sup>3</sup> diseases, as well as other pathologic states like inflammatory, renal, pulmonary, endocrine disorders and cancer.<sup>7</sup> The high therapeutic potential of adenosine receptors has been largely documented. Despite the large numbers of selective adenosine receptor agonists and antagonists reported in the literature, the clinical application of adenosine ligands is lacking. One reason for this may be the ubiquitous distribution of adenosine receptors and, consequently, the high possibility of side effects. In addition species differences in the affinity in selective ligands complicate preclinical testing in animal models.<sup>13, 18</sup>

Other ways to affect and modulate ARs activity could be the use of allosteric enhancer of agonist action<sup>32-34</sup> or the inhibition of adenosine metabolism<sup>35</sup> or its extracellular uptake. In particular, the allosteric modulators could selectively amplify the effects of endogenous adenosine in an event-responsive manner, with a series of therapeutic advantages when compared with agonists acting on the orthosteric binding site.<sup>36, 37</sup>



## REFERENCES

1. Cacciari, B.; Pastorin, G.; Bolcato, C.; Spalluto, G.; Bacilieri, M.; Moro, S., A2B adenosine receptor antagonists: recent developments. *Mini reviews in medicinal chemistry* **2005**, *5*, 1053-60.
2. Gomes, C. V.; Kaster, M. P.; Tome, A. R.; Agostinho, P. M.; Cunha, R. A., Adenosine receptors and brain diseases: neuroprotection and neurodegeneration. *Biochimica et biophysica acta* **2011**, *1808*, 1380-99.
3. Ribeiro, J. A.; Sebastião, A. M.; de Mendonça, A., Adenosine receptors in the nervous system: pathophysiological implications. *Progress in Neurobiology* **2002**, *68*, 377-392.
4. Ferré, S.; Quiroz, C.; Woods, A. S.; Cunha, R.; Popoli, P.; Ciruela, F.; Lluís, C.; Franco, R.; Azdad, K.; Schiffmann, S. N., An Update on Adenosine A(2A)-Dopamine D(2) receptor interactions. Implications for the Function of G Protein-Coupled Receptors. *Current pharmaceutical design* **2008**, *14*, 1468-1474.
5. Karmouty-Quintana, H.; Xia, Y.; Blackburn, M. R., Adenosine Signaling During Acute and Chronic Disease States. *Journal of molecular medicine (Berlin, Germany)* **2013**, *91*, 173-81.
6. Johnson, D. S.; Weerapana, E.; Cravatt, B. F., Strategies for discovering and derisking covalent, irreversible enzyme inhibitors. *Future medicinal chemistry* **2010**, *2*, 949-64.
7. Jacobson, K. A.; Gao, Z.-G., Adenosine receptors as therapeutic targets. *Nat. Rev. Drug Discovery* **2006**, *5*, 247-264.
8. Jacobson, K. A., Introduction to adenosine receptors as therapeutic targets. *Handb. Exp. Pharmacol.* **2009**, *193*, 1-24.
9. Fredholm, B. B., Adenosine, an endogenous distress signal, modulates tissue damage and repair. *Cell death and differentiation* **2007**, *14*, 1315-23.
10. Fredholm, B. B.; Ijzerman, A. P.; Jacobson, K. A.; Klotz, K.-N.; Linden, J., International union of pharmacology. XXV. Nomenclature and classification of adenosine receptors. *Pharmacol. Rev.* **2001**, *53*, 527-552.

11. Ham, J.; Evans, B. A., An emerging role for adenosine and its receptors in bone homeostasis. *Frontiers in endocrinology* **2012**, 3, 113.
12. Schulte, G.; Fredholm, B. B., Signalling from adenosine receptors to mitogen-activated protein kinases. *Cellular signalling* **2003**, 15, 813-27.
13. Chen, J.-F.; Eltzschig, H. K.; Fredholm, B. B., Adenosine receptors as drug targets - what are the challenges? *Nat. Rev. Drug Discovery* **2013**, 12, 265-286.
14. Hervé, D., Identification of a Specific Assembly of the G Protein Golf as a Critical and Regulated Module of Dopamine and Adenosine-Activated cAMP Pathways in the Striatum. *Frontiers in Neuroanatomy* **2011**, 5.
15. Mundell, S.; Kelly, E., Adenosine receptor desensitization and trafficking. *Biochimica et biophysica acta* **2011**, 1808, 1319-28.
16. Klaasse, E. C.; Ijzerman, A. P.; de Grip, W. J.; Beukers, M. W., Internalization and desensitization of adenosine receptors. *Purinergic Signalling* **2008**, 4, 21-37.
17. Jacobson, K. A.; Klutz, A. M.; Tosh, D. K.; Ivanov, A. A.; Preti, D.; Baraldi, P. G., Medicinal Chemistry of the A(3) Adenosine Receptor: Agonists, Antagonists, and Receptor Engineering. *Handbook of experimental pharmacology* **2009**, 123-59.
18. Mueller, C. E.; Jacobson, K. A., Recent developments in adenosine receptor ligands and their potential as novel drugs. *Biochim. Biophys. Acta, Biomembr.* **2011**, 1808, 1290-1308.
19. Jaakola, V. P.; Griffith, M. T.; Hanson, M. A.; Cherezov, V.; Chien, E. Y.; Lane, J. R.; Ijzerman, A. P.; Stevens, R. C., The 2.6 angstrom crystal structure of a human A2A adenosine receptor bound to an antagonist. *Science (New York, N.Y.)* **2008**, 322, 1211-7.
20. Congreve, M.; Andrews, S. P.; Dore, A. S.; Hollenstein, K.; Hurrell, E.; Langmead, C. J.; Mason, J. S.; Ng, I. W.; Tehan, B.; Zhukov, A.; Weir, M.; Marshall, F. H., Discovery of 1,2,4-triazine derivatives as adenosine A(2A) antagonists using structure based drug design. *J Med Chem* **2012**, 55, 1898-903.
21. Dore, A. S.; Robertson, N.; Errey, J. C.; Ng, I.; Hollenstein, K.; Tehan, B.; Hurrell, E.; Bennett, K.; Congreve, M.; Magnani, F.; Tate, C. G.; Weir, M.; Marshall, F. H., Structure of the adenosine A(2A) receptor in complex with ZM241385 and the xanthines XAC and caffeine. *Structure (London, England : 1993)* **2011**, 19, 1283-93.

22. Jacobson, K. A.; Balasubramanian, R.; Deflorian, F.; Gao, Z. G., G protein-coupled adenosine (P1) and P2Y receptors: ligand design and receptor interactions. *Purinergic Signalling* **2012**, *8*, 419-36.
23. Jacobson, K. A., Introduction to adenosine receptors as therapeutic targets. *Handb Exp Pharmacol* **2009**, 1-24.
24. Houston, D.; Costanzi, S.; Jacobson, K. A.; Harden, T. K., Development of Selective High Affinity Antagonists, Agonists, and Radioligands for the P2Y(1) Receptor. *Combinatorial chemistry & high throughput screening* **2008**, *11*, 410-9.
25. Federico, S.; Ciancetta, A.; Porta, N.; Redenti, S.; Pastorin, G.; Cacciari, B.; Klotz, K. N.; Moro, S.; Spalluto, G., Scaffold decoration at positions 5 and 8 of 1,2,4-triazolo[1,5-c]pyrimidines to explore the antagonist profiling on adenosine receptors: a preliminary structure-activity relationship study. *J Med Chem* **2014**, *57*, 6210-25.
26. Khanapur, S.; Paul, S.; Shah, A.; Vatakuti, S.; Koole, M. J.; Zijlma, R.; Dierckx, R. A.; Luurtsema, G.; Garg, P.; van Waarde, A.; Elsinga, P. H., Development of [18F]-labeled pyrazolo[4,3-e]-1,2,4- triazolo[1,5-c]pyrimidine (SCH442416) analogs for the imaging of cerebral adenosine A2A receptors with positron emission tomography. *J Med Chem* **2014**, *57*, 6765-80.
27. Meyer, P. T.; Elmenhorst, D.; Boy, C.; Winz, O.; Matusch, A.; Zilles, K.; Bauer, A., Effect of aging on cerebral A1 adenosine receptors: A [18F]CPFPX PET study in humans. *Neurobiology of aging* **2007**, *28*, 1914-24.
28. Middleton, R. J.; Briddon, S. J.; Cordeaux, Y.; Yates, A. S.; Dale, C. L.; George, M. W.; Baker, J. G.; Hill, S. J.; Kellam, B., New fluorescent adenosine A1-receptor agonists that allow quantification of ligand-receptor interactions in microdomains of single living cells. *J Med Chem* **2007**, *50*, 782-93.
29. Knight, A.; Hemmings, J. L.; Winfield, I.; Leuenberger, M.; Frattini, E.; Frenguelli, B. G.; Dowell, S. J.; Lochner, M.; Ladds, G., Discovery of Novel Adenosine Receptor Agonists That Exhibit Subtype Selectivity. *J Med Chem* **2016**, *59*, 947-64.
30. Briddon, S. J.; Hill, S. J., Pharmacology under the microscope: the use of fluorescence correlation spectroscopy to determine the properties of ligand-receptor complexes. *Trends in pharmacological sciences* **2007**, *28*, 637-45.

31. Headrick, J. P.; Ashton, K. J.; Rose'meyer, R. B.; Peart, J. N., Cardiovascular adenosine receptors: expression, actions and interactions. *Pharmacology & therapeutics* **2013**, 140, 92-111.
32. Narlawar, R.; Lane, J. R.; Doddareddy, M.; Lin, J.; Brussee, J.; Ijzerman, A. P., Hybrid ortho/allosteric ligands for the adenosine A(1) receptor. *J Med Chem* **2010**, 53, 3028-37.
33. Gao, Z. G.; Ye, K.; Goblyos, A.; Ijzerman, A. P.; Jacobson, K. A., Flexible modulation of agonist efficacy at the human A3 adenosine receptor by the imidazoquinoline allosteric enhancer LUF6000. *BMC pharmacology* **2008**, 8, 20.
34. Du, L.; Gao, Z. G.; Nithipatikom, K.; Ijzerman, A. P.; Veldhoven, J. P.; Jacobson, K. A.; Gross, G. J.; Auchampach, J. A., Protection from myocardial ischemia/reperfusion injury by a positive allosteric modulator of the A(3) adenosine receptor. *The Journal of pharmacology and experimental therapeutics* **2012**, 340, 210-7.
35. Peart, J.; Matherne, G. P.; Cerniway, R. J.; Headrick, J. P., Cardioprotection with adenosine metabolism inhibitors in ischemic-reperfused mouse heart. *Cardiovascular research* **2001**, 52, 120-9.
36. Goeblyoes, A.; Ijzerman, A. P., Allosteric modulation of adenosine receptors. *Biochim. Biophys. Acta, Biomembr.* **2011**, 1808, 1309-1318.
37. Cristalli, G.; Costanzi, S.; Lambertucci, C.; Lupidi, G.; Vittori, S.; Volpini, R.; Camaioni, E., Adenosine deaminase: functional implications and different classes of inhibitors. *Medicinal research reviews* **2001**, 21, 105-28.

### **3 SYNTHESIS AND BIOLOGICAL EVALUATION OF 1-PROPYL-8-(PIPERAZINE-1-SOLPHONYL)PHENYL XANTHINES AS SELECTIVE ANTAGONISTS OF ADENOSINE A<sub>2B</sub> RECEPTORS.**

#### **3.1 INTRODUCTION TO A<sub>2B</sub> RECEPTOR**

##### **3.1.1 A<sub>2B</sub> receptor. Structure and therapeutic potential**

The preeminent role of adenosine A<sub>2B</sub> receptors have been recognized in the aetiology of several pathologic states. A<sub>2B</sub> are low affinity receptors that are thought to be activated when the extracellular adenosine concentration reaches micromolar levels.<sup>1</sup> Hence they are generally silent during normal physiological conditions, in which adenosine levels are very low. As a consequence of their low affinity for the endogenous ligand, A<sub>2B</sub> receptors have been considered, for a long time, less physiologically relevant than the high-affinity A<sub>2A</sub> receptors. However, the observation that the A<sub>2B</sub> receptors expression, as well as the high concentration levels reached by extra-cellular adenosine, are dramatically increased during low oxygen tension and inflammation, points out the relevance of this receptor subtype during pathophysiological conditions. Worth noting, A<sub>2B</sub> receptors are highly responsive to many mediators, which are also able to induce their expression at a transcriptional or post-transcriptional level.<sup>2</sup> As an example it has been observed that different mediators, associated with inflammation, increase A<sub>2B</sub>AR expression.<sup>2</sup> The pro-inflammatory cytokine TNF- $\alpha$  increased A<sub>2B</sub>AR transcription in several cell types, both *in vitro* and *in vivo*. It has been proposed that in vascular smooth muscle cells a TNF- $\alpha$  mediated increase in NAD(P) H oxidase enzymes is responsible for the upregulation of A<sub>2B</sub>AR expression.<sup>3,4</sup> In line with these studies, the pro-inflammatory cytokine, IL-1 $\beta$ , induced A<sub>2B</sub>AR transcription in endothelial cells. Finally, IFN- $\gamma$  was demonstrated to increase A<sub>2B</sub>AR mRNA expression in macrophages, with a concurrent increased expression of the receptor on the cell surface.<sup>5</sup> Interestingly, IFN- $\gamma$  treatment of intestinal epithelial cells did not alter A<sub>2B</sub>AR cell-surface expression, suggesting that A<sub>2B</sub> receptor regulation, by inflammatory mediators, is likely to be cell-type specific.<sup>6</sup>

As part of P1 receptor family, A<sub>2B</sub> are G protein-coupled receptors, whose stimulation can activate either adenylate cyclase or phospholipase C, through the activation of G<sub>s</sub> and G<sub>q</sub> proteins, respectively, or both of them simultaneously. Coupling to mitogen-activated protein kinases and the activation of membrane ion channels have also been described.<sup>7</sup> The activation mechanism of membrane ion channels is not completely understood and could involve the  $\beta\gamma$  subunit of G proteins.<sup>8,9</sup>

Consistently with the structural studies deriving from the crystal of A<sub>2A</sub>AR, several structural features of A<sub>2B</sub>AR have been established. The topological structure is typical of GPCRs family A and is characterized by seven alpha-helical trans-membrane domains

(TM), connected each other by three extracellular (ELs) and three intracellular loops (ILs). The average sequence identity for the receptors subtypes of this family is around 47% for each species and increases approximately to 57% if only the TM domain is considered. The residues in the binding cavity involved in the ligand recognition are conserved among the AR subtypes. In the context of ARs the major differences were found in the active site of A<sub>3</sub>. Importantly, the differences in amino acid residues at the binding site are likely responsible of the ligand selectivity and reflect the unique pharmacologic profile of each adenosine receptor.<sup>9-11</sup>

The wide expression of A<sub>2B</sub>ARs on mast cells, lungs, bladder and on gastrointestinal tract accounts for the effects of their activation. Numerous evidences suggest that A<sub>2B</sub> receptors may play a role in different pathologic states among which asthma, diabetes, diabetic retinopathy and cancer are the most dissected,<sup>12</sup> but additional therapeutic indications have been detected in the treatment of inflammatory pain and in the attenuation of neurodegenerative disorders, as Alzheimer disease.<sup>8</sup>

The putative role of these receptors in asthma is supported by activation of this receptor in mast cells leading to degranulation, releasing of pro-inflammatory cytokines (e.g. interleukines IL-4, -8 and -13) and histamine.<sup>13</sup> In addition, activation of these receptors on bronchial smooth muscle cells leads to the release of the inflammatory cytokines monocyte chemoattractant protein 1 (MCP-1) and IL-6.<sup>14</sup> A series of experiments described the A<sub>2B</sub> receptor-mediated release of pro-inflammatory cytokines from a number of cells and tissues, including bronchial smooth muscle and epithelial cells, lung fibroblasts, and intestinal epithelial cells.<sup>9</sup> It was demonstrated that activation of the A<sub>2B</sub>AR promotes the differentiation of human fibroblasts into myofibroblasts via IL-6 release, resulting in airway remodelling, which is known to play an important role in the pathophysiology of inflammatory airway diseases.<sup>15</sup> A<sub>2B</sub> antagonists are also proved to attenuate the release of IL-19 from human bronchial epithelial cells and to prevent the secretion of IL-13 from mouse bone marrow-derived mast cells.<sup>8, 12</sup> These evidences led CVT 6883, an A<sub>2B</sub> AR antagonist, in phase I clinical trial for the development of an anti-asthma drug (CV Therapeutics).<sup>14</sup> Moreover, studies in animals models show that A<sub>2B</sub> antagonists may reduce airway reactivity and inflammation in allergic asthma.<sup>14</sup> However, since activation of A<sub>2B</sub> receptors on human bronchial epithelial cells (HBECS) may have an important function in the CFTR-Cl<sup>-</sup> (Cystic fibrosis transmembrane conductance regulator) channel control, A<sub>2B</sub> antagonists may reduce airway hydration, promoting secretion inspissation, mucus overproduction and plugging in patients with asthma. Although this effect of A<sub>2B</sub> antagonists on airway hydration and mucus viscosity in asthmatics has not been demonstrated, it could be a limit for safety and efficacy of this class of drugs in asthmatic patients.<sup>13</sup>

As adenosine is an ubiquitous metabolic sensing molecule, it is not surprising that the activation of its receptors is implicated in different aspects of glucose homeostasis.<sup>16</sup> In this respect, different findings outlined that A<sub>2B</sub> antagonists and/or mixed A<sub>2B</sub>/A<sub>1</sub>

antagonists may be useful in the treatment of diabetes. Some studies demonstrated that adenosine agonist analogues, NECA (non-selective), CPA ( $A_1$  selective) and CGS-21680 ( $A_{2A}$  selective) stimulate glucose production from rat hepatocytes, with NECA having the most pronounced effect.<sup>17, 18</sup> High affinity  $A_{2B}$  antagonists block NECA-induced glucose production in rat hepatocytes, although the compounds do not have high selectivity over  $A_1$ AR and  $A_{2A}$ AR.<sup>18</sup> In a separate study, the inhibition of glucose production was proved to have better correlation with the  $A_{2B}$ AR affinity.<sup>19</sup> A non-selective high affinity  $A_{2B}$  antagonist was shown to lower plasma glucose following oral dosing (10 and 30 mg/kg bodyweight) in a mouse model of non-insulin-dependent diabetes mellitus (NIDDM), KK-Ay mice.<sup>19</sup> However, due to the low selectivity of the antagonists used in the study, the role of  $A_{2B}$  antagonism has not been defined absolutely.<sup>12, 16</sup> Interestingly, an elevated gene expression of  $A_{2B}$ AR has been found in women with gestational diabetes mellitus (GDM), a pathology characterized by chronic insulin resistance and pancreatic  $\beta$ -cell dysfunction.<sup>16, 20</sup> The overexpression of  $A_{2B}$  receptors on maternal leukocyte has been associated with a series of complex alterations in the expression of diabetes-related genes involved in insulin action, carbohydrate and lipid metabolism, oxidative stress and inflammation. Therefore, the higher expression of this receptor could reflect the elevated plasma glucose level in diabetic patients.<sup>16, 21</sup>

The involvement of  $A_{2B}$  receptors has also been demonstrated in some pathologic conditions related to diabetes, like diabetic nephropathy and diabetic retinopathy.<sup>16</sup> The pathophysiologic mechanisms of diabetic nephropathy are not yet completely understood. Since the diabetic nephropathy is mediated by the modulation of vascular endothelial growth factor (VEGF)-nitric oxide (NO) balance in renal tissue, the adenosine signalling has been suggested as a target for a possible therapeutic intervention. As reported in some studies,  $A_{2B}$  receptors regulate VEGF expression under normoxic and hypoxic conditions in different tissues.<sup>22</sup> In particular, it has been observed that the renal content of  $A_{2B}$ ARs and VEGF was increased after 8 weeks of diabetes induction whilst the renal and plasma NO levels were reduced in these animals, suggesting that adenosine signalling might be the critical event in regulating VEGF-NO axis in diabetic nephropathy.<sup>22</sup> These data attribute a protective role for antagonists toward VEGF-induced diabetic glomerulopathy. It is important to highlight that the role of  $A_{2B}$  agonists and antagonists as potential treatment of this condition is still controversial. In fact, in contrast with these results, other studies demonstrated that CD73-dependent production of adenosine attenuates the diabetic nephropathy acting on endothelial  $A_{2B}$  receptors.<sup>16</sup>

Proliferative diabetic retinopathy is a process involving the human retinal endothelial cells (HREC). During the pathogenic process, ischaemic events lead to new vessel formation and disruption of normal vasculature, which are driven by the activation of  $A_{2B}$ ARs.<sup>23</sup> A further confirmation on the role of  $A_{2B}$  receptors is given by the increase in VEGF-mRNA in HRECs caused by NECA, which is then blocked by  $A_{2B}$ AR antisense oligonucleotides.<sup>12, 16</sup>

A recent study showed that A<sub>2B</sub>AR knockout mice exhibit attenuated tumour growth and decreased levels of VEGF in the tumours after inoculation with Lewis lung carcinoma when compared to wild-type mice, pointing at the involvement of A<sub>2B</sub>AR activation in the neovascularization of tumours.<sup>24</sup> The release of VEGF was increased by the nonselective agonist NECA but not by the A<sub>2A</sub>-selective agonist CGS-21680 (2-*p*-(2-carboxyethyl) phenethylamino-5'-*N*-ethylcarboxamidoadenosine), whereas a combination of NECA and the selective A<sub>2B</sub>AR antagonist did not show this effect, indicating that A<sub>2B</sub> antagonists might have the potential to inhibit tumour vascularization.<sup>25</sup> With regards to certain cancers, researchers at CV Therapeutics suggest that labelled antibodies directed against the A<sub>2B</sub>AR are potentially useful tools in detecting and possibly preventing the angiogenesis associated with gliomas, colon cancer and solid tumours.<sup>8, 12</sup>

As caffeine is known to have intrinsic anti-nociceptive properties when used in combination with NSAID's or opiates, Müller *et al.*<sup>26</sup> explored the anti-nociceptive effects of selective adenosine antagonists in a hot-plate test, and A<sub>2B</sub> antagonists were found to possess the best anti-nociceptive effects. Furthermore, an A<sub>2B</sub> AR antagonist was found to synergise with morphine for an enhanced anti-nociceptive effect in the same manner as caffeine.<sup>26</sup>

Finally, another potential application of A<sub>2B</sub> antagonists might be the attenuation of neurodegenerative disorders, such as Alzheimer disease, in which the neurodegeneration process could be in part related to A<sub>2B</sub>AR-mediated IL-6 release in human astrocytoma cells.<sup>8</sup>

Considering the social impact of the pathologic states in which A<sub>2B</sub> receptors are involved, both in terms of health care costs and life quality of patients, is obvious that further efforts are needed for the development of high selective agonists and antagonists that could be proposed as useful pharmacologic tool for the fundamental research and/or as drugs candidates.

### **3.1.2 A<sub>2B</sub> receptor. Agonists and antagonists**

Due to its clinical relevance, significant efforts were dedicated to the development of A<sub>2B</sub>AR interacting compounds and, over the last years, large progresses have been made in the identification of high affinity A<sub>2B</sub> agonists and antagonists.<sup>27</sup>

Based on the good results obtained for the other adenosine receptor subtypes, the starting point for the synthesis of agonists were the endogenous agonist adenosine. Despite the high number of adenosine analogues synthesized and investigated for their ability to activate A<sub>2B</sub> receptors, the non-selective NECA (5'-*N*-ethylcarboxamido adenosine) and its derivative (*S*)-PHP NECA show the highest affinity. However, the most active compound synthesized so far as A<sub>2B</sub> agonist belong to a class of non-ribose derivatives, known as dicarbonitrilepyridines.<sup>27</sup>



By contrast, different classes of antagonists, including xanthines, pyrrolopyrimidines, triazoles, aminothiazoles, and quinazolines derivatives, have been identified. Notably, each class possesses compounds endowed with both high affinity and selectivity for the adenosine A<sub>2B</sub> receptor, but among these, xanthines have been the most extensively studied compounds.<sup>27</sup>

The natural xanthine derivatives caffeine and theophylline act as nonselective antagonists on adenosine receptors, particularly on A<sub>1</sub>, A<sub>2A</sub> and A<sub>2B</sub> subtypes. Some synthetic xanthine derivatives, with the exception of the theophylline (which is a naturally occurring product), are reported in Figure 3.1.<sup>28</sup> Theophylline (**1**), which has 9 μM affinity for the A<sub>2B</sub>AR, displays no selectivity against the other adenosine receptors. Enprofylline (**2**), a 3-propyl-xanthine derivative has moderate A<sub>2B</sub> affinity and low selectivity over the other AdoRs. However, further structural explorations of this scaffold by several groups lead to the discovery of 8-phenylxanthines as selective A<sub>2B</sub>AR antagonists. Among these, different 8-phenylxanthine derivatives, including a p-cyanoanilide derivative MRS-1754 (**3**) of Jacobson et al.<sup>29</sup> and a negatively charged PSB-1115 (**4**) of Müller et al.<sup>30</sup> stand out as selective A<sub>2B</sub> antagonists. To address the metabolic stability of MRS-1754 (**3**) in human liver microsomal enzymes, Zablocki et al.<sup>31</sup> synthesized CVT-5440 (**5**), in which the metabolically labile amide group present in **3** has been substituted with a oxadiazole bioisoster group. Compound **5** demonstrated good affinity for the A<sub>2B</sub>AR, selectivity over the other AdoRs and improved *in vitro* metabolic stability with respect to compound **3**. However, a very low systemic exposure in rats has been observed when this compound were dosed orally, presumably due to low solubility.<sup>28</sup>

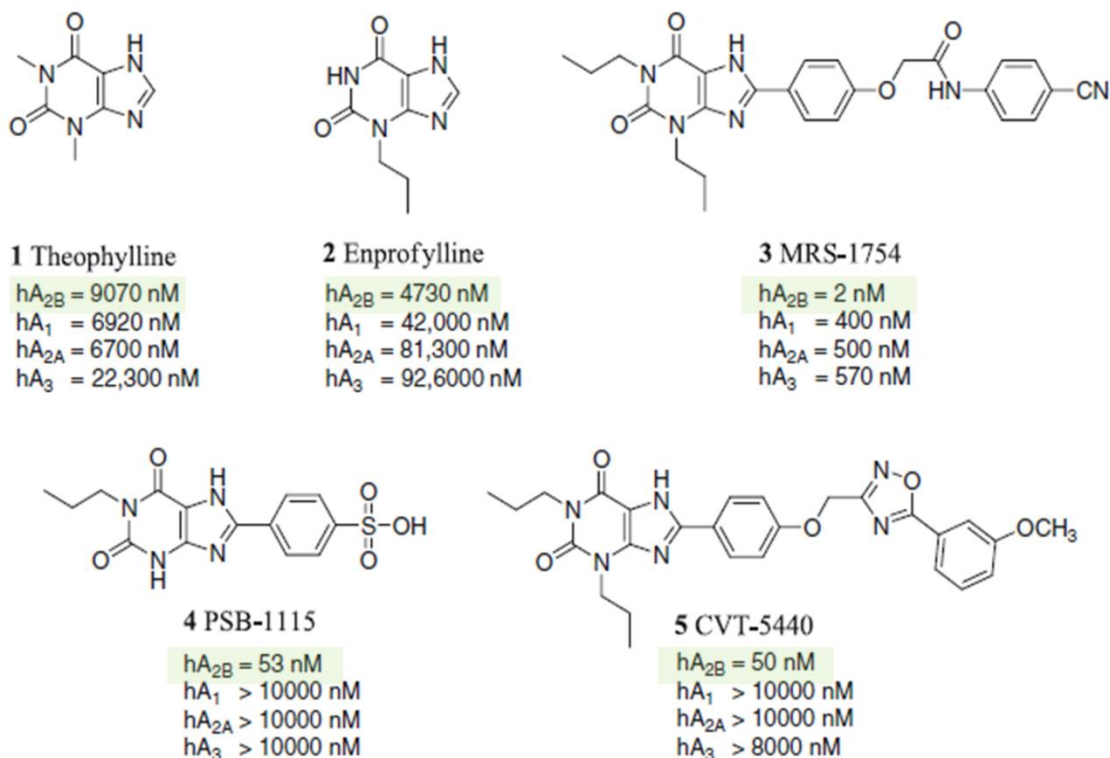


**Figure 3.1.** Prototypical xanthine-derived  $A_{2B}R$  antagonists.<sup>28</sup>

Starting from these evidences, different research groups explored various substitutions to achieve selective and high affinity  $A_{2B}$  antagonists. As an example, the bioisosteric replacement of the phenyl group at the position 8 with different heterocycles led to the discovery that 8-(pyrazol-4-yl)xanthines are characterized by a good affinity for  $A_{2B}$  receptors. The prototypical compound 1,3-dipropyl-8-(1H-pyrazol-4-yl)xanthine (CVT-5450) showed high affinity but very low selectivity. The most encouraging data with respect to this compound was the high systemic exposure after oral dosing in rat. Therefore, different structural modifications have been made on the 8-(pyrazol-4-yl)xanthine to increase the selectivity.<sup>32</sup> This optimization process included:

1. the insertion of an aromatic group on the pyrazole ring, obtaining different compounds among which the benzylic derivatives showed the best selectivity value compared to the phenyl, phenethyl, and phenpropyl derivatives. A further modification of benzylic group, introducing the electron withdrawing groups F and  $CF_3$  at the meta-position increased the selectivity toward the  $A_{2B}$  AdoR.
2. Replacing the 1,3-dipropyl groups of the xanthine core with various alkyl groups like methyl, ethyl, butyl, and isobutyl groups suggested that smaller alkyl groups relative to propyl increase the  $A_{2B}$  AdoR affinity and selectivity compared to the large groups.
3. Investigation of the monosubstitution at the N-1 position of the 8-pyrazolyl xanthine provided  $A_{2B}$  AR antagonists with very high affinity and selectivity. For example,

the compound CVT-7124 (1-propyl-8-(1-(3-(trifluoromethyl)benzyl)-1H-pyrazol-4-yl)-xanthine) displays high  $A_{2B}$  affinity (6 nM) and very good selectivity. Observation in the 8-phenyl xanthine series of compounds demonstrated that the monosubstitution at the N-1 position of the xanthine core enhances the  $A_{2B}$ AR selectivity.<sup>27, 28, 32</sup>

Similarly to 8-(pyrazol-4-yl)xanthines, several xanthine derivatives were synthesized and improved in terms of affinity and selectivity. Even though substituted xanthine derivatives show the most promising combination of high affinity and selectivity, they often show poor water solubility and thus low oral bioavailability. Thus, a further optimization of this scaffold is required to obtain new compounds with enhanced pharmacokinetic properties.<sup>8, 27, 28</sup>

## 3.2 SYNTHESIS OF 1,8-SUBSTITUED XANTHINES AS SELECTIVE ANTAGONISTS OF $A_{2B}$ AR.

### 3.2.1 Structural features and synthetic pathway

Since the majority of the non-xanthine  $A_{2B}$  antagonists developed so far is characterized by only moderate selectivity toward other AdoR subtypes, this work focuses on the synthesis of xanthine-based  $A_{2B}$  antagonists. Taking into account a pharmacophore model developed by Yan et al.,<sup>33</sup> the aim of this study is to develop high-affinity  $A_{2B}$  antagonists endowed with high selectivity in humans as well as in rodents.<sup>33</sup> This model, reported in Figure 3.2, has been obtained by the structural comparison of the most active  $A_{2B}$  antagonists and is characterized by a xanthine- or, less frequently, a deazapurine-central core and an aromatic portion linked each other by a long spacer (7-10 atoms long), consisting in a cyclic, aromatic or non-aromatic portion with a hydrogen bond acceptor.

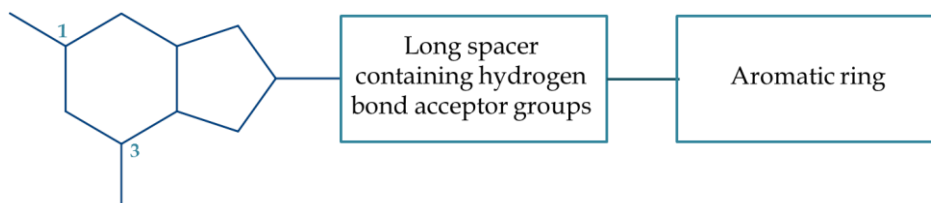


**Figure 3.2.** Pharmacophore model for the synthesis of high-affinity  $A_{2B}$  antagonists.<sup>33</sup>

The central core bears a hydrogen bond acceptor and a hydrogen bond donor in C6-oxygen and N7-hydrogen of xanthine moiety, respectively. The positions 1 and 3 of this core may be substituted with alkyl residues that can fill two lipophilic pockets found in AdoRs. In particular, small alkyl substituent (propyl, ethyl and methyl) at position 1 proved to increase  $A_{2B}$ AR affinity, whereas additional alkylation at position 3 led to a decrease in  $A_{2B}$ AR affinity and an increase in  $A_1$  and  $A_{2A}$ ARs affinity. Several studies

demonstrated that the lipophilic propyl residue in position 1 is the best one for enhancing A<sub>2B</sub>AR affinity. Position 8 is substituted with the spacer, which is further connected to an aromatic residue. Therefore, taking 1-propyl-8-*p*-sulphophenylxanthine, PSB-1115, (Figure 3.1, compound **4**) as a lead structure, several structural features were found.<sup>8, 33</sup> More in detail:

1. The central core is a 1-propyl-xanthine derivative. In this portion unsubstituted N-3 and N-7 are also important for the receptor interaction.

2. The spacer, tied to the central core in position 8 of xanthine moiety, consists in an aromatic ring, bearing a sulphonamidic group in position 4. The insertion of a sulfamidic group in this position may improve the bioavailability with respect to the lead compound PSB-1115. In this compound, the sulphonic acid group in the aromatic spacer seems to contribute to the high selectivity at A<sub>2B</sub> over the other AdoRs. Additionally, it contributes to the high water-solubility, which makes PSB-1115 a useful tool for *in vivo* studies. However, the polar character of free sulphonic acid groups (deprotonated under physiological conditions) is associated with a poor per-oral bioavailability. Thus, the introduction of a basic piperazine, which can be protonated under physiological conditions, improves water solubility. Importantly, the connection of piperazine via sulphonamidic bond leads to a sterically restricted spacer.<sup>33</sup>

These structural features are reported in Figure 3.3.

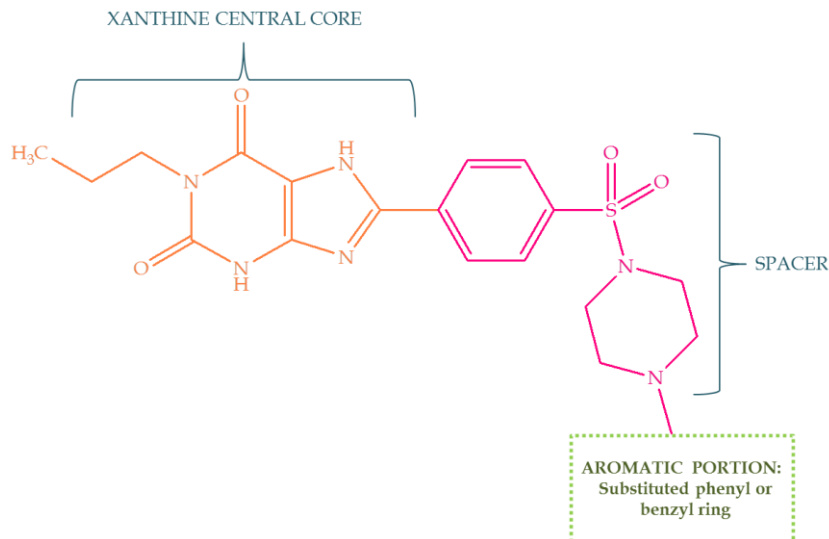


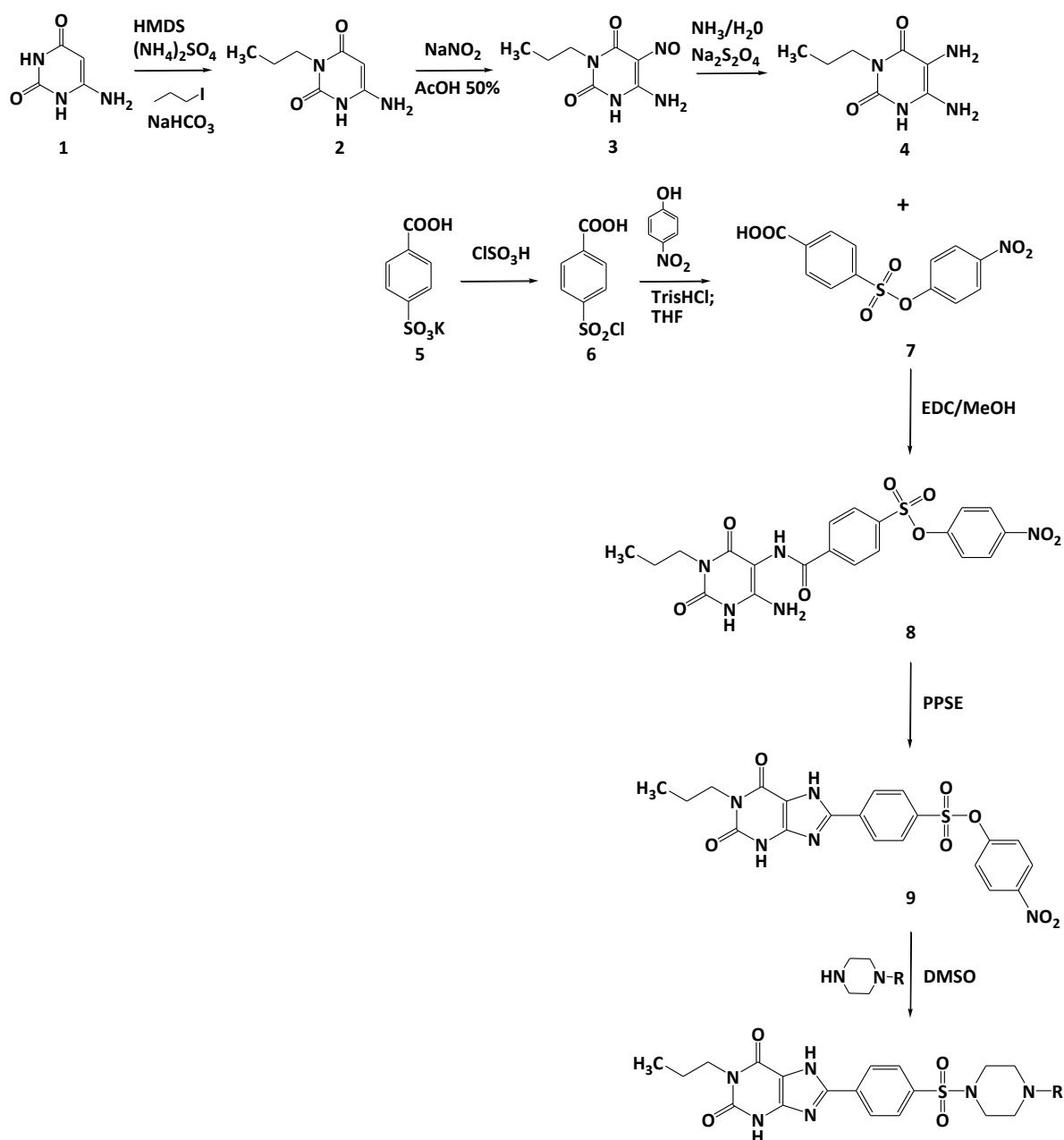
**Figure 3.3.** Structural feature of synthesized compounds.

Starting from this previous study, and considering the importance of the aromatic portion, this work is focused on the synthesis of different derivatives in which the influence of substituted-phenyl and -benzyl piperazine is analysed, both in terms of affinity and selectivity for A<sub>2B</sub> receptors.

Based on the abovementioned pharmacophore model, different compounds have been synthesized according to the procedure depicted in Scheme 3.1.

The synthetic procedure is divided in several steps, including:

1. the synthesis of precursors 1-propyl-5,6-diaminouracil and 4-(*p*-nitrophenoxysulphonyl) benzoic acid;
2. the amide coupling between 1-propyl-5,6-diaminouracil and 4-(*p*-nitrophenoxysulphonyl) benzoic acid;
3. the ring closure, leading to the xanthine formation;
4. the aminolysis of *p*-nitrophenylsulphonates with substituted 4-phenyl- or benzyl-piperazine.



**Scheme 3.1.** General scheme of reaction

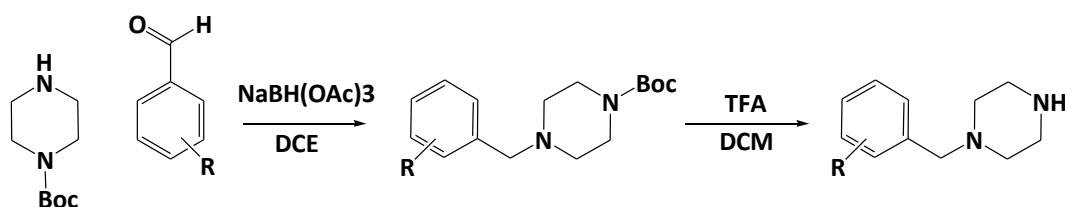
Substituted 5,6-diaminouracil and 4-(*p*-nitrophenoxysulphonyl) benzoic acid were obtained according to following procedures.

The precursor 3-propyl-6-aminouracil (**2**) is obtained via a regioselective synthesis starting from commercially available 6-aminouracil. During this reaction, the silylation with HMDS (hexamethyldisilazane) enables specific alkylation of the uracil N3-position of 6-aminouracil, leading to 1-propyl-6-aminouracil.<sup>34</sup> After nitrosation at the uracil 5-position (affording derivative **3**)<sup>35</sup> and subsequent reduction, 5,6-diamino-3-propyluracil (**4**) was obtained. This derivative is unstable towards oxidation and therefore has to be freshly prepared each time before performing the subsequent amide coupling reaction.

Amide coupling was performed reacting 1-propyl-5,6-diaminouracil with 4-(*p*-nitrophenoxysulphonyl)benzoic acid (**7**), using EDC (*N*-(3-(dimethylamino)-propyl)-*N'*-ethylcarbodiimide) as condensing agent to yield amides (**8**).<sup>36</sup> Compound **7** was obtained by a two steps methodology. In particular, the required 4-(chlorosulphonyl)benzoic acid (**5**) can be obtained starting from the corresponding sulphonic acid potassium salt, which is converted to **5** using chlorosulphonic acid. In the following step, **5** is reacted with *para*-nitrophenol forming **6**. Introduction of the *p*-nitrophenyl substituent (connected via a sulphonic acid ester bond) is necessary to insert a good leaving group which activates the sulphonate group for nucleophilic substitution.<sup>33</sup>

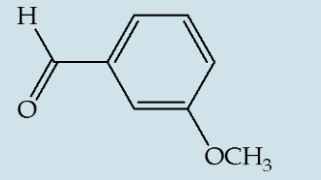
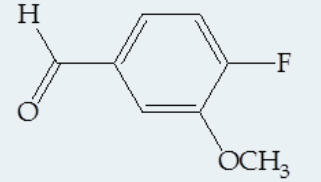
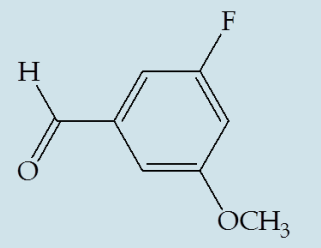
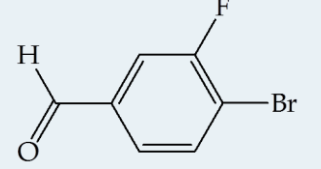
Ring closure to the corresponding xanthine derivatives was achieved by heating with polyphosphoric acid trimethylsilyl ester (PPSE), obtaining compound **9**. In case of *N*-propyl-substitution, PPSE (trimethylsilyl polyphosphate) proved to be the best reagent.

The final sulphonamides were obtained in the last step by aminolysis of *p*-nitrophenylsulphonates with substituted 4-phenyl or benzylpiperazine. Substituted 4-phenylpiperazine were commercially available, while 4-benzylpiperazine were obtained via reductive amination using sodium triacetoxyborohydride, starting from boc-protected piperazine and an excess of the required benzaldehyde. The subsequent deprotection using TFA give the expected compound.<sup>37</sup> The reaction is reported in the Scheme 3.2, while Table 3.1 reports the used benzaldehydes.



**Scheme 3.2.** General scheme for the synthesis of benzylpiperazines

**Table 3.1.** Substituted benzaldehydes: group R in scheme 3.2.

Benzaldehydes (R)	
3-methoxybenzaldehyde	
4-fluoro-3-methoxybenzaldehyde	
3-fluoro-5-methoxybenzaldehyde	
4-bromo-3-fluorobenzaldehyde	

The procedure for the final step (aminolysis of the *p*-nitrophenylsulphonate) was carried out using DMSO as a solvent at 160-170°C. The formation of yellow-coloured side-products during the final coupling step was observed in all cases. The nature of these coloured compounds were elucidated in a previous study, indicating that two competing reactions for the nucleophilic substitution of the *p*-nitrophenylsulphonates are possible (Figure 3.4):

1. The nucleophilic attack at the sulphur atom leading to S-O bond cleavage;
2. The nucleophilic attack at the 1-carbon atom of the phenyl ring resulting in C-O bond cleavage.

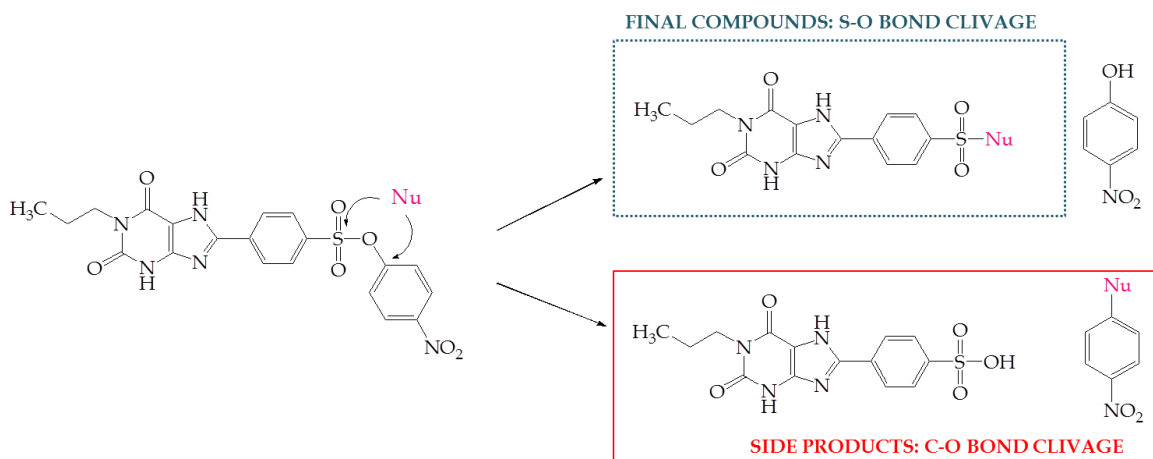


**Figure 3.4.** Nucleophilic substitution of *p*-nitrophenylsulfonate.

For the aminolysis of *p*-nitrophenylsulfonate, predominant S-O bond cleavage is desirable, while C-O bond cleavage results in reduced yields. Mechanistic investigations by Choi et al.<sup>38</sup> pointed to several possibilities to influence S-O or C-O bond cleavage (e.g. substitution of the sulphur and/or the phenol ester moiety, nucleophile and solvent). Importantly, several investigation suggested an important influence of the solvent on S-O versus C-O bond. However, in most cases both pathways are likely to occur. In addition to this side reaction, the formation of several by-products are observed and has been related to high temperatures.<sup>8, 33</sup>

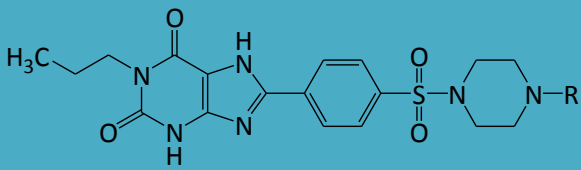
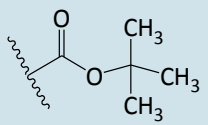
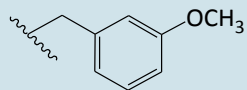
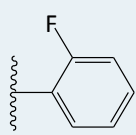
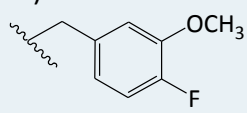
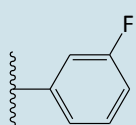
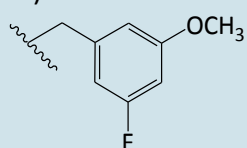
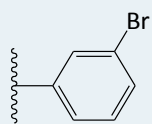
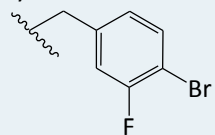
The synthetic pathway adopted for the synthesis of compound **JJ1533** (Table 3.2) differs from the procedures previously indicated. In this specific case, the use of a protected piperazine in the last step (aminolysis reaction) is necessary. However, the deprotection reaction of nitrogen in position 4 of piperazine, necessary to obtain the final product, is a critical step. In fact, the use of strong conditions can lead to hydrolysis of the sulphonamide group, with a drastic reduction of the yields. For this reason, the synthesis was carried out using N-acetylpiperazine, instead Boc-piperazine, that requires mild hydrolysis conditions. The used conditions are reported in the section 3.4.2.6.

Final compounds were subsequently purified by reverse-phase high performance liquid chromatography (RP-HPLC). All the synthesized xanthine-8-yl-benzenesulphonamides are reported in Table 3.2.

The structures of final products were confirmed by mass spectrometry employing electron spray ionization (ESI) and by <sup>1</sup>H and <sup>13</sup>CNMR spectroscopy. Purity was determined by RP-HPLC analysis coupled to UV detection at 254 nm and found to be higher than 95% in all cases.



**Table 3.2.** Structure of synthesized compounds.

	
(JJ1533) H	(JJ1520) CH <sub>3</sub>
(JJ1532) 	(JJ1517) 
(JJ1521) 	(JJ1534) 
(JJ1522) 	(JJ1535) 
(JJ1523) 	(JJ1536) 

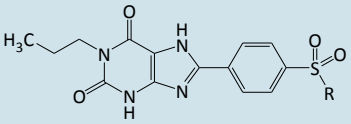
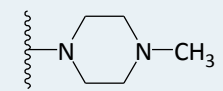
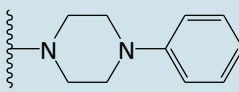
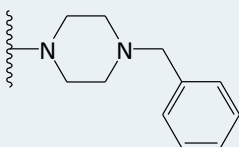
### 3.2.2 Results and discussion

While maintaining the optimized xanthine core structure, a set of new compounds was synthesized, introducing different aromatic portions in position 4 of piperazine. These newly synthesized compounds should contribute to extend the understanding of structure-activity relationships for the class of xanthine derivatives and, in particular, the influence of phenyl and benzyl substituent in the piperazine moiety. Since each compound bear different substituents in these aromatic portions, a deeper analysis of pharmacological results enables to obtain more detailed information about the nature and/or position of substituent in the aromatic portion. As only a part of the synthesized compounds has been tested, it is not possible to provide a detailed analysis of structure-activity relationships of these compounds.

Therefore, the activity of **JJ1520** and **JJ1521** is shown in Table 3.3 and Table 3.4, respectively, and compared to the activity of other compounds, previously synthesized in the same laboratory. The data reported in these tables show the affinity values ( $K_i$ ,  $\mu\text{M}$ ) obtained in a competitive radioligand binding assay.

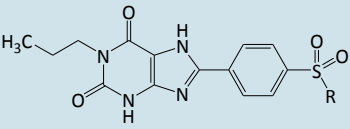
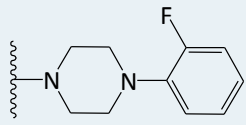
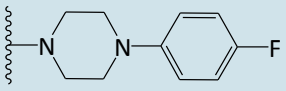
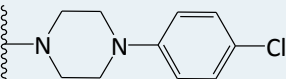
The activity of **JJ1520**, bearing a methyl group in position 4 of the piperazine, has been compared with an unsubstituted 4-phenylpiperazine and the 4-benzylpiperazine. The obtained data indicates that the presence of an aromatic group in this position enhance the affinity for  $A_{2B}$  receptor, further confirming the pharmacophore model predictions. In addition, the different activities of 4-phenyl and 4-benzyl piperazine suggest an influence of the length of the spacer between these two moieties.

**Table 3.3.** **JJ1520** activity compared to the activity of other compounds, previously synthesized, with  $K_i$  expressed in  $\mu\text{M}$ .

Compounds	Receptors			
	$A_{1A}$ AR (human recombinant) $[^3\text{H}]\text{CCP}$ A	$A_{2A}$ AR (human recombinant) $[^3\text{H}]\text{MS}$ X-2	$A_{2B}$ AR (human recombinant) $[^3\text{H}]\text{PSB}$ -603	$A_{3A}$ AR (human recombinant) $[^3\text{H}]\text{PSB}$ -11
				
<b>JJ1520</b> 	$334 \pm 109$	$140 \pm 91$	$48.2 \pm 10.9$	$>1000$
	$364 \pm 57$	$122 \pm 32$	$0.643 \pm 0.035$	$>1000$
	$2,067 \pm 261$	$484 \pm 115$	$3.6 \pm 0.4$	$>1000$

The compound **JJ1521**, instead, presents in the position 4 of the piperazine a 2-fluorophenyl group and is compared with halogenated structural analogues, having a *p*-fluorophenyl and a *p*-chlorophenyl in position 4 of piperazine moiety. For this set of compounds is possible to observe that chlorine is the best substituent and the para position is the preferred one.

**Table 3.4.** JJ1521 activity compared to the activity of other compounds, previously synthesized, with  $K_i$  expressed in  $\mu\text{M}$ .

Compounds	Receptors			
	$A_1\text{AR}$ (human recombinant) $[^3\text{H}]\text{CCP}$ A	$A_{2A}\text{AR}$ (human recombinant) $[^3\text{H}]\text{MSX}$ -2	$A_{2B}\text{AR}$ (human recombinant) $[^3\text{H}]\text{PSB}$ -603	$A_3\text{AR}$ (human recombinant) $[^3\text{H}]\text{PSB}$ -11
<b>JJ1521</b> 	>1000	>1000	$3.22 \pm 1.39$	>1000
	>1000	$108 \pm 25$	$0.644 \pm 0.154$	>1000
	>10000	>10000	0.553	>10000

### 3.3 CONCLUSIONS

In this work a series of xanthine derivatives were synthesized as high affinity  $A_{2B}$  antagonists. Some of synthesized compounds (**JJ1520** and **JJ1521**) were tested in a competition radioligand binding assay, confirming the structural features predicted in the pharmacophore model. A further step toward the understanding of the structure-activity relationships will be obtained following the biological results of each compound of this series. The critical analysis of these results will be essential to define the structural features required to further refine the affinity and selectivity for  $A_{2B}\text{AdoR}$ .

## 3.4 EXPERIMENTAL SECTION

### 3.4.1 Materials and methods

All the materials, reagents and solvents, if not specified, were purchased from commercial suppliers and used without any further purification.

Each reaction and purification method were monitored using Thin Layer Chromatography (TLC), using precoated Merk Silica gel 60 254F. Detection was carried out using UV light at 254 nm and 366 nm.

Purification methods were performed by chromatographic columns for precursors, when needed, and by HPLC for final compounds. Chromatographic columns were performed using Silica gel, while preparative HPLC was performed on a Knauer HPLC system using a Wellchrome K-1800 pump, a WellChrome K-2600 spectrophotometer, and a Eurospher 100 C18 column (250 mm × 20 mm, particle size 10 μm). A gradient of methanol in water was used as indicated below with a flow rate of 20 mL/min.

Melting points (Mp) were measured using a Buchi 530 apparatus and are uncorrected.

The <sup>1</sup>H and <sup>13</sup>CNMR spectra of synthesized compounds were recorded either on a Bruker Avance 500 MHz or on a Bruker Ascend™ 600 MHz spectrometer, using tetramethylsilane (TMS) as internal standard. Chemical shifts are reported in ppm, with the use of a δ scale, and the coupling constants J in Hz.

To determine purity and identity of final compounds and precursors, mass spectra were recorded on an API 2000 (Applied Biosystems, Darmstadt, Germany) mass spectrometer (turbo spray ion source) coupled with an Agilent 1100 HPLC system (Agilent, Böblingen, Germany). The standard method uses a gradient of water : methanol 90:10 to 0:100 with triethylamine as additive. The UV absorption was detected from 190-900 nm using a diode array detector (DAD). The purity of all compounds was determined at 220-400 nm.

### 3.4.2 Chemistry and structural characterization

The general method of reaction for the synthesis of 1-propyl-8-(piperazine -1-sulphonyl)phenylxanthines and 1-propyl-8-(benzylpiperazine -1-sulphonyl)phenylxanthines has been discussed in the Section 3.2.1. In this paragraph a more detailed overview of the synthesis of each compound will be provided.

## Synthesis of 1-propyl-5,6-diamino uracil

### *Synthesis of 6-amino-3-propyl-uracil*

A mixture of 4-(6)-aminouracil (1 mmol), ammonium sulfate (0.03 mmol) and 1,1,1,3,3,3-hexamethyldisilazane, HMDS, (2.4 mmol) was heated at 190°C until the solution was clear, obtaining a brown solution. The solution was cooled (65°C) and 1-iodopropane (1.5 mmol) was added. Then the solution was heated for other 2 hours at 125°C. The viscous solution was cooled in an ice bath and a saturated solution of sodium hydrogen carbonate (200 ml) was gradually added. In this way the viscous residue turned into a suspension. The resulting brown precipitate was collected by filtration, washed with water, dried and directly used for the next step.

Light brown powder; Yield 85%; MW 169.18 g/mol

$^1\text{H}$  NMR (600 MHz, DMSO- $d_6$ ):  $\delta$  10.26 (s, 1H, -NH), 6.13 (s, 2H, -NH<sub>2</sub>) 4.53 (s, 1H, -CH), 3.59 (t, 2H, -CH<sub>2</sub>CH<sub>2</sub>CH<sub>3</sub>), 1.45 (m=6, 2H, -CH<sub>2</sub>CH<sub>2</sub>CH<sub>3</sub>), 0.80 (t, 3H, -CH<sub>2</sub>CH<sub>2</sub>CH<sub>3</sub>)

$^{13}\text{C}$  NMR (151 MHz, DMSO- $d_6$ ):  $\delta$  162.98, 153.94, 150.92, 74.71, 40,61, 21.57, 11.56.

### *Synthesis of 6-amino-5-nitroso-3-propyluracil*

A solution of 6-amino-3-propyl-uracil (1 mmol) in aq AcOH 50% was prepared heating at 70-80°C. The mixture was stirred until it became a clear solution. Then sodium nitrite (1.5 mmol) was added in small portions over a period of 20 minutes, leading to the formation of a suspension. The mixture was heated (70-80°C) for 30-45 minutes and cooled at room temperature. The orange precipitate was separated by filtration under reduced pressure, washed with 200 mL of water and then dried.

Orange solid; Yield 91%; MW 198.18 g/mol

$^1\text{H}$  NMR (600 MHz, DMSO- $d_6$ ):  $\delta$  11.45 (s, 1H, -NH), 7.92(s, 2H, -NH<sub>2</sub>), 3.79 (t, 2H, -CH<sub>2</sub>CH<sub>2</sub>CH<sub>3</sub>), 1.59 (m=6, 2H, -CH<sub>2</sub>CH<sub>2</sub>CH<sub>3</sub>), 0.89 (t, 3H, -CH<sub>2</sub>CH<sub>2</sub>CH<sub>3</sub>)

$^{13}\text{C}$  NMR (151 MHz, DMSO):  $\delta$  161.32, 149.28, 144.22, 41.59, 21.27, 11.17.

### *Synthesis of 5,6-diamino-3-propyluracil*

A mixture of 5,6-diamino-propyl-uracil (1 mmol) in aqueous ammonia solution 12,5% was heated at 70°C, observing the formation of a red clear solution. A huge amount of sodium dithionite (2.8 mmol) was added in small portions over a period of 20 minutes, until the solution became colourless. The reaction was monitored with TLC (DCM/MeOH 3:1, R<sub>f</sub>=5.4). The solution was cooled at room temperature and concentrated to obtain a solid. The solid was filtered obtaining a light yellow powder. The obtained compound is not stable, thus it was dried (ca. 30') and directly used for the next step.

Light yellow solid; Yield 73%; MW 184.2 g/mol

## Synthesis of 4-[(4-nitrofenoxy)sulphonyl]benzoic acid

### *Synthesis of 4-(chlorosulphonyl)benzoic acid*

Chlorosulphonic acid (10.7 mmol) was slowly added to p-sulphobenzoic acid potassium salt (1 mmol) while the temperature was kept below 30°C using an ice bath. The mixture turned gradually to a clear solution and was stirred overnight at room temperature. The solution was carefully added in a beaker containing chipped ice. In this way a white precipitate was obtained. Such precipitate was then filtered and washed with 250 mL of cold water. The dried solid was directly used for the next step without any further purification.

White solid; Yield 60%; MW 220.63 g/mol

### *Synthesis of 4-[(4-nitrofenoxy)sulphonyl]benzoic acid*

A solution of 4-(chlorosulphonyl)benzoic acid (1 mmol) in THF was slowly added to a second solution of p-nitrophenol (1 mmol) in THF and tris HCl buffer using an injection pump (6 mL/h). The pH value of the solution was kept around 8-9 by the addition of a solution of NaOH 2,5N.

After stirring at room temperature (at least for other 2 h) the pH value of solution was decreased to 7, adding of a solution of HCl 1N and THF was removed under reduced pressure. The product of the reaction precipitated when the aqueous solution was further acidified to pH 1. The precipitate was collected by filtration and dried over vacuum pump.

White solid; Yield 86%; MW 323.28 g/mol

<sup>1</sup>H NMR (600 MHz, DMSO-d<sub>6</sub>): δ 13.70 (bs, 1H, -COOH), 8.26 (d, 2H, aromatic, J<sub>o</sub>=9, J<sub>m</sub>=3), 8.17 (d, 2H, aromatic, J<sub>o</sub>=8.4), 8.02(d, 2H, Aromatic, J<sub>o</sub>=8.4), 7.35 (d, 2H, aromatic, J<sub>o</sub>=9, J<sub>m</sub>=3)

<sup>13</sup>C NMR (151 MHz, DMSO-d<sub>6</sub>) δ 165.97, 153.25, 146.25, 137.59, 137.21, 131.18, 128.84, 126.21, 123.89.

## Synthesis of 4-nitrofenil-4-[(6-amino-2,4-dioxo-3-propyl-1,2,3,4-tetrahydropyrimidin-5-yl) carbamoyl] benzenesulphonate

A solution of 5,6-diamino-3-propyluracil (1 mmol), 4-[(4-nitrofenoxy)sulphonyl]benzoic acid (1.03 mmol) and 1-ethyl-3-(3-dimethylaminopropyl)carbodiimide, EDC, (1.3 mmol) was stirred for at least 5 h at room temperature, using methanol as a solvent. The mixture was stirred under Argon atmosphere obtaining a light yellow suspension. The precipitate was filtered obtaining a sticky product. The product was washed with water and dried over vacuum pump, obtaining a light yellow powder.

Light yellow solid; Yield 45%; MW 489.46 g/mol

LC/MS: positive mode ( $m/z$ )=490.4  $[M+H]^+$ ; Purity 68%

### Synthesis of 4-nitrofenil-4-(2,6-dioxo-1-propyl-2,3,6,7-tetrahydro-1H-purin-8-yl)benzenesulphonate

A mixture of compound 4-nitrofenil-4-[(6-amino-2,4-dioxo-3-propyl-1,2,3,4-tetrahydropyrimidin-5-yl)carbamoyl]benzenesulphonate (8) (1 mmol) and trimethylsilyl polyphosphate, PPSE, (four times the weight of compound 8) was stirred for 1 hour at 170°C, obtaining a clear solution. After cooling at room temperature, a small amount of methanol was added, leading to the formation of a precipitate. The solid was separated by filtration, washed with methanol and dried over vacuum pump. The reaction product was purified by chromatography, using DCM/MeOH in gradient, starting from a mixture 12:1 as eluent.

White solid; Yield 67%; MW 471.44 g/mol

LC/MS: positive mode  $m/z$ =472.3  $[M+H]^+$ ; Purity 99%

$^1\text{H}$  NMR (600 MHz, DMSO- $d_6$ ):  $\delta$  14.12 (s, 1H, -NH), 11.97 (s, 1H, -NH), 8.34 (d, 2H, -CH aromatic,  $J_o=8,4$ ), 8.26 (d, 2H, -CH aromatic,  $J_o=9.5$ ), 8.03(d, 2H, -CH aromatic,  $J_o=8.4$ ), 7.38 (d, 2H, -CH aromatic,  $J_o=9.5$ ), 3.82 (t, 2H,  $-\underline{\text{CH}_2\text{CH}_2\text{CH}_3}$ ), 1.57 (m=6, 2H,  $-\text{CH}_2\underline{\text{CH}_2}\text{CH}_3$ ), 0.87 (t, 3H,  $-\text{CH}_2\text{CH}_2\underline{\text{CH}_3}$ ).

$^{13}\text{C}$  NMR (151 MHz, DMSO- $d_6$ ):  $\delta$  155.07 (-C6xanth.), 153.22 (-C2xanth.), 151,13 (-C8xanth.), 147.77 (-C4xanth.), 147.47 (-C aromatic), 146.33 (-C aromatic), 135.02 (-C aromatic), 134.29 (-C aromatic), 129.25 (-CH aromatic), 127.49 (-CH aromatic), 126,04 (-CH aromatic), 123.61 (-CH aromatic), 108.96 (-C5xanth.), 41.66 ( $-\underline{\text{CH}_2\text{CH}_2\text{CH}_3}$ ), 20.99 ( $-\text{CH}_2\underline{\text{CH}_2}\text{CH}_3$ ), 11.34 ( $-\text{CH}_2\text{CH}_2\underline{\text{CH}_3}$ ).

### Synthesis of 4-benzylpiperazines

Boc-piperazine (1 mmol) and a benzaldehyde (1 mmol) were mixed in 1,2-dichloroethane and treated with sodium triacetoxyborohydride (1.3 mmol). The mixture was stirred overnight at room temperature and under Argon atmosphere. The reaction was stopped adding aqueous saturated Sodium hydrogen carbonate ( $\text{NaHCO}_3$ ) and the product was washed with a saturated solution of Sodium Chloride ( $\text{NaCl}$ ), then dried with Magnesium Sulphate ( $\text{MgSO}_4$ ). The solvent was evaporated to give an oily sample for the column.

To a solution of boc-benzylpiperazine (1 mmol) in dichloromethane, trifluoro acetic acid, TFA, (10 mmol) was added dropwise, while the temperature was kept at 0°C using an ice bath. The reaction was stirred vigorously overnight. The mixture was poured in 25mL of water. The aqueous layer was collected and treated with a saturated solution of

NaHCO<sub>3</sub> to adjust the pH to 8. Then the mixture was extracted with DCM (3x30mL). The organic layer was treated with MgSO<sub>4</sub> and concentrated to obtain the expected product.

#### **1-(3-methoxybenzyl)piperazine**

Yellow-orange liquid; Yield 83%; MW 206.28 g/mol

LC/MS: positive mode  $m/z=207$  [M+H]<sup>+</sup>; Purity 95%

<sup>1</sup>H NMR (600 MHz, chloroform-d):  $\delta$  7.21 (t, 1H, -CH aromatic,  $J_{o1,2}=7.8$ ), 6.86 (m, 2H, -CH aromatic), 6.80 (dd, 1H, -CH aromatic,  $J_o=8$ ;  $J_m=2.4$ ), 3.78 (s, 3H, -OCH<sub>3</sub>), 3.53 (s, 2H, -CH<sub>2</sub>), 3.17 (bs, 4H, -CH<sub>2</sub> piperazine), 2.70 (bs, 4H, -CH<sub>2</sub> piperazine).

<sup>13</sup>C NMR (151 MHz, chloroform-d):  $\delta$  159.87, 129.55 (-CH aromatic), 121.32 (-CH aromatic), 114.32 (-CH aromatic), 113.05 (-CH aromatic), 62.42 (-CH<sub>2</sub>), 55.18 (-OCH<sub>3</sub>), 49.45 (-CH<sub>2</sub> piperazine), 43.47 (-CH<sub>2</sub> piperazine).

#### **1-(4-fluoro-3-methoxybenzyl)piperazine**

White solid; Yield 94%; MW 224.27 g/mol; Mp 90-92°C

LC/MS: positive mode  $m/z=225$  [M+H]<sup>+</sup>; Purity 95%

<sup>1</sup>H NMR (600 MHz, chloroform-d):  $\delta$  7.00 (dd, 1H, -CH aromatic,  $J_{oH-H}=8.4$ ;  $J_{oH-F}=11.4$ ), 6.92 (dd, 1H, -CH aromatic,  $J_o=7.8$ ;  $J_m=1.2$ ), 6.79-6.77 (m, 1H, -CH aromatic), 3.87 (s, 3H, -OCH<sub>3</sub>), 3.49 (s, 2H, -CH<sub>2</sub>), 3.16 (bs, 4H, -CH<sub>2</sub> piperazine), 2.67 (bs, 4H, -CH<sub>2</sub> piperazine).

<sup>13</sup>C NMR (151 MHz, chloroform-d):  $\delta$  152.66, 150.99, 121.03(-CH aromatic), 115.69 (-CH aromatic), 113.72 (-CH aromatic), 62.02 (-CH<sub>2</sub>), 56.19 (-OCH<sub>3</sub>), 49.50 (-CH<sub>2</sub> piperazine), 43.52 (-CH<sub>2</sub> piperazine).

#### **1-(3-fluoro-5-methoxybenzyl)piperazine**

White solid; Yield 90%; MW 224.27 g/mol; Mp 97-99°C

LC/MS: positive mode  $m/z=225$  [M+H]<sup>+</sup>; Purity 92%

<sup>1</sup>H NMR (600 MHz, chloroform-d):  $\delta$  6.63-6.61 (m, 2H, -CH aromatic), 6.51 (dt, 1H, -CH aromatic,  $J_m=1.8$  and  $2.4$ ;  $J_{oH-F}=10.8$ ), 3.77 (s, 3H, -OCH<sub>3</sub>), 3.49 (s, 2H, -CH<sub>2</sub>), 3.18 (bs, 4H, -CH<sub>2</sub> piperazine), 2.69 (bs, 4H, -CH<sub>2</sub> piperazine).

<sup>13</sup>C NMR (151 MHz, chloroform-d):  $\delta$  164.51, 162.89, 161.08, 110.21 (-CH aromatic), 107.63 (-CH aromatic), 100.52 (-CH aromatic), 62.30 (-CH<sub>2</sub>), 55.97 (-OCH<sub>3</sub>), 49.64 (-CH<sub>2</sub> piperazine), 43.63 (-CH<sub>2</sub> piperazine).

#### **1-(4-bromo-3-fluorobenzyl)piperazine**

White solid; Yield 88%; MW 272.03 g/mol; 82-85°C

LC/MS: positive mode  $m/z=272.9$  [M+H]<sup>+</sup>; Purity 91%

<sup>1</sup>H NMR (600 MHz, chloroform-d):  $\delta$  7.47-7.44 (m, 1H, -CH aromatic), 7.09 (d, 1H, -CH aromatic,  $J_o=8.4$ ), 6.95 (d, 1H, -CH aromatic,  $J_o=8.4$ ), 3.47 (s, 2H, -CH<sub>2</sub>), 3.09 (bs, 4H, -CH<sub>2</sub> piperazine), 2.61 (bs, 4H, -CH<sub>2</sub> piperazine).



<sup>13</sup>C NMR (151 MHz, chloroform-d): δ 159.93, 158.29, 139.52, 133.80 (-CH aromatic), 125.82 (-CH aromatic), 116.72 (-CH aromatic), 61.57 (-CH<sub>2</sub>), 50.90 (-CH<sub>2</sub> piperazine), 44.26 (-CH<sub>2</sub> piperazine).

### **Synthesis of 1-propyl-8-(piperazine-1-sulphonyl)phenyl xanthine and 1-propyl-8-(benzylpiperazine-1-sulphonyl)phenyl xanthine derivatives**

Final compounds were obtained reacting 4-nitrophenyl-4-(2,6-dioxo-1-propyl-2,3,6,7-tetrahydro-1H-purin-8-yl)benzenesulphonate with an excess of a proper substituted piperazine (3 eq. for the substituted benzylpiperazines and 1.5 eq. for all other piperazines). The reaction was performed using the minimum amount of anhydrous DMSO as a solvent and heating, under argon atmosphere, at 160-170°C at least for three hours. It is worth noting that the lower reactivity of benzylpiperazines requires the use of longer reaction times (10-12h).

The obtained solution was cooled at room temperature and the reaction product was precipitated by the addition of water. The solid was washed with methanol and or acetonitrile to facilitate the subsequent purification step. The purification was carried out by HPLC, using as eluent a mixture of water and methanol as a gradient. Since the poor solubility in this mixture, each final product required a small amount of triethylamine to be solubilized in water and methanol (ratio H<sub>2</sub>O/MeOH/triethylamine 1:1:0.01).

After the reaction each compound was submitted to LC/MS analysis, to verify the formation of the expected reaction product.

#### **(JJ1517) 8-(4-(4-(3-methoxybenzyl)piperazin-1-ylsulphonyl)phenyl)-1-propyl-3,7-dihydropurine-2,6-dione**

White solid; MW 538.62 g/mol; Mp >350°C

LC/MS: positive mode  $m/z=539.4$  [M+H]<sup>+</sup>; negative mode  $m/z=537.19$  [M-H]<sup>-</sup>; Purity 97%

<sup>1</sup>H NMR (600 MHz, DMSO-d<sub>6</sub>): δ 14.03 (bs, 1H, -NH), 11.95 (bs, 1H, -NH), 8.33 (d, 2H, -CH aromatic,  $J_o=8.4$ ), 7.84 (d, 2H, -CH aromatic,  $J_o=8.4$ ), 7.17 (t, 1H, -CH aromatic,  $J_o=7.8$ ), 6.79-6.76 (m, 3H, -CH aromatic), 3.82 (t, 2H, -CH<sub>2</sub>CH<sub>2</sub>CH<sub>3</sub>), 3.68 (s, 3H, -OCH<sub>3</sub>), 3.42 (s, 2H, -CH<sub>2</sub>), 2.94 (bs, 4H, -CH<sub>2</sub> piperazine), 2.42 (bs, 4H, -CH<sub>2</sub> piperazine), 1.58 (m=6, 2H, -CH<sub>2</sub>CH<sub>2</sub>CH<sub>3</sub>), 0.87 (t, 3H, -CH<sub>2</sub>CH<sub>2</sub>CH<sub>3</sub>).

<sup>13</sup>C NMR (151 MHz, DMSO-d<sub>6</sub>): δ 159.38, 155.11, 151.10, 148.24, 147.77, 139.44, 135.84, 133.22, 129.35 (-CH aromatic), 128.40 (-CH aromatic), 127.09 (-CH aromatic), 121.02 (-CH aromatic), 114.35 (-CH aromatic), 112.53 (-CH aromatic), 109.13, 61.71 (-CH<sub>2</sub>), 55.00 (-OCH<sub>3</sub>), 51.59 (-CH<sub>2</sub> piperazine), 46.33 (-CH<sub>2</sub> piperazine), 41.97 (-CH<sub>2</sub>CH<sub>2</sub>CH<sub>3</sub>), 21.27 (-CH<sub>2</sub>CH<sub>2</sub>CH<sub>3</sub>), 11.54 (-CH<sub>2</sub>CH<sub>2</sub>CH<sub>3</sub>).

**(JJ1520) 8-(4-(4-methylpiperazine-1-sulphonyl)phenyl)-1-propyl-3,7-dihydropurine-2,6-dione**

White solid; MW 432.5 g/mol; Mp 338-339°C

LC/MS: positive mode  $m/z=433.4$  [M+H]<sup>+</sup>; negative mode  $m/z=431.15$  [M-H]<sup>-</sup>; Purity 99%

<sup>1</sup>H NMR (500 MHz, DMSO-d<sub>6</sub>): δ 14.12 (s, 1H, -NH, *nd*), 11.88 (bs, 1H, -NH), 8.31 (d, 2H, -CH aromatic,  $J_o=8.5$ ), 7.83 (d, 2H, -CH aromatic,  $J_o=8.5$ ), 3.82 (t, 2H, -CH<sub>2</sub>CH<sub>2</sub>CH<sub>3</sub>), 2.93 (bs, 4H, -CH<sub>2</sub> piperazine), 2.35 (t, 4H, -CH<sub>2</sub> piperazine), 2.12 (s, 3H, -CH<sub>3</sub>), 1.57 (m=6, 2H, -CH<sub>2</sub>CH<sub>2</sub>CH<sub>3</sub>), 0.87 (t, 3H, -CH<sub>2</sub>CH<sub>2</sub>CH<sub>3</sub>).

<sup>13</sup>C NMR (126 MHz, DMSO-d<sub>6</sub>): δ 155.24, 151.11, 151.13, 148.36, 147.77, 135.71, 133.59, 128.31, 126.96, 109.30, 53.77 (-CH<sub>2</sub> piperazine), 46.16 (-CH<sub>2</sub> piperazine), 45.45 (-CH<sub>3</sub>), 41.58 (-CH<sub>2</sub>CH<sub>2</sub>CH<sub>3</sub>), 21.01 (-CH<sub>2</sub>CH<sub>2</sub>CH<sub>3</sub>), 11.31 (-CH<sub>2</sub>CH<sub>2</sub>CH<sub>3</sub>).

**(JJ1521) 8-(4-(4-(2-fluorophenyl)piperazine-1-sulphonyl)phenyl)-1-propyl-3,7-dihydropurine-2,6-dione**

White solid; MW 512.56 g/mol; Mp 339-341°C

LC/MS: positive mode  $m/z=513.4$  [M+H]<sup>+</sup>; negative mode  $m/z=511.15$  Purity 97%

NMR data for this compound are not available.

**(JJ1522) 8-(4-(4-(3-fluorophenyl)piperazine-1-sulphonyl)phenyl)-1-propyl-3,7-dihydropurine-2,6-dione**

White solid; MW 512.56 g/mol; Mp 338-340°C

LC/MS: positive mode  $m/z=513.4$  [M+H]<sup>+</sup>; negative mode  $m/z=511.15$  [M-H]<sup>-</sup>; Purity 96%

<sup>1</sup>H NMR (600 MHz, DMSO-d<sub>6</sub>): δ 14.01 (bs, 1H, -NH), 11.94 (s, 1H, -NH), 8.33 (d, 2H, -CH aromatic,  $J_o=8.4$ ), 7.88 (d, 2H, -CH aromatic,  $J_o=8.4$ ), 7.20-7.16 (m, 1H, -CH aromatic), 6.71 (m, 2H, -CH aromatic), 6.56-6.53 (m, 1H, -CH aromatic), 3.81 (t, 2H, -CH<sub>2</sub>CH<sub>2</sub>CH<sub>3</sub>), 3.26 (bs, 4H, -CH<sub>2</sub> piperazine), 3.05 (bs, 4H, -CH<sub>2</sub> piperazine), 1.57 (m=6, 2H, -CH<sub>2</sub>CH<sub>2</sub>CH<sub>3</sub>), 0.87 (t, 3H, -CH<sub>2</sub>CH<sub>2</sub>CH<sub>3</sub>).

<sup>13</sup>C NMR (151 MHz, DMSO-d<sub>6</sub>): δ 164.09, 162.49, 155.14, 152.24, 151.09, 135.57, 133.43, 130.46, 128.71, 127.12, 111.66, 105.86, 102.94, 102.48, 47.59 (-CH<sub>2</sub> piperazine), 45.57 (-CH<sub>2</sub> piperazine), 41.53 (-CH<sub>2</sub>CH<sub>2</sub>CH<sub>3</sub>), 21.15 (-CH<sub>2</sub>CH<sub>2</sub>CH<sub>3</sub>), 11.56 (-CH<sub>2</sub>CH<sub>2</sub>CH<sub>3</sub>).

**(JJ1523) 8-(4-(4-(3-bromophenyl)piperazine-1-sulphonyl)phenyl)-1-propyl-3,7-dihydropurine-2,6-dione**

White solid; MW 573.46 g/mol; Mp 322-324°C

LC/MS: positive mode  $m/z=575.3$  [M+H]<sup>+</sup>; negative mode  $m/z=573.07$ ; Purity 98%

<sup>1</sup>H NMR (500 MHz, DMSO-d<sub>6</sub>): δ 14.02 (bs, 1H, -NH), 11.93 (s, 1H, -NH), 8.33 (d, 2H, -CH aromatic,  $J_o=8.4$ ), 7.88 (d, 2H, -CH aromatic,  $J_o=8.4$ ), 7.12 (t, 1H, -CH aromatic,  $J_{o1-2}=8.5$ ), 7.04 (s, 1H, -CH aromatic), 6.92 (d, 1H, -CH aromatic  $J_o=8.5$ ), 6.89 (d, 1H, -CH aromatic,  $J_o=8.5$ ), 3.82 (t, 2H, -CH<sub>2</sub>CH<sub>2</sub>CH<sub>3</sub>), 3.26 (bs, 4H, -CH<sub>2</sub> piperazine), 3.05 (bs, 4H, -CH<sub>2</sub> piperazine), 1.57 (m=6, 2H, -CH<sub>2</sub>CH<sub>2</sub>CH<sub>3</sub>), 0.87 (t, 3H, -CH<sub>2</sub>CH<sub>2</sub>CH<sub>3</sub>).

<sup>13</sup>C NMR (126 MHz, DMSO-d<sub>6</sub>): δ 155.33, 151.88, 150.98, 148.12, 147.70, 135.84, 133.34, 131.14, 128.61, 127.20, 122.73, 121.87, 118.38, 114.94, 47.43 (CH<sub>2</sub> piperazine), 46.02 (-CH<sub>2</sub> piperazine), 41.49 (-CH<sub>2</sub>CH<sub>2</sub>CH<sub>3</sub>), 21.23 (-CH<sub>2</sub>CH<sub>2</sub>CH<sub>3</sub>), 11.31 (-CH<sub>2</sub>CH<sub>2</sub>CH<sub>3</sub>).

**(JJ1532) tert-butyl 4-(4-(2,6-dioxo-1-propyl-2,3,6,7-tetrahydro-1H-purin-8-yl)phenylsulphonyl)piperazine-1-carboxylate**

White solid; MW 518.59 g/mol; Mp 340°C

LC/MS: positive mode *m/z*=519.2 [M+H]<sup>+</sup>; negative mode *m/z*=517.18 [M-H]<sup>-</sup>; Purity 99%

<sup>1</sup>H NMR (500 MHz, DMSO-d<sub>6</sub>): δ 14.00 (bs, 1H, -NH), 11.94 (s, 1H, -NH), 8.35 (d, 2H, -CH aromatic, *J*<sub>o</sub>=8.4), 7.85 (d, 2H, -CH aromatic, *J*<sub>o</sub>=8.4), 3.82 (t, 2H, -CH<sub>2</sub>CH<sub>2</sub>CH<sub>3</sub>), 3.39 (t, 4H, -CH<sub>2</sub> piperazine), 2.91 (t, 4H, -CH<sub>2</sub> piperazine), 1.58 (m=6, 2H, -CH<sub>2</sub>CH<sub>2</sub>CH<sub>3</sub>), 1.32 (s, 9H, -CH<sub>3</sub> tert-butyl), 0.87 (t, 3H, -CH<sub>2</sub>CH<sub>2</sub>CH<sub>3</sub>).

<sup>13</sup>C NMR (126 MHz, DMSO-d<sub>6</sub>): δ 155.20, 153.51, 151.01, 147.86, 147.70, 135.90, 133.40, 128.55(-CH aromatic), 127.05 (-CH aromatic), 79.46, 45.84 (-CH<sub>2</sub> piperazine), 41.62 (-CH<sub>2</sub>CH<sub>2</sub>CH<sub>3</sub>), 28.14 (-CH<sub>3</sub> tert-butyl), 20.99 (-CH<sub>2</sub>CH<sub>2</sub>CH<sub>3</sub>), 11.31 (-CH<sub>2</sub>CH<sub>2</sub>CH<sub>3</sub>).

**(JJ1533) 8-(4-(piperazin-1-ylsulphonyl)phenyl)-1-propyl-3,7-dihydropurine-2,6-dione**

Final compound JJ1533 was obtained reacting 4-nitrophenyl-4-(2,6-dioxo-1-propyl-2,3,6,7-tetrahydro-1H-purin-8-yl)benzenesulphonate (1 mmol) with N-acetyl-piperazine (1.5 mmol) in DMSO, heating for 3 hours, under Argon atmosphere, at 160°C. The solution was cooled at room temperature. A solid was obtained after the addition of water. This solid was filtered out and analysed by LC/MS. The acetyl derivative was deprotected by aqueous sodium hydroxide 2M, heating in ethanol for eight hours.

White solid; MW 418.47 g/mol; Mp >350°C

LC/MS: positive mode *m/z*=419.3 [M+H]<sup>+</sup>; negative mode *m/z*=417.13 [M-H]<sup>-</sup>; Purity 97%;

<sup>1</sup>H NMR (500 MHz, DMSO-d<sub>6</sub>): δ 8.35 (d, 2H, -CH aromatic, *J*<sub>o</sub>=8.4), 7.87 (d, 2H, -CH aromatic, *J*<sub>o</sub>=8.4), 3.82 (t, 2H, -CH<sub>2</sub>CH<sub>2</sub>CH<sub>3</sub>), 3.07-2.89 (m, 8H, -CH<sub>2</sub> piperazine), 1.58 (m=6, 2H, -CH<sub>2</sub>CH<sub>2</sub>CH<sub>3</sub>), 0.88 (t, 3H, -CH<sub>2</sub>CH<sub>2</sub>CH<sub>3</sub>).

<sup>13</sup>C NMR (126 MHz, DMSO-d<sub>6</sub>): δ 155.13, 151.08, 148.07, 147.69, 135.40, 133.48, 128.48 (-CH aromatic), 127.12 (-CH aromatic), 108.96, 44.72 (-CH<sub>2</sub> piperazine), 43.46 (-CH<sub>2</sub> piperazine), 41.62 (-CH<sub>2</sub>CH<sub>2</sub>CH<sub>3</sub>), 20.99 (-CH<sub>2</sub>CH<sub>2</sub>CH<sub>3</sub>), 11.31 (-CH<sub>2</sub>CH<sub>2</sub>CH<sub>3</sub>).

**(JJ1534) 8-(4-(4-(4-fluoro-3-methoxybenzyl)piperazin-1-ylsulphonyl)phenyl)-1-propyl-3,7-dihydropurine-2,6-dione**

White solid; MW 556.61 g/mol; Mp >350°C

LC/MS: positive mode *m/z*=557.3 [M+H]<sup>+</sup>; negative mode *m/z*=555.18 [M-H]<sup>-</sup>; Purity 98%

<sup>1</sup>H NMR (500 MHz, DMSO-d<sub>6</sub>): δ 14.01 (bs, 1H, -NH), 11.94 (bs, 1H, -NH), 8.33 (d, 2H, -CH aromatic, *J*= 8.3), 7.84 (d, 2H, -CH aromatic, *J*= 8.3), 7.07 (t, 1H, -CH aromatic, *J*<sub>oH-F</sub>=9.5), 6.98 (d, 2H, -CH aromatic, *J*<sub>oH-H</sub>=7.5), 6.78 (s, 1H, -CH aromatic), 3.82 (t, 2H, -

CH<sub>2</sub>CH<sub>2</sub>CH<sub>3</sub>), 3.75 (s, 3H, -OCH<sub>3</sub>), 3.42 (s, 2H, -CH<sub>2</sub>), 2.95 (bs, 4H, -CH<sub>2</sub> piperazine), 2.42 (bs, 4H, -CH<sub>2</sub> piperazine), 1.58 (m=6, 2H, -CH<sub>2</sub>CH<sub>2</sub>CH<sub>3</sub>), 0.88 (t, 3H, -CH<sub>2</sub>CH<sub>2</sub>CH<sub>3</sub>).

<sup>13</sup>C NMR (126 MHz, DMSO-d<sub>6</sub>): δ 155.04, 151.07, 148.12, 147.05, 135.99, 134.56, 133.13, 128.39 (-CH aromatic), 127.11 (-CH aromatic), 120.95 (-CH aromatic), 115.55 (-CH aromatic), 114.22 (-CH aromatic), 108.63, 61.10 (-CH<sub>2</sub>), 56.05 (-OCH<sub>3</sub>), 51.76 (-CH<sub>2</sub> piperazine), 46.04 (-CH<sub>2</sub> piperazine), 41.63 (-CH<sub>2</sub>CH<sub>2</sub>CH<sub>3</sub>), 20.89 (-CH<sub>2</sub>CH<sub>2</sub>CH<sub>3</sub>), 11.39 (-CH<sub>2</sub>CH<sub>2</sub>CH<sub>3</sub>).

**(JJ1535) 8-(4-(4-(3-fluoro-5-methoxybenzyl)piperazin-1-ylsulphonyl)phenyl)-1-propyl-3,7-dihydropurine-2,6-dione**

White solid; MW 556.61 g/mol; Mp >350°C

LC/MS: positive mode *m/z*=557.3 [M+H]<sup>+</sup>; negative mode *m/z*=555.18 [M-H]<sup>-</sup>; Purity=100%

<sup>1</sup>H NMR (500 MHz, DMSO-d<sub>6</sub>): δ 13.99 (bs, 1H, -NH), 11.93 (bs, 1H, -NH), 8.32 33 (d, 2H, -CH aromatic, J= 8.3), 7.83 33 (d, 2H, -CH aromatic, J= 8.3), 6.66-6.60 (m, 3H, -CH aromatic), 3.82 (t, 2H, -CH<sub>2</sub>CH<sub>2</sub>CH<sub>3</sub>), 3.70 (s, 3H, -OCH<sub>3</sub>), 3.42 (s, 2H, -CH<sub>2</sub>), 2.96 (bs, 4H, -CH<sub>2</sub> piperazine), 2.43 (bs, 4H, -CH<sub>2</sub> piperazine), (m=6, 2H, -CH<sub>2</sub>CH<sub>2</sub>CH<sub>3</sub>), 0.88 (t, 3H, -CH<sub>2</sub>CH<sub>2</sub>CH<sub>3</sub>).

<sup>13</sup>C NMR (126 MHz, DMSO) δ 164.03, 162.17, 160.74, 155.16, 151.10, 148.36, 147.72, 141.48, 135.87, 133.36, 128.35 (-CH aromatic), 127.05 (-CH aromatic), 110.63 (-CH aromatic), 107.13 (-CH aromatic), 100.18 (-CH aromatic), 61.06 (-CH<sub>2</sub>), 55.64 (-OCH<sub>3</sub>), 51.98 (-CH<sub>2</sub> piperazine), 46.14 (-CH<sub>2</sub> piperazine), 41.83 (-CH<sub>2</sub>CH<sub>2</sub>CH<sub>3</sub>), 21.41 (-CH<sub>2</sub>CH<sub>2</sub>CH<sub>3</sub>), 11.32 (-CH<sub>2</sub>CH<sub>2</sub>CH<sub>3</sub>).

**(JJ1536) 8-(4-(4-(4-bromo-3-fluorobenzyl)piperazin-1-ylsulphonyl)phenyl)-1-propyl-3,7-dihydropurine-2,6-dione**

White solid; MW 605.48 g/mol; Mp >350°C

LC/MS: positive mode *m/z*=605.1 [M+H]<sup>+</sup>; negative mode *m/z*=376.11 [M-H]<sup>-</sup>; Purity=98%

<sup>1</sup>H NMR (600 MHz, DMSO-d<sub>6</sub>): δ 14.02 (bs, 1H, -NH), 11.94 (bs, 1H, -NH), 8.33 (d, 2H, -CH aromatic, J= 8.4), 7.84 (d, 2H, -CH aromatic, J= 8.4), 7.58 (t, 1H, -CH aromatic, J<sub>o</sub>=7.8), 7.21 (d, 1H, -CH aromatic, J<sub>oH-F</sub>=10.2), 7.04 (d, 1H, -CH aromatic, J<sub>o</sub>=8.4), 3.82 (t, 2H, -CH<sub>2</sub>CH<sub>2</sub>CH<sub>3</sub>), 3.46 (s, 2H, -CH<sub>2</sub>), 2.95 (bs, 4H, -CH<sub>2</sub> piperazine), 2.43 (bs, 4H, -CH<sub>2</sub> piperazine), 1.58 (m=6, 2H, -CH<sub>2</sub>CH<sub>2</sub>CH<sub>3</sub>), 0.88 (t, 3H, -CH<sub>2</sub>CH<sub>2</sub>CH<sub>3</sub>).

<sup>13</sup>C NMR (151 MHz, DMSO-d<sub>6</sub>): δ 159.09, 157.46, 155.14, 151.09, 148.23, 147.76, 140.78, 133.28 (-CH aromatic), 128.39 (-CH aromatic), 127.06 (-CH aromatic), 126.31 (-CH aromatic), 116.78 (-CH aromatic), 116.63, 106.29, 106.16, 60.04 (-CH<sub>2</sub>), 51.48 (-CH<sub>2</sub> piperazine), 46.07 (-CH<sub>2</sub> piperazine), 41.61 (-CH<sub>2</sub>CH<sub>2</sub>CH<sub>3</sub>), 21.05 (-CH<sub>2</sub>CH<sub>2</sub>CH<sub>3</sub>), 11.32 (-CH<sub>2</sub>CH<sub>2</sub>CH<sub>3</sub>).

### 3.5 REFERENCES

1. Jacobson, K. A., Introduction to adenosine receptors as therapeutic targets. *Handbook of experimental pharmacology* **2009**, 1-24.
2. Ryzhov, S.; Zaynagetdinov, R.; Goldstein, A. E.; Novitskiy, S. V.; Blackburn, M. R.; Biaggioni, I.; Feoktistov, I., Effect of A2B adenosine receptor gene ablation on adenosine-dependent regulation of proinflammatory cytokines. *The Journal of pharmacology and experimental therapeutics* **2008**, 324, 694-700.
3. St Hilaire, C.; Koupenova, M.; Carroll, S. H.; Smith, B. D.; Ravid, K., TNF-alpha upregulates the A2B adenosine receptor gene: The role of NAD(P)H oxidase 4. *Biochemical and biophysical research communications* **2008**, 375, 292-6.
4. Kolachala, V.; Asamoah, V.; Wang, L.; Obertone, T. S.; Ziegler, T. R.; Merlin, D.; Sitaraman, S. V., TNF-alpha upregulates adenosine 2b (A2b) receptor expression and signaling in intestinal epithelial cells: a basis for A2bR overexpression in colitis. *Cellular and molecular life sciences : CMLS* **2005**, 62, 2647-57.
5. Xaus, J.; Mirabet, M.; Lloberas, J.; Soler, C.; Lluís, C.; Franco, R.; Celada, A., IFN-gamma up-regulates the A2B adenosine receptor expression in macrophages: a mechanism of macrophage deactivation. *Journal of immunology (Baltimore, Md. : 1950)* **1999**, 162, 3607-14.
6. Aherne, C. M.; Kewley, E. M.; Eltzhig, H. K., The resurgence of A2B adenosine receptor signaling. *Biochimica et Biophysica Acta (BBA) - Biomembranes* **2011**, 1808, 1329-1339.
7. Schulte, G.; Fredholm, B. B., Signalling from adenosine receptors to mitogen-activated protein kinases. *Cellular signalling* **2003**, 15, 813-27.
8. Borrmann, T.; Hinz, S.; Bertarelli, D. C.; Li, W.; Florin, N. C.; Scheiff, A. B.; Müller, C. E., 1-alkyl-8-(piperazine-1-sulfonyl)phenylxanthines: development and characterization of adenosine A2B receptor antagonists and a new radioligand with subnanomolar affinity and subtype specificity. *Journal of medicinal chemistry* **2009**, 52, 3994-4006.
9. Hasko, G.; Csoka, B.; Nemeth, Z. H.; Vizi, E. S.; Pacher, P., A(2B) adenosine receptors in immunity and inflammation. *Trends in immunology* **2009**, 30, 263-70.

10. Jacobson, K. A.; Balasubramanian, R.; Deflorian, F.; Gao, Z. G., G protein-coupled adenosine (P1) and P2Y receptors: ligand design and receptor interactions. *Purinergic Signalling* **2012**, 8, 419-36.
11. Piirainen, H.; Ashok, Y.; Nanekar, R. T.; Jaakola, V. P., Structural features of adenosine receptors: from crystal to function. *Biochimica et biophysica acta* **2011**, 1808, 1233-44.
12. Zablocki, J.; Elzein, E.; Kalla, R., A2B adenosine receptor antagonists and their potential indications. *Expert Opin. Ther. Pat.* **2006**, 16, 1347-1357.
13. Brown, R. A.; Spina, D.; Page, C. P., Adenosine receptors and asthma. *British journal of pharmacology* **2008**, 153 Suppl 1, S446-56.
14. Wilson, C. N., Adenosine receptors and asthma in humans. *Br. J. Pharmacol.* **2008**, 155, 475-486.
15. Sun, C. X.; Zhong, H.; Mohsenin, A.; Morschl, E.; Chunn, J. L.; Molina, J. G.; Belardinelli, L.; Zeng, D.; Blackburn, M. R., Role of A2B adenosine receptor signaling in adenosine-dependent pulmonary inflammation and injury. *The Journal of clinical investigation* **2006**, 116, 2173-2182.
16. Merighi, S.; Borea, P. A.; Gessi, S., Adenosine receptors and diabetes: Focus on the A2B adenosine receptor subtype. *Pharmacol. Res.* **2015**, 99, 229-236.
17. Rusing, D.; Muller, C. E.; Verspohl, E. J., The impact of adenosine and A(2B) receptors on glucose homeostasis. *The Journal of pharmacy and pharmacology* **2006**, 58, 1639-45.
18. Yasuda, N.; Inoue, T.; Horizoe, T.; Nagata, K.; Minami, H.; Kawata, T.; Hoshino, Y.; Harada, H.; Yoshikawa, S.; Asano, O.; Nagaoka, J.; Murakami, M.; Abe, S.; Kobayashi, S.; Tanaka, I., Functional characterization of the adenosine receptor contributing to glycogenolysis and gluconeogenesis in rat hepatocytes. *European journal of pharmacology* **2003**, 459, 159-66.
19. Figler, R. A.; Wang, G.; Srinivasan, S.; Jung, D. Y.; Zhang, Z.; Pankow, J. S.; Ravid, K.; Fredholm, B.; Hedrick, C. C.; Rich, S. S.; Kim, J. K.; LaNoue, K. F.; Linden, J., Links between insulin resistance, adenosine A2B receptors, and inflammatory markers in mice and humans. *Diabetes* **2011**, 60, 669-79.

20. Wojcik, M.; Zieleniak, A.; Mac-Marcjanek, K.; Wozniak, L. A.; Cypryk, K., The elevated gene expression level of the A(2B) adenosine receptor is associated with hyperglycemia in women with gestational diabetes mellitus. *Diabetes/metabolism research and reviews* **2014**, 30, 42-53.
21. Burnstock, G.; Novak, I., Purinergic signalling and diabetes. *Purinergic Signalling* **2013**, 9, 307-324.
22. San Martin, R.; Valladares, D.; Roa, H.; Troncoso, E.; Sobrevia, L., Do adenosine receptors offer new therapeutic options for diabetic nephropathy? *Current vascular pharmacology* **2009**, 7, 450-9.
23. Grant, M. B.; Davis, M. I.; Caballero, S.; Feoktistov, I.; Biaggioni, I.; Belardinelli, L., Proliferation, migration, and ERK activation in human retinal endothelial cells through A(2B) adenosine receptor stimulation. *Investigative ophthalmology & visual science* **2001**, 42, 2068-73.
24. Gessi, S.; Merighi, S.; Sacchetto, V.; Simioni, C.; Borea, P. A., Adenosine receptors and cancer. *Biochimica et biophysica acta* **2011**, 1808, 1400-12.
25. Ryzhov, S.; McCaleb, J. L.; Goldstein, A. E.; Biaggioni, I.; Feoktistov, I., Role of adenosine receptors in the regulation of angiogenic factors and neovascularization in hypoxia. *The Journal of pharmacology and experimental therapeutics* **2007**, 320, 565-72.
26. Bilkei-Gorzo, A.; Abo-Salem, O. M.; Hayallah, A. M.; Michel, K.; Muller, C. E.; Zimmer, A., Adenosine receptor subtype-selective antagonists in inflammation and hyperalgesia. *Naunyn-Schmiedeberg's archives of pharmacology* **2008**, 377, 65-76.
27. Beukers, M. W.; Meurs, I.; Ijzerman, A. P., Structure-affinity relationships of adenosine A2B receptor ligands. *Medicinal research reviews* **2006**, 26, 667-98.
28. Kalla, R. V.; Zablocki, J., Progress in the discovery of selective, high affinity A(2B) adenosine receptor antagonists as clinical candidates. *Purinergic Signalling* **2009**, 5, 21-9.
29. Kim, S. A.; Marshall, M. A.; Melman, N.; Kim, H. S.; Muller, C. E.; Linden, J.; Jacobson, K. A., Structure-activity relationships at human and rat A2B adenosine receptors of xanthine derivatives substituted at the 1-, 3-, 7-, and 8-positions. *Journal of medicinal chemistry* **2002**, 45, 2131-8.

30. Hayallah, A. M.; Sandoval-Ramirez, J.; Reith, U.; Schobert, U.; Preiss, B.; Schumacher, B.; Daly, J. W.; Muller, C. E., 1,8-disubstituted xanthine derivatives: synthesis of potent A2B-selective adenosine receptor antagonists. *Journal of medicinal chemistry* **2002**, 45, 1500-10.
31. Zablocki, J.; Kalla, R.; Perry, T.; Palle, V.; Varkhedkar, V.; Xiao, D.; Piscopio, A.; Maa, T.; Gimbel, A.; Hao, J.; Chu, N.; Leung, K.; Zeng, D., The discovery of a selective, high affinity A(2B) adenosine receptor antagonist for the potential treatment of asthma. *Bioorganic & medicinal chemistry letters* **2005**, 15, 609-12.
32. Kalla, R. V.; Elzein, E.; Perry, T.; Li, X.; Palle, V.; Varkhedkar, V.; Gimbel, A.; Maa, T.; Zeng, D.; Zablocki, J., Novel 1,3-disubstituted 8-(1-benzyl-1H-pyrazol-4-yl) xanthines: high affinity and selective A2B adenosine receptor antagonists. *Journal of medicinal chemistry* **2006**, 49, 3682-92.
33. Yan, L.; Bertarelli, D. C. G.; Hayallah, A. M.; Meyer, H.; Klotz, K.-N.; Muller, C. E., A new synthesis of sulfonamides by aminolysis of p-nitrophenylsulfonates yielding potent and selective adenosine A2B receptor antagonists. *Journal of medicinal chemistry* **2006**, 49, 4384-91.
34. Müller, C. E., Synthesis of 3-substituted 6-aminouracils. *Tetrahedron Letters* **1991**, 32, 6539-6540.
35. Müller, C. E., General synthesis and properties of 1-monosubstituted xanthines. *Synthesis* **1993**, 125-128.
36. Mueller, C. E.; Sandoval-Ramirez, J., A new versatile synthesis of xanthines with variable substituents in the 1-, 3-, 7-, and 8-positions. *Synthesis* **1995**, 1295-9.
37. Abdel-Magid, A. F.; Carson, K. G.; Harris, B. D.; Maryanoff, C. A.; Shah, R. D., Reductive Amination of Aldehydes and Ketones with Sodium Triacetoxyborohydride. Studies on Direct and Indirect Reductive Amination Procedures(1). *The Journal of organic chemistry* **1996**, 61, 3849-3862.
38. Choi, J. H.; Lee, B. C.; Lee, H. W.; Lee, I., Competitive reaction pathways in the nucleophilic substitution reactions of aryl benzenesulfonates with benzylamines in acetonitrile. *The Journal of organic chemistry* **2002**, 67, 1277-81.



## **Acknowledgments.**

PhD has been not only a professional experience, but a great life experience.

Foremost, I would like to thank my supervisor, Prof. Elias Maccioni, for giving me the opportunity to experience the "research" life and for his kind supervision.

I would like to express my gratitude to the entire research team, for having made available their knowledges and expertise.

Among them, a special mention goes to Simona, Giulia and Claudia for their generosity and sincere friendship, without them nothing would have been the same.

In particular, I would like to express my immense gratitude to Simona for being present in all the possible ways, for her encouragement and support, as well as for the life and professional teachings.

To Giulia for the time she dedicated to me and for her adorable craziness, precious elements in the last three years.

To Claudia for her positivity and for the stimulating discussions that have radically changed my days in the lab.

My thanks and appreciation goes also to Prof. Antonio Maccioni, a pillar of the research group, for his kindness, the work advices and his endless wisdom.

I am thankful to Prof. Christa Müller, for the huge opportunity to spend some months in the laboratories at the University of Bonn. It has been an experience that tremendously enriched my knowledges, my thesis work and my personal growth.

I would like to thank all the people who made these months in Germany unforgettable.

In particular, I am appreciative to Jie, a very good mentor and friend, Yuliya, Marco and Samer for the nice conversations and the time we spent together in the lab.

A special thank is for each member of my family, my main supporters during this experience. For this, I would like to dedicate this thesis to my parents, my sister, my brother, Pietro, Carmen and my aunts, whose presence has been essential in my life.

I am thankful to Chiara and Tonino for their kindness, and to Alessandro and Stefania for their support, also logistic, during these years.

Deep gratitude goes to my friends, which always encouraged me during this exciting and difficult experience. In particular, to Angelica, for her unconditioned friendship.

Finally, there are no words that can express my gratitude for Marco, for his invaluable support in every step and mood of the last six years, for taking care of me, for supporting my ambitions and having never allowed me to give up in front of the

difficulties. For this I dedicate to him each effort, each sacrifice and above all each joy of this journey. Without him nothing of this would have been possible.